Development and Implementation of Control System for an Advanced Multi-Regime Series-Parallel Plug-in Hybrid Electric Vehicle

by

Daniel Prescott
B.Eng, University of Victoria, 2009

A Thesis Submitted in Partial Fulfillment
of the Requirements for the Degree of

Master of Applied Science

in the Department of Mechanical Engineering

Supervisory Committee

Development and Implementation of Control System for an Advanced Multi-Regime Series-Parallel Plug-in Hybrid Electric Vehicle

by

Daniel Prescott
B.Eng, University of Victoria, 2009

Supervisory Committee

Dr. Zuomin Dong, (Department of Mechanical Engineering)
Supervisor

Dr. Curran Crawford, (Department of Mechanical Engineering)
Departmental Member

Dr. Brad Buckham, (Department of Mechanical Engineering)
Departmental Member

Supervisory Committee

Dr. Zuomin Dong, (Department of Mechanical Engineering)
Supervisor

Dr. Curran Crawford, (Department of Mechanical Engineering)
Departmental Member

Dr. Brad Buckham, (Department of Mechanical Engineering)
Departmental Member

Abstract

Following the Model-Based-Design (MBD) development process used presently by the automotive industry, the control systems for a new Series-Parallel Multiple-Regime Plug-in Hybrid Electric Vehicle (PHEV), UVic EcoCAR2, have been developed, implemented and tested. Concurrent simulation platforms were used to achieve different developmental goals, with a simplified system power loss model serving as the low-overhead control strategy optimization platform, and a high fidelity Software-in-Loop (SIL) model serving as the vehicle control development and testing platform. These two platforms were used to develop a strategy-independent controls development tool which will allow deployment of new strategies for the vehicle irrespective of energy management strategy particulars. A rule-based energy management strategy was applied and calibrated using genetic algorithm (GA) optimization. The concurrent modeling approach was validated by comparing the vehicle equivalent fuel consumption between the simplified and SIL models. An equivalency factor (EF) of 1 was used in accounting for battery state of charge (SOC) discrepancies at cycle end. A recursively-defined subsystem efficiency-based EF was also

applied to try to capture real-world equivalency impacts. Aggregate results between the two test platforms showed translation of the optimization benefits though absolute results varied for some cycles. Accuracy improvements to the simplified model to better capture dynamic effects are recommended to improve the utility of the newly introduced vehicle control system development method. Additional future work in redefining operation modes and mode transition threshold conditions to approximate optimal vehicle operation is recommended and readily supported by the control system platform developed.

Table of Contents

Supervisory Committee ii
Abstract iii
Table of Contents v
List of Tables ix
List of Figures xi
List of Abbreviations xv
Acknowledgments xviii
Dedication xix
Chapter 1: Introduction 1
1.1. EcoCAR2 Student Competition 1
1.2. Overview of Vehicle Architecture 3
1.3. Considerations for Control Development for Selected Architecture 4
1.3.1. Connection to Existing Research 4
1.3.2. Driveability Challenges of Controlling Selected Architecture 6
1.4. Controls Implementation Platform and Development Process 7
Chapter 2: Introduction to Hybrid Powertrain Technology 9
2.1. The Benefit of Hybrid Powertrain Technology 9
2.1.1. A Brief History of Hybrid Electric Vehicles 11
2.1.2. Powertrain Electrification 13
2.1.3. Manipulating Engine Operating Point 15
2.2. Major Enabling Technologies 16
2.2.1. High Power Density Traction Motors 16
2.2.2. Battery Energy Storage Systems 17
2.2.3. Optimization Design via Model-Based-Design 19
2.3. Production Hybrid Vehicle Architecture Variations 20
2.3.1. Mild Hybrid 21
2.3.2. Parallel Hybrid 22
2.3.3. Series Hybrid 23
2.3.4. Power-Split Hybrid 24

2.3.5. Series-Parallel Hybrid 26
2.4. Hybridization Benefits and Applicability of Advanced Controls to Marine Vessel Powertrains 27
2.4.1. Marine Vessel Power System Overview and Hybridization Potential 27
2.4.2. Current Marine Vessel Emissions 30
2.4.3. Availability of Hardware 32
2.4.4. Challenges Associated with Optimal Design of Marine Hybrid Powertrains 34
Chapter 3: Vehicle Control System Development 37
3.1. Vehicle Component Details 37
3.1.1. GM 2.4L EcoTEC Engine 38
3.1.2. GM 6T40 Transmission 39
3.1.3. Magna E-Drive Rear Traction Motor 42
3.1.4. TM4 Motive B Belted Alternator Starter Motor 44
3.1.5. A123 Lithium Ion Battery Pack 47
3.1.6. Driver Interface 49
3.2. Operational Performance Targets 50
3.2.1. Vehicle Technical Specifications 50
3.2.2. Operational Flexibility 52
3.3. Model-Based-Design Process 56
3.3.1. Development Process Flow 56
3.3.2. Design Failure Mode Effects Analysis and Test Case Feedback 59
3.3.3. Automated Testing 61
3.3.4. Process Documentation and Development Team Organization 64
3.3.5. Multi-Platform Controls Development 68
3.3.6. SIL to HIL to Vehicle Validation 76
3.3.7. Linear Vehicle Dynamics 78
3.4. Control System Development Summary 79
Chapter 4: Vehicle Control System Logic and Strategy 80
4.1. High Level Controller Logic Hierarchy 80

4.2. Safety Critical System Design 82
4.2.1. Subsystem Level Requirements Handling 82
4.2.2. System Driver Torque Request Handling 84
4.2.3. System Level Failure Mitigation Algorithms 86
4.2.4. System Level Operation State Diagnostics 87
4.3. Strategy Override Tactics for Strategy-Independent Controls 88
4.3.1. ICE Starting While Driving 89
4.3.2. Component Torque Transition Overrides 91
4.4. Rule-Based Control Strategy Employed for Validation 94
4.4.1. Energy Management Logic and Rationale 95
4.4.2. Road-Tuned Variables 96
4.4.3. Drive-Cycle Tuned Variables 99
4.4.4. Operational Limitations 102
4.5. System Logic Development Summary 104
Chapter 5: Assessments of Performance of Control System Architecture 105
5.1. Methodology and Metrics for Assessment 105
5.1.1. Global Optimization Algorithm and Method 106
5.1.2. Calculation of Performance Metrics 108
5.1.3. Equivalency Factor 108
5.1.4. Driver Model Tuning Effects 110
5.2. Drive Cycle Schedules Used for Assessment 111
5.2.1. US06 City Cycle 111
5.2.2. US06 Highway Cycle 112
5.2.3. HWFET Cycle 113
5.2.4. FU505 Cycle 114
5.2.5. 4-Cycle Mixed 115
5.3. Non-Optimized Rule-Based Strategy System Performance 115
5.4. Optimized Strategy System Performance of Simplified Model 117
5.4.1. Equivalency Factor 1 Optimization Results 118
5.4.2. Sensitivity of Results to Equivalency Factor 119
5.4.3. Recursive Equivalency Factor Analysis Scheme 121

5.4.4. Recursive Equivalency Factor Optimization Results 122
5.4.5. Parallel Coordinate Visualization of Recursive Equivalency Factor Optimization 124
5.5. Translated Optimized Strategy System Performance of SIL Model 127
5.5.1. Equivalency Factor 1 Optimized 127
5.5.2. Recursive Equivalency Factor Optimized 129
5.6. SIL Model Behaviour for Optimal Calibrations 130
5.6.1. US06 City Cycle Behaviour for Optimal Calibration 130
5.6.2. HWFET Cycle Behaviour for Optimal Calibration 135
5.7. Performance Evaluation Summary 139
Chapter 6: Conclusions and Recommendations 140
6.1. Strategy-Independent Controls Implementation and Effects 140
6.2. Two-Model Development Approach 140
6.3. Recommended Future Vehicle Work 142
6.3.1. Mechanical Deficiencies 142
6.3.2. Engine-Throttle Relationship Verification 143
6.3.3. Use of Manumatic Transmission Functionality 144
6.4. Recommended Future Research Development of Work 144
6.4.1. Application of Industry Standard Driveability Tools 144
6.4.2. Development of Higher Accuracy Lightweight Models for Optimization 145
6.4.3. Development of Quasi-Optimal Rule-Based Controls Strategy 146
6.5. Summary of Contributions 146
Bibliography 148
Appendix A – System Interfacing Details 152
Appendix B – Development of Transmission Gearing Estimation Curve and Rationale 155
Appendix C – Optimization Routine Sample Code 158

List of Tables

Table 1: 6T40 Transmission Gear Ratios 41
Table 2: Magna E-Drive Specifications 43
Table 3: TM4 Motive B Specifications 45
Table 4: A123 6x15s3p ESS Specifications 48
Table 5: Driver Interface 49
Table 6: UVic Vehicle Architecture Vehicle Technical Specifications 51
Table 7: Master Test Case Summary Document Excerpt 65
Table 8: Comparison of Model Features for SIL and MIL Models 69
Table 9: SIL Component Model Summary Information 71
Table 10: Simplified MIL Component Model Summary Information 73
Table 11: Normalized Root Meet Square Error of SIL and MIL Model Platforms 76
Table 12: Strategic Operation Mode Definitions for Control Platform 89
Table 13: Drive-Cycle Strategy Tuning Variables for Optimization 101
Table 14: Fuel Energy Density Comparison 108
Table 15: 4-Cycle Mixed Relative Weightings 115
Table 16: Non-Optimized SIL Model Consumption Performance CD Mode 116
Table 17: Non-Optimized SIL Model Consumption Performance CS Mode 116
Table 18: Non-Optimized SIL Model Consumption Performance UF Weighted 116
Table 19: Non-Optimized SIL Model Consumption Performance CD Mode with Recursively-Defined Equivalency Factor 117
Table 20: Optimization Results by Drive Cycle with Equivalency Factor 1 118
Table 21: Lge/100km Consumption Performance of Simplified Model at Optimal Set-point Calibrations with Equivalency Factor 1 119
Table 22: Optimization Results by Drive Cycle with Recursive Equivalency Factor Calculation Applied 122
Table 23: Lge/100km Consumption Performance of Simplified Model at Optimal Set-point Calibrations with Recursive Equivalency Factor Calculation Applied 123

Table 24: Optimally-Calibrated Resultant Equivalency Factors 123

Table 25: Lge/100km Consumption Performance of SIL Model at Optimal Set-point Calibrations with Equivalency Factor 1 Applied..... 127

Table 26: Consumption Percent Difference between Simplified Model and SIL Model for Equivalency Factor 1..... 128

Table 27: Consumption Improvement over Benchmark Equivalency Factor 1 128

Table 28: Lge/100km Consumption Performance of SIL Model at Optimal Set-point Calibrations with Recursive Equivalency Factor Scheme..... 129

Table 29: Consumption Percent Difference between Simplified Model and SIL Model for Recursive Equivalency Factor Scheme..... 129

Table 30: Consumption Improvement over Benchmark Recursively-Defined Equivalency Factor..... 130

Table 31: MicroAutoBoxII VSU Interfacing..... 152

List of Figures

Figure 1: EcoCAR2 Development Process....2
Figure 2: UVic EcoCAR Vehicle Architecture....4
Figure 3: Strategy Independent Controls Concept....7
Figure 4: Conventional Vehicle Power Demand Control Constraints....9
Figure 5: HEV Power Demand Control Process....10
Figure 6: Degree of Hybridization....11
Figure 7: Utility Factor Plot Based on SAE J2841 and National Household Transportation Survey 2005....14
Figure 8: GM EcoTEC LE9 Engine Efficiency Plot....15
Figure 9: Comparison of ESS Types....18
Figure 10: PHEV and EV U.S. Sales....21
Figure 11: HEV U.S. Sales....21
Figure 12: 2013 Chevrolet Malibu Eco....22
Figure 13: Parallel Hybrid Architecture....23
Figure 14: Series Hybrid Architecture....24
Figure 15: Power-Split Hybrid Architecture....25
Figure 16: Series-Parallel Hybrid Architecture....26
Figure 17: Power Flow and Losses in Marine Powertrain Systems....28
Figure 18: Marine Powertrain System Architecture with Supplemental Power Sources....29
Figure 19: Canadian transportation SO_2 emissions in 2002 by vehicle type....31
Figure 20: Port Particulate Emission Composition....32
Figure 21: Simplified Powertrain Modelling Configuration....36
Figure 22: UVic EcoCAR Vehicle Component Layout....37
Figure 23: GM LE9 Engine....38
Figure 24: Transmission Upshift Curves....40
Figure 25: Transmission Downshift Curves....40
Figure 26: Magna E-Drive Integrated with Rear Sub-Frame....42
Figure 27: Magna E-Drive Efficiency Map....43

Figure 28: Magna E-Drive Maximum Torque Curve 44
Figure 29: TM4 Motive B 44
Figure 30: TM4 Belted Interface 45
Figure 31: TM4 Motor Maximum Torque Curve 46
Figure 32: TM4 Motor Efficiency Map 46
Figure 33: A123 6x15s3p Li-Ion ESS 47
Figure 34: A123 6x15s3p Open Cell Voltage Curve 48
Figure 35: A123 6x15s3p Cell Resistance Curve 48
Figure 36: EV Operation Power Path 53
Figure 37: Conventional Operation Power Path 54
Figure 38: BAS Hybrid Operation Power Path 54
Figure 39: Series-Parallel High Power Operation Power Path 55
Figure 40: Series Hybrid Operation Power Path 55
Figure 41: Controls Development V-Diagram 56
Figure 42: Controller Requirement Feedback 60
Figure 43: Process Flow from Algorithm Development to Automated Regression Test Platform Integration 62
Figure 44: Accelerator Pedal Example Test 63
Figure 45: Sample Test Case Document 66
Figure 46: SIL Platform Soft-ECU Interaction 70
Figure 47: SIL and MIL Model Comparison – ESS Energy Consumed 74
Figure 48: SIL and MIL Model Comparison – Fuel Consumed 75
Figure 49: SIL and MIL Model Comparison – ESS Current 75
Figure 50: SIL and MIL Model Comparison – Fuel Rate 75
Figure 51: SIL Platform Configuration 77
Figure 52: HIL Platform Configuration 77
Figure 53: Vehicle Glider Free Body Diagram 78
Figure 54: Control Logic Hierarchy Interactions 81
Figure 55: RTM De-rating Process Overheating 83
Figure 56: Driver Torque Distribution Safety Diagnostics 85
Figure 57: BAS Failure Simulated System Response 86
Figure 58: System Operation Status Diagnostics 87

Figure 59: Mode Switch Overrides 88
Figure 60: On-the-Fly ICE Start-Up Procedure 90
Figure 61: On-the-Fly ICE Start-Up Results 91
Figure 62: Gaussian Error Function versus Hyperbolic Tangent 92
Figure 63: AWD Series-Parallel to EV Transition Strategy Target Values 93
Figure 64: AWD Series-Parallel to EV Transition Output Values 93
Figure 65: EV to AWD Series-Parallel Transition Strategy Target Values 94
Figure 66: EV to AWD Series-Parallel Transition Output Values 94
Figure 67: Rule-Based Controller State Logic 96
Figure 68: Uncorrected System Torque Response Map 97
Figure 69: Corrected System Torque Response Map 98
Figure 70: Vehicle Creep Torque Curve 98
Figure 71: ICE Minimum Torque Application Multiplier 99
Figure 72: Mode Switch Criteria Timer Delays Operation 102
Figure 73: BAS-ICE Interface Mechanical Failure at Engine Crankshaft 103
Figure 74: Broken Crankshaft Snout and Sheared Key 103
Figure 75: US06 City Drive Cycle 111
Figure 76: US06 City Speed Distribution 111
Figure 77: US06 City Acceleration Distribution 112
Figure 78: US06 Highway Drive Cycle 112
Figure 79: US06 Highway Speed Distribution 112
Figure 80: US06 Highway Acceleration Distribution 113
Figure 81: HWFET Drive Cycle 113
Figure 82: HWFET Speed Distribution 113
Figure 83: HWFET Acceleration Distribution 114
Figure 84: FU505 Drive Cycle 114
Figure 85: FU505 Speed Distribution 114
Figure 86: FU505 Acceleration Distribution 115
Figure 87: US06 Highway BAS Charge Sustain Algorithm Tuning Variable Optimization Equivalence Factor Sensitivity 120
Figure 88: US06 Highway Engine Torque Tuning Variable Optimization Equivalence Factor Sensitivity 120

Figure 89: Recursive Equivalency Factor Scheme 121
Figure 90: Equivalency Factor 1 4-Cycle Optimization Parallel Axis Plot 124
Figure 91: Linear Relationship between Fuel Consumption and Minimum ICE Torque 125
Figure 92: Recursive Equivalency Factor 4-Cycle Optimization Parallel Axis Plot 126
Figure 93: Recursive Equivalency Factor 4-Cycle High Consumption Filtered Data Set 126
Figure 94: Overall Vehicle Behaviour over US06 City Cycle 131
Figure 95: Vehicle Acceleration and Hybrid Mode Transitions over US06 City Cycle 131
Figure 96: ICE Operation over US06 City Cycle 132
Figure 97: RTM Operation over US06 City Cycle 132
Figure 98: BAS Operation over US06 City Cycle 133
Figure 99: Hybrid Mode Selection over US06 City Cycle 134
Figure 100: Driver Operation Validation US06 City Cycle 134
Figure 101: Overall Vehicle Behaviour over HWFET Cycle 135
Figure 102: Vehicle Acceleration and Hybrid Mode Transitions over HWFET Cycle 136
Figure 103: ICE Operation over HWFET Cycle 136
Figure 104: RTM Operation over HWFET Cycle 137
Figure 105: BAS Operation over HWFET Cycle 137
Figure 106: Hybrid Mode Selection over HWFET Cycle 138
Figure 107: Driver Operation Validation HWFET Cycle 138
Figure 108: Vehicle CAN Architecture 154
Figure 109: Vehicle Control System Connections 154
Figure 110: Transmission Gear Bounce Scenario 155
Figure 111: Transmission Ratio Estimator Curve 156
Figure 112: Engine Torque Target Increase Results in No Bounce Acceleration 157

List of Abbreviations

AC	Alternating Current
APM	Auxiliary Power Module
ANL	Argonne National Laboratory
ASM	Automotive Simulation Model (dSPACE)
AVTC	Advanced Vehicle Technology Competition
AWD	All-Wheel-Drive
BAS	Belted Alternator Starter
CO	Carbon Monoxide
CO_2	Carbon Dioxide
CD	Charge Deplete
CS	Charge Sustain
cVT	Continuously Variable Transmission
DC	Direct Current
DFMEA	Design Failure Mode Effects Analysis
DOE	United States Department of Energy
DOF	Degrees of Freedom
EC	Energy Consumption
ECA	Emission Controlled Areas
ECM	Engine Control Module
ECU	Electronic Control Unit
EF	(Fuel-Electricity Energy Consumption) Equivalency Factor
EPA	Environmental Protection Agency

EPO	“emergency power off” (controls flag)
EREV	Extended Range Electric Vehicle
ESS	(Battery) Energy Storage System
EV	Electric Vehicle
FWD	Front-Wheel Drive
GA	Genetic Algorithm
GHG	Greenhouse Gas (Emissions)
GM	General Motors
HIL	Hardware-in-Loop
HEV	Hybrid Electric Vehicle
HV	High Voltage
HWFET	Highway Fuel Economy Driving Schedule
ICE	Internal Combustion Engine
IMO	International Maritime Organization
I/O	Inputs and Outputs (interfacing)
Li-Ion	Lithium Ion
MG	Motor/Generator
MBD	Model-Based-Design
MIL	Model-in-Loop
Ni-MH	Nickel Metal Hydride
NO_x	Nitrous Oxides
NVH	Noise Vibration and Harshness
OCV	Open Cell Voltage
PM	Permanent Magnet
PEU	Petroleum Energy Use

PHEV	Plug-in Hybrid Electric Vehicle
PRNDL	Automatic transmission shift selection lever
RTM	Rear Traction Motor
R&D	Research and Development
RSG	“ready, set, go” (controls flag)
SAE	Society of Automotive Engineers
SIL	Software-in-Loop
SLA	Sealed Lead Acid
SOC	State of Charge
SO_2	Sulphur Dioxide
TCM	Transmission Control Module
TtR	Through-the-Road (parallel architecture)
UDDS	Urban Dynamometer Driving Schedule
UF	Utility Factor
VDP	(General Motors) Vehicle Development Process
VFD	Variable Frequency Drive
VOC	Volatile Organic Compounds
VTS	Vehicle Technical Specifications
VSU	Vehicle Supervisory Controller
WTW	Wheel-to-Well

Acknowledgments

Given the team-based nature of the EcoCAR2 competition, many individuals had a role in the development of enabling works used within the work presented. The development of the UVic PHEV vehicle was a significant team effort which included mechanical design, component fabrication, electrical design, vehicle wiring, component testing, vehicle troubleshooting, and team management, and the entire extended team is credited with this process. Of specific note is the work developed by Stefan Kaban and David Killy in Year 1 of the competition, which laid the developmental framework and basic model structure used in the ongoing development of the vehicle control system and Software-in-Loop (SIL) simulation platform. Also, Rui Cheng and Jackie Dong were responsible for early development and algorithm testing of a rule-based control strategy for the UVic vehicle architecture which served as an initial basis for the development of the rule-based control strategy presented. Finally, the vehicle development project in general would not have been possible without the efforts of the UVic EcoCAR2 team faculty advisors, Dr. Zuomin Dong, and Dr. Curran Crawford, who both provided mentorship, development guidance, and research funding to complete the design implementation.

Dedication

I dedicate my Master's thesis work to my family and my friends who have worked on this project with me along the way. I am thankful for the technical help, moral support, and willingness to toil together in solidarity displayed by all my friends and acquaintances that have also had a hand in the greater project and research endeavours associated with my work. I am also grateful for the encouraging support granted by my parents, who watched me leave a perfectly good, secure, well-paying job without putting forward too much criticism. Finally, I wish to send a very special thanks to my wife, Robyn, who supported my interest in pursuing this work despite the requisite long-distance relationship that it would necessitate. You have selflessly supported me in my endeavours, all the while pursuing your own educational goals, and words cannot express my gratitude for your understanding throughout this entire process. You have been my compass in times of disillusionment, my confidante in times of frustration, and my cheerleader in times of success. Thank you.

Chapter 1: Introduction

Modern Hybrid Electric Vehicles (HEVs) are increasingly employing more complex architectures with more sophisticated underlying system controls. With advancements in vehicle powertrain component technology and reduction of prices associated with higher volume productions, advanced architectures with more system degrees of freedom (DOF) are becoming possible, with greater potential to beneficially employ real-time optimization schemes and global optimization tuning. Each additional system DOF dramatically increases the control system development burden, as robust and safety-critical systems require extensive testing of cross interactions between all independently-controlled components and subsystem functionality within the vehicle control system. Additionally, this increased flexibility complicates driveability considerations which must be incorporated into the development process. Controls development in industry uses iterative testing and validation procedures to arrive at a robust system deployment. This includes the tight integration of energy management strategies with underlying system control. For the purposes of deploying advanced strategies developed through academic research, a system which can be developed and validated using a given energy management strategy and then safely and robustly interface with newly developed advanced strategies is highly beneficial. With a high DOF architecture, this can provide for a long term test platform for advanced HEV control strategy validation. This goal requires an approach that allows for parallel development of controls implementation details and energy management strategies.

1.1.EcoCAR2 Student Competition

EcoCAR2: Plugging into the Future was a 3-year university student competition which ran between 2011 and 2014. The program was sponsored by the U.S. Department of Energy (DOE) and administered by Argonne National Laboratory (ANL), and is part of a longer series of Advanced Vehicle Technology Competitions (AVTCs). The competition was sponsored by a multitude of automotive industry sponsors, including General Motors (GM), dSPACE, MathWorks, among others. AVTCs enable unique research

collaboration between government, industry, and university academic departments, with a focus on sustainable vehicle solutions.

EcoCAR2 had an overarching goal of reducing the overall environmental impact of a vehicle while maintaining consumer safety, performance, and comfort standards demanded by the domestic auto market. Each team integrated a custom developed plug-in hybrid electric vehicle (PHEV) powertrain into a 2013 Chevrolet Malibu. Vehicles were evaluated across multiple metrics in controlled test situations including fuel consumption, Wheel-To-Well (WTW) emissions, criteria emissions, total energy consumption, acceleration, braking, dynamic handling, ride comfort, Noise Vibration and Harshness (NVH) characteristics, and static consumer acceptability.

The vehicle development process was intended to simulate the GM Vehicle Development Process (VDP) for advanced technology implementation. Development was broken into 3 streams (mechanical, electrical, controls) with the yearly plan objectives as follows:

- **Year 1:** concept design and performance estimation modelling
- **Year 2:** vehicle construction and model refinement
- **Year 3:** vehicle refinement, controls optimization and robustness *improvements*

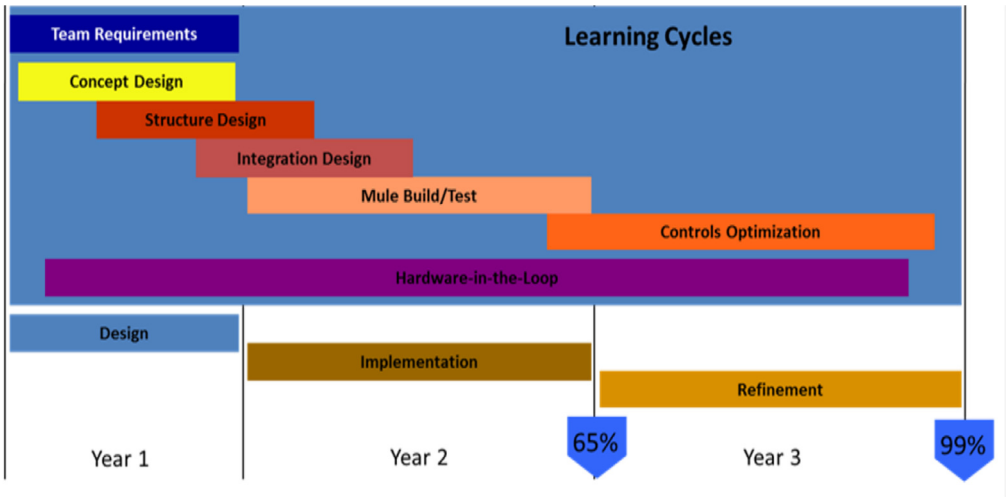

Figure 1: EcoCAR2 Development Process

(Image courtesy of EcoCAR2 Competition[1])

Access to the advanced technologies provided by the competition sponsors, including dSPACE, MathWorks, Siemens, GM, Magna E-Car, among others, has allowed the UVic Hybrid Powertrain Research Group led by Dr. Zuomin Dong to conduct novel and compelling research with industry-relevant objectives. The availability of advanced toolsets and hardware has allowed for the development of real-time powertrain optimization techniques, component degradation models, powertrain global optimization techniques, and advanced modeling activities. Associated research at UVic is being conducted in areas outside of the consumer automotive sector, including heavy transport, light rail, and marine transport applications. The modeling and controls development techniques being researched have particular application to these fields as existing motor and ESS technologies are employed in new ways to provide hybrid powertrain functionality.

1.2.Overview of Vehicle Architecture

The UVic EcoCAR2 vehicle architecture uses an advanced configuration to produce multiple-regime series-parallel All-Wheel-Drive (AWD) PHEV functionality. The vehicle components and energy transfer paths are displayed in Figure 2.

This powertrain configuration provides many substantial improvements over the production 2013 Malibu. These are accomplished by virtue of the tremendous operational flexibility the architecture is capable of providing. A Magna E-Drive motor and transaxle gearbox unit serves as the Rear Traction Motor (RTM) for the vehicle, providing electric only capability. It also allows for AWD functionality during engine-on operation. The front wheels are powered by a GM LE9 4-cylinder Internal Combustion Engine (ICE) and TM4 MotiveB Belted Alternator Starter (BAS) motor/generator (MG). The BAS torque can thus be used to manipulate the operating characteristics of the ICE irrespective of vehicle load demand, allowing for high overall system efficiency in Charge Sustain (CS) operation. Electric power and resulting Charge Deplete (CD) range is supplied with a donated A123 6s 15s3p Lithium Ion (Li-Ion) Energy Storage System (ESS). In addition to efficiency gains associated with the architecture, the addition of 2 high power electric motors to the vehicle allows for substantial improvements to the acceleration performance compared to the stock vehicle, despite significant mass addition.

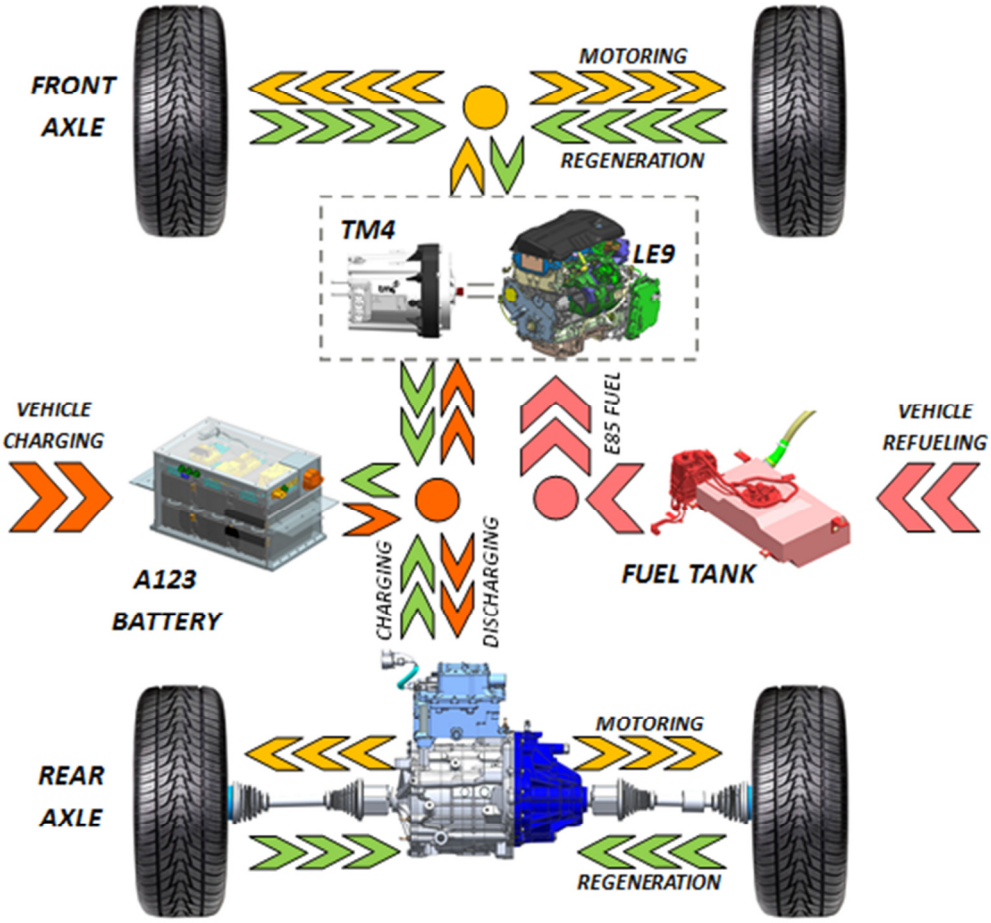

Figure 2: UVic EcoCAR Vehicle Architecture

1.3. Considerations for Control Development for Selected Architecture

The Series-Parallel PHEV architecture developed by the UVic EcoCAR2 team is a complex platform for developing robust controls. Complications in the development process are due to the constraints of various components and the complexity of developing a control system that allows the various drive systems to work together in tandem.

1.3.1. Connection to Existing Research

The UVic EcoCAR2 architecture was originally conceived as an ideal platform to conduct research and development (R&D) in hybrid powertrain optimization techniques, building off of previous work completed within the department. Early work at UVic,

associated with the EcoCAR: The NeXt Challenge, focussed on real-time optimization of an advanced PHEV employing the GM Two-Mode hybrid transmission. A novel application of equivalent consumption minimization strategy using two degrees of freedom was developed by *Wise* and evaluated in simulation during year one of the competition[2]. Subsequent implementation and in-vehicle testing of the vehicle control system by *Waldner* produced results which suggest that components of the real-time optimization routine related to torque split between the RTM and 2-Mode ICE assembly could suitably be replaced by an optimized rule-based strategy to equivalent effect[3]. Additionally, in-vehicle testing demonstrated a lack of operating point stability in the vehicle resulting in a large number of hybrid mode changes[3]. In both cases, the goal was optimization of fuel consumption while maintaining minimum performance and driveability constraints.

The UVic EcoCAR2 PHEV architecture allows for similar operational flexibility to the EcoCAR1 Two-Mode PHEV, but without the operational complications arising from controlling the GM Two-Mode hybrid transmission, as discussed by *Wise*[2]. The system allows for three degrees of freedom (DOFs): ICE torque, RTM torque, and BAS torque. Development of explicit transmission gear selection via the manumatic transmission functionality would add a fourth DOF. When the transmission is set to neutral, the ICE and BAS speeds also become unconstrained. This operational flexibility is the key feature of the architecture. The original architecture conceptualization anticipated the use of multiple operating regimes in controlling the vehicle.

Recent work at UVic has been focussed on understanding of how to constrain the system operation for maximum vehicle efficiency. A backwards-looking model was developed by *Kaban* to facilitate use of dynamic programming theory to arrive at optimal component torque inputs for a given drive cycle[4]. The output was framed in terms of several defined operating regimes. While these results are useful for understanding ideal operation of the given architecture, the resultant component inputs are deterministic in nature and not directly useful for in-vehicle control. The dynamic programming results developed by *Kaban* thus provide a useful roadmap for the development of control logic for the UVic PHEV architecture[4].

1.3.2. Driveability Challenges of Controlling Selected Architecture

A balance must be achieved between seeking maximum vehicle efficiency and maintaining driveability characteristics. Frequent mode switches, if poorly executed, will cause intermittence and inconsistencies in vehicle acceleration response and driver feedback. Developing the vehicle controller to allow consistent and frequent mode switches irrespective of instantaneous driving conditions is a major challenge with implementing the control system. Mode switches that involve a transfer of torque between front and rear axles add another design consideration, as any abrupt torque transfer could result in traction instability and driver startle leading to a motor vehicle accident.

The front drive components, the ICE and BAS, are coupled to the wheels through the automatic transmission, while the RTM is coupled to the wheels via a fixed transaxle gearbox. While the torque limitations of the RTM are well defined based on instantaneous vehicle speed, the torque limitations of the front drive components step in response to the transmission gearing. As the torque at the wheels defines the vehicle acceleration response to driver torque requests, the inconsistent gear ratios between front and rear propulsion systems further complicates the controls development. The automatic transmission, as implemented within the UVic PHEV, does not allow for explicit selection of the front gear ratios, which adds some unpredictability to the drive ratio of the ICE and BAS.

Another factor complicating mode switching is the periodic requirement for on-the-fly ICE start-up events. This occurs when the vehicle must transition from driving off the RTM to deriving propulsion power from the ICE. In order for this event to occur smoothly and predictably, the procedure needs to be designed into the transition between all affected modes. This includes a requisite time delay for ICE start-up and road rev-matching for enhanced driveability. Commercialized vehicles are able to employ crankshaft position control to streamline hybrid ICE start-up processes by stopping the ICE rotation at a cycle position which allows starting to be aided by direct fuel injection combustion. These techniques are outside of the scope of the UVic vehicle integration plan due to the highly detailed ICE-specific control required to realize such functionality.

1.4.Controls Implementation Platform and Development Process

A strategy-independent controls platform foundation is beneficial for highly-flexible advanced powertrain configurations such as the UVic EcoCAR2 PHEV architecture, as it allows for the delineation of strategy optimization and vehicle controls development, while providing flexibility for future improvements.

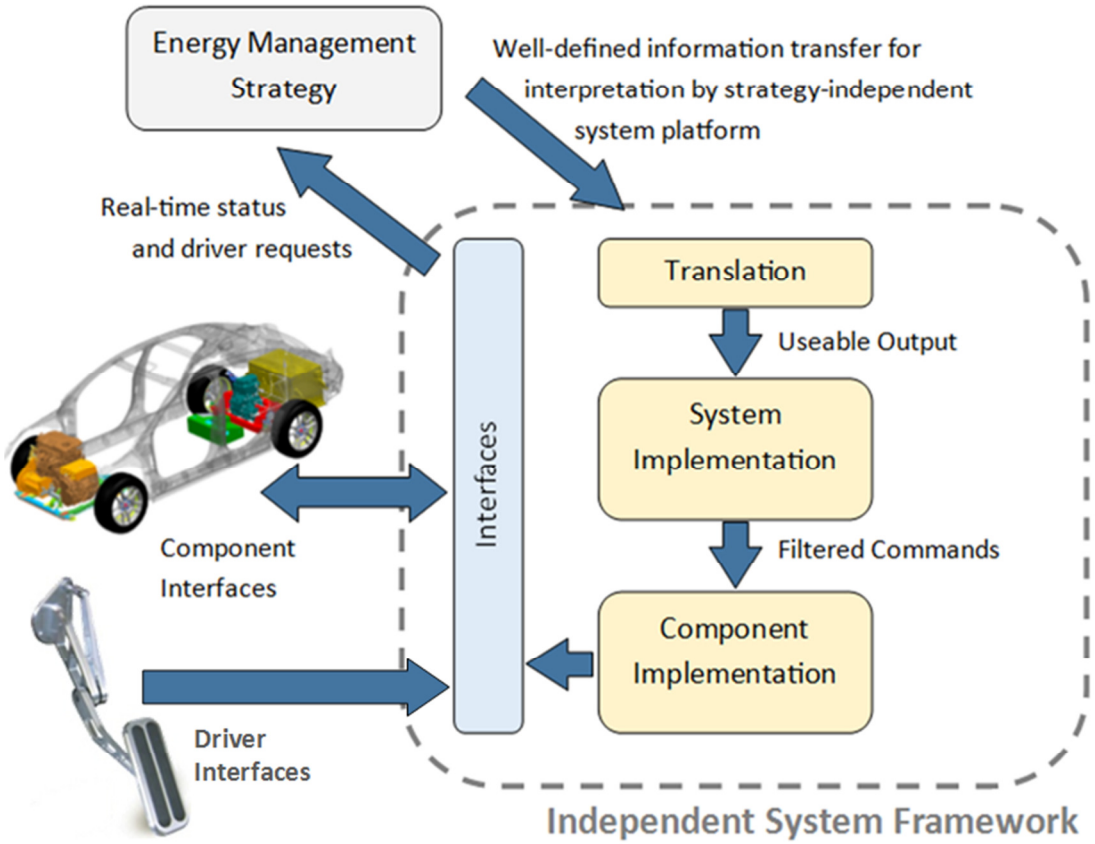

Figure 3: Strategy Independent Controls Concept

A strategy-independent controls platform as shown in Figure 3 was developed for the UVic EcoCAR2 PHEV architecture. System constraints and driveability limitations were extracted from the core strategy and implemented as a system of overrides and additive torque management algorithms ensuring robust operation. These algorithms form the upper logic hierarchy of the overall vehicle control system platform, which was developed within a Model-Based-Design (MBD) framework. This allowed for the separate development and global optimization of a modular rule-based energy

management strategy within a simplified modeling environment. The energy management strategy is limited to determining ideal torque set-points for each component. When the foundation controls platform reached operational maturity and was tested within the vehicle on-road, the strategy was extracted from the simplified model platform and placed on top of the vehicle control system platform and assessed for performance carry-through. This approach was used for the purposes of achieving two primary benefits:

- The delineation of control strategy optimization and functional controls development was beneficial for meeting the aggressive development timeline targets of the EcoCAR2 competition.

- The platform will allow for future control strategies developed at UVic to be applied within the vehicle and high fidelity development model for validation. This provides more meaningful validation compared to using a simplified model and helps to support long-term powertrain optimization research at UVic.

The following Chapters document in detail the developments described above. Chapter 2 provides a review of HEV technology and clarification on the different possible HEV architectures, as well as possible tie-ins with marine hybrid development. Chapter 3 provides details about the UVic PHEV architecture, modeling platforms used, and MBD controls development process. Chapter 4 documents the rule-based energy management strategy that was developed for use within the vehicle. Chapter 5 documents the optimization of the rule-based strategy and provides assessment of the carry-through of performance between the two development platforms. The results are summarized in Chapter 6, and future research development is proposed.

Chapter 2: Introduction to Hybrid Powertrain Technology

2.1. The Benefit of Hybrid Powertrain Technology

In a conventional internal combustion vehicle, tractive power is derived solely from the ICE, which is attached to the vehicle's drive wheels via one of several mechanical transmission configurations which exist in typical vehicle applications today: automatic transmission with torque converter, manual transmission with driver-operated clutch mechanism, or Continuously Variable Transmission (cVT). In all cases, power is requested by the driver, and that power must be instantaneously supplied by the ICE. This process is illustrated in Figure 4, and results in overall system efficiency that is constrained by the operational efficiency of the ICE, with the only system level manipulation possible being the selection of gear ratio at the transmission.

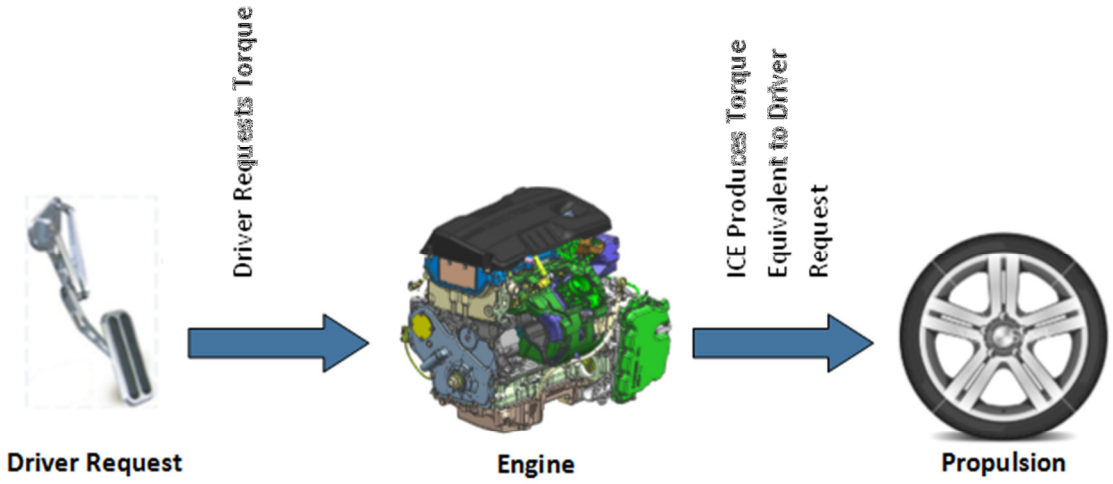

Figure 4: Conventional Vehicle Power Demand Control Constraints

In a HEV, the addition of an ESS and one or more MGs allows for additional system controllability. The end result is that the ICE is no longer constrained in needing to produce precisely the instantaneous power demand of the user, allowing for more system operational flexibility, and higher net efficiency. The resulting system control process is illustrated in Figure 5.

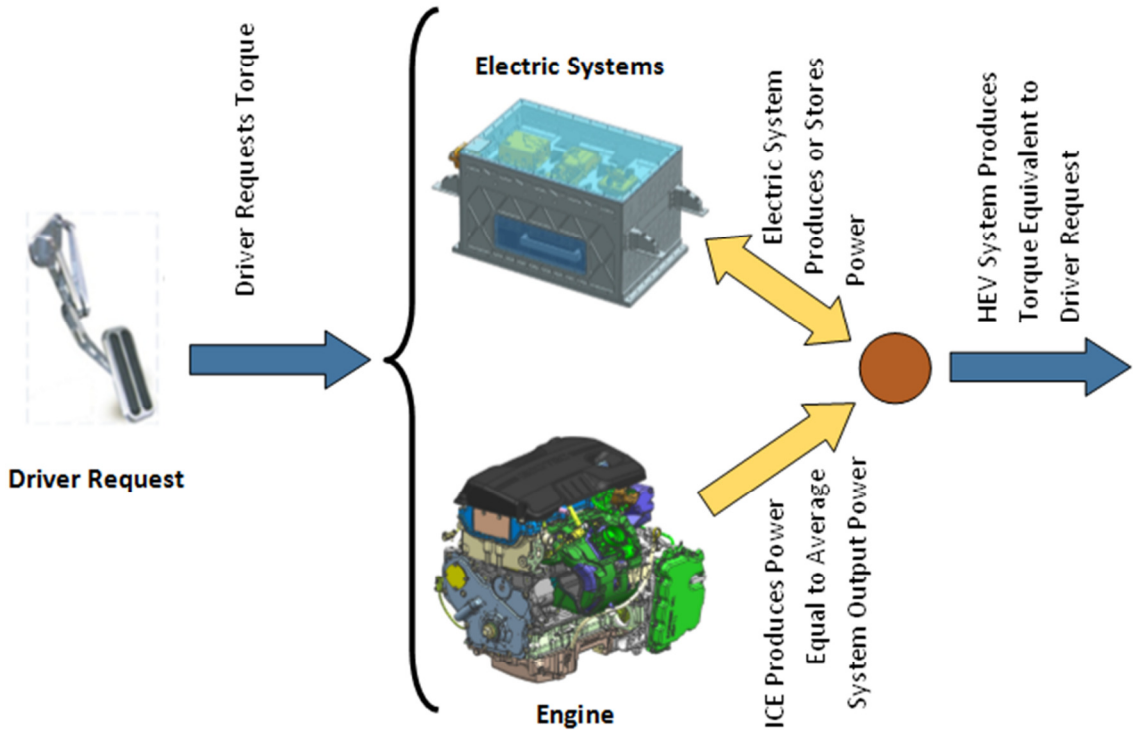

Figure 5: HEV Power Demand Control Process

Many different hybrid architectures exist, with varying levels of hybridization. The degree of hybridization is described by *Capata and Coccia* as the ratio of power capacity supplied by the electric vehicle propulsion systems versus the ICE [5]. Figure 6 shows the relative importance of MG and ICE sub-components in a vehicle architecture based on the degree of hybridization [6].

It is important to note that although HEV powertrain technology is trending towards higher degrees of hybridization, advanced modern powertrains with optimal operational efficiency do not necessarily imply a largely electric propulsion source (high degree of hybridization). Indeed, many newer vehicle entrants in the consumer vehicle market have been on the mild hybrid end of the hybridization spectrum, with relative fuel savings in the order of 10-15% [7].

High degrees of hybridization and the associated high power electrical powertrain subsystems can allow for additional functionality, including full Electric Vehicle (EV) capability and PHEV functionality with CD and CS operational regimes.

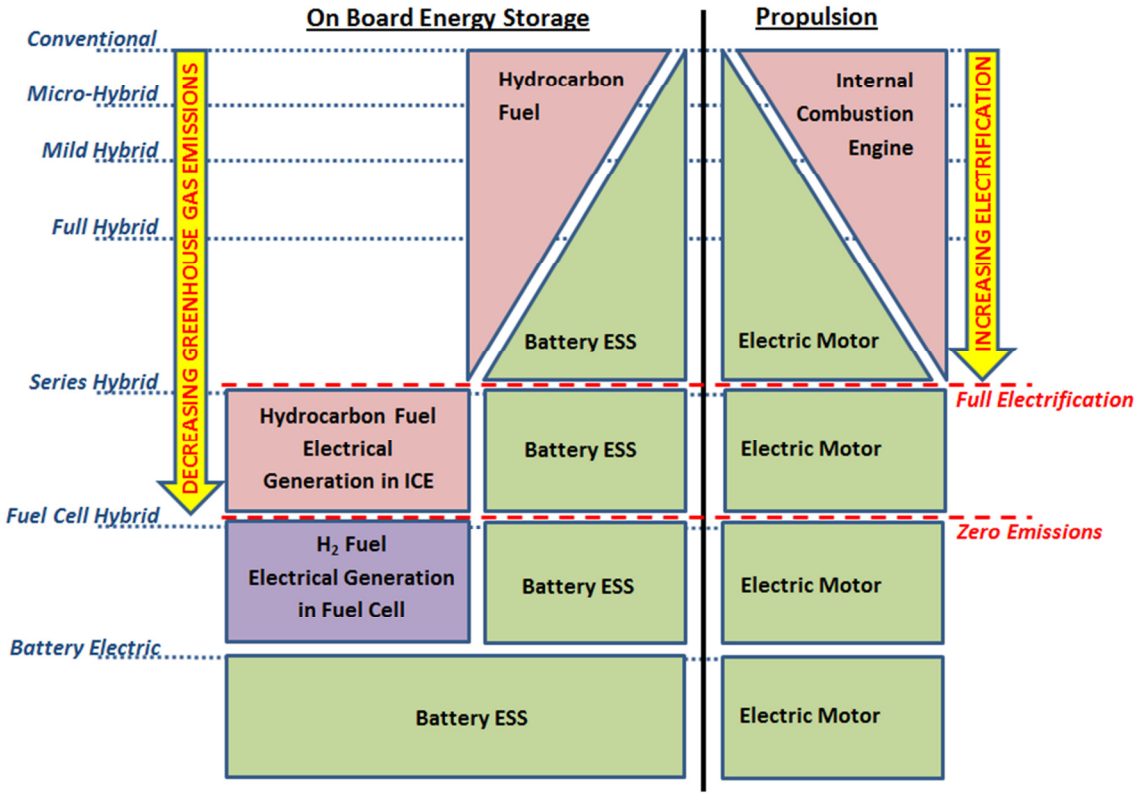

Figure 6: Degree of Hybridization

(Adapted image concept from greencarcongress.com[6])

2.1.1.A Brief History of Hybrid Electric Vehicles

The history of HEV development reaches back much further than more recent commercialized development, but was preceded significantly by early EV development. Full EVs were developed much earlier than the first ICE-driven vehicles, with the first recorded EV being constructed by Robert Andersen of Aberdeen, Scotland in 1839[8]. Kinetic engine vehicle development continued for the rest of the 19th century, with heavy focus on steam cycle engines, while EVs were employed for various urban commercial purposes. The first HEV followed as a series hybrid developed by Dr. Ferdinand Porsche in 1898. The vehicle was a second revision of Dr. Porsche's Lohner Electric Chaise. It

used an ICE to turn a generator and power wheel hub motors and could achieve an electric range of 40 miles[8, 9].

In 1900, a Belgian company, Pieper developed a patent for an early primitive parallel HEV. The design used a lower power gasoline ICE coaxially-coupled to an electric motor. Together the two drive components propelled the vehicle, with the motor charging the batteries during low power operation, and the motor assisting the ICE during high power operation[8].

In the early 1900's, advancements by the Ford Motor Company allowed for the low cost production of gasoline ICE powered vehicles. Additionally, advancements in ICE reliability, noise, vibration balancing, and the development of starter motor systems allowed widespread uptake of ICE vehicle and the formation of the modern automotive industry. Consequently, the mid-20th century was a relatively quiet period for HEV development[8].

The late-20th century saw isolated concept vehicle development employing HEV technologies. Emphasis was on the development of high fuel efficiency concepts, with limited speed and power. The 1970's oil crisis sparked new industrial and governmental interest in viable consumer EV technology. In 1991, the D.O.E. launched an industry collaboration program called the United States Advanced Battery Consortium (USABC) to produce viable EV battery technology[8].

In 1997, Toyota introduced the first generation Prius within the Japanese market which produced first year sales of close to 18,000 vehicles. This represented the first large-scale consumer sale of HEV technology. In 1999, the Honda Insight was released in the North American market, with the North American Prius following in 2000. Since these first consumer releases, consumer HEV development has become widespread and diverse, spanning vehicle classifications and varying HEV architectures. Modern HEV technology initiatives include the incorporation of plug-in capabilities, furthering the industry along the path to electrification. Ongoing PHEV development seeks to provide a counterpart path to EV development, both combining to address the diverse transportation needs of motorists while reducing environmental impact of driving[8].

2.1.2. Powertrain Electrification

Increasing the degree of electrification of a vehicle powertrain to the extent at which the electric systems provide a substantial component of the vehicle's drive system has inherent efficiency benefits, as well as functional use benefits. Modern EV propulsion system components have significantly higher energy use efficiencies than modern ICE technology. While the thermal efficiency of the modern direct-injection ICE is limited to approximately 25-30%[10], electric powertrains can produce efficiencies as high as 80%[11]. The operational efficiency of EV systems is further augmented by the ability to recapture energy through regenerative braking which has been shown *by Clegg* to reduce and EV fuel consumption over a drive cycle by up to 23% for a 1600 kg passenger sedan[12].

When a vehicle has some level of CD EV operability, overall fuel usage and emissions are reduced in practice since a portion of the cycle is completed with zero fuel usage. On average, Americans drive 61 km per day[13]. As a result, limited EV range effectively offsets some of the petroleum use and emissions associated with an average day of driving. This is based off the assumption that users will typically fully charge the ESS of their vehicles each day at the end of the drive cycle use. Thus, in an Extended Range Electric Vehicle (EREV), there are two components of energy use and emissions which need to be accounted for and numerically balanced for the CD and CS operation regimes respectively. A Society of Automotive Engineers (SAE) standard method (SAE J2841) for objectively and numerically quantifying this is the Utility Factor (UF)[14].

The UF is a weighting factor for computing weighted average energy consumption, emissions, Petroleum Energy Use (PEU) based on a given drive cycle. The EcoCAR2 competition thus provided numerical tuning (National Household Travel Survey, 2005) for the UF as follows[1]:

$$UF = 1 - e^{-\left[c_1*\left(\frac{x}{D_{norm}}\right)+c_2*\left(\frac{x}{D_{norm}}\right)^2+\cdots+c_6*\left(\frac{x}{D_{norm}}\right)^6\right]} \quad (1)$$

$$D_{norm} = 399.9$$

$$c_1 = 10.52, c_2 = -7.282, c_3 = -26.37, c_4 = 79.08, c_5 = -77.36, c_6 = 26.07$$

where x is the EV range in miles. The UF curve plotted against EV range in miles is shown in Figure **7**. Note that the curve describes diminishing benefit of additional EV range. This captures the fact that many users will not see additional benefit, as their daily driving is satisfied with purely EV operation at a relatively low range. The curve moves towards unity more slowly at higher range capabilities, reflecting the fact that there are always use patterns which exceed the EV range such as long day trips.

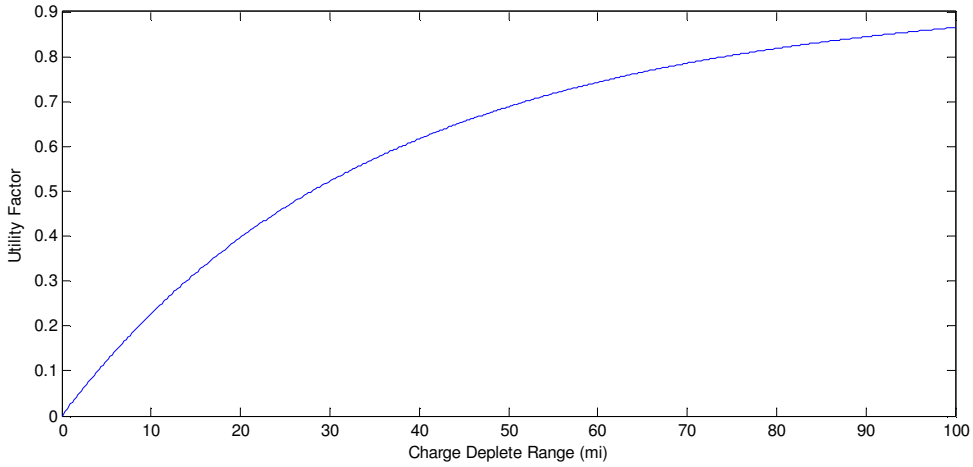

Figure 7: Utility Factor Plot Based on SAE J2841 and National Household Transportation Survey 2005

(Plotted curve courtesy of EcoCAR2 Competition[1])

Effective EREV Energy Consumption (EC) can thus be calculated from the individual CD and CS values for a given drive cycle as follows[1]:

$$EC = EC_{CD} * UF + EC_{CS} * (1 - UF) \quad (2)$$

Any aggregate quantitative performance metric which varies from CD to CS operation may be calculated as a weighted overall average using this methodology. As efficiency tends to be higher during CD regimes in a HEV, the resultant operational efficiency for typical use conditions improves through consideration of the effects represented by the UF calculation methodology.

2.1.3. Manipulating Engine Operating Point

The instantaneous constraint of a conventional ICE-driven powertrain needing to supply all of the user torque demand from the ICE alone is a major source of system operational inefficiency. Figure 8 shows the efficiency map against ICE speed and torque production for a GM EcoTEC LE9 ICE[15]. It can be seen that operational efficiency is lowest in the low torque regions of operation.

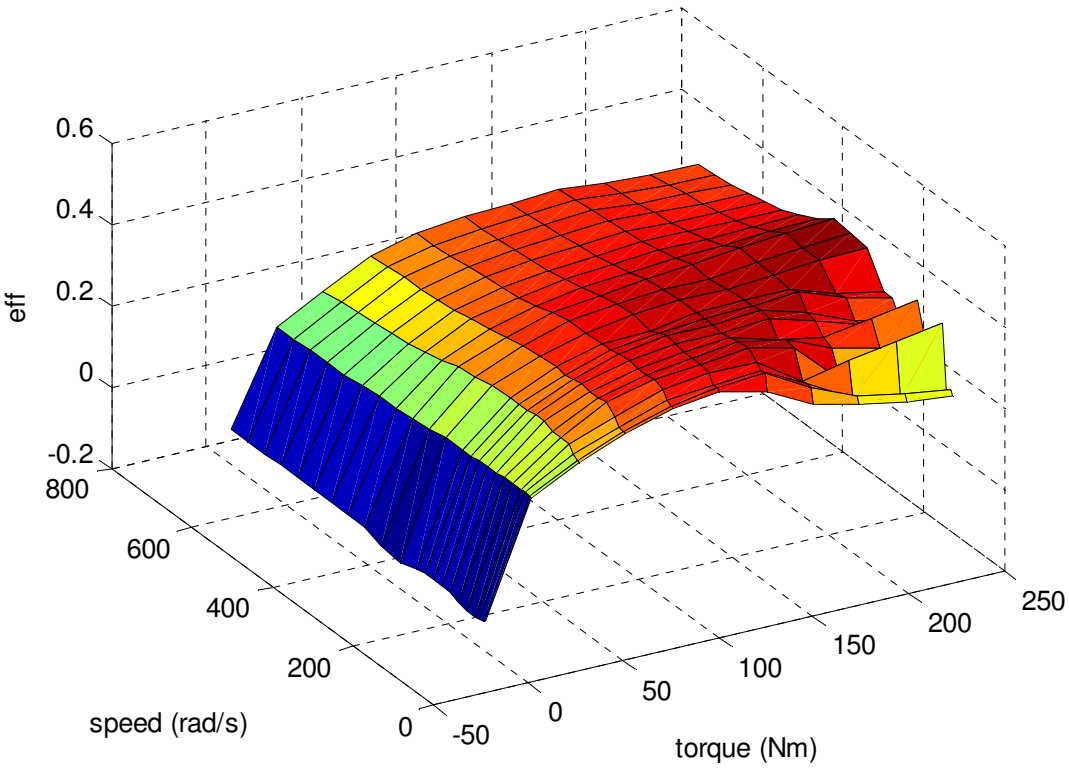

Figure 8: GM EcoTEC LE9 Engine Efficiency Plot

(Data extracted from Autonomie courtesy of EcoCAR2 team[15])

User torque demand while driving at constant speeds in the city, and to a lesser extent on the highway, are typically low in comparison to ICE output capacity. The ICE is sized this way to allow for surplus power for hill-climbing and reasonable acceleration performance. As a result, the ICE is often forced to operate in this lower efficiency region. Another region of comparative inefficiency can be seen in the lower speed but very high torque area of the map.

With the introduction of a hybrid ESS, power demand and ICE power production can be effectively decoupled to an extent which is limited by the electric hybrid system power capacity. As a result, the ICE operation point can be biased towards the ideal operation range of the efficiency map to increase aggregate efficiency over a drive cycle. This operation must obviously be balanced against system-level factors such as ESS State of Charge (SOC), system component temperature, driveability constraints, and emissions production.

2.2.Major Enabling Technologies

The past 15 years have been accompanied by the mainstream production of various key powertrain components required to realize advanced HEV architectures. Physically, previously limiting hardware includes high power density motors as well as high energy density ESS. The mainstream production of mild HEVs and more recently PHEV and EREV vehicle architectures has pushed these component technologies to be developed to a point of mass-market feasibility. In addition, development processes using MBD allow for rapid development of advanced control strategies and optimization schemes for controlling complex HEV architectures.

2.2.1. High Power Density Traction Motors

MGs provide an alternative power source for vehicle drive systems, converting electrical energy into kinetic energy at the output shaft which may be used for propulsion. There are many varieties of MGs available today, including alternating current (AC) MG, synchronous MG, direct current (DC) MG, and permanent magnet (PM) MG. The drive types which are best suited, and most readily applied to consumer automotive vehicles are AC induction motors, and PM motors (DC brushless motors)[16].

PM motors employ rare earth magnets on the rotor to develop a rotating magnetic field and improving the power density by eliminating a set of electromagnets. Wire coils on the stator are used to develop a leading rotating magnetic field through high speed switching of polarities to develop torque at the rotor, creating an inside-out functional representation of the traditional DC split-commutator motor[17]. The ESS powers the

motor through a 3-phase inverter which provides the switching mechanism which controls the motor speed and torque.

Induction motors are similar in construction to PM motors, with the main difference being the design of the rotor[16]. Instead of magnets, the induction motor rotor contains only a series laminated steel cage structure, sometimes referred to as a squirrel cage. The stator is constructed with phase offset electromagnet windings which reverse polarity in rotating sequence. The rotating electric field in the stator generates a counteracting inductance current within the rotor windings which is proportional to the rotational speed differential between the rotating electric field of the stator and the physical rotation of the rotor. This in turn develops lagging magnetic fields which reacts to the stator fields to produce drive torque, which at zero stator-rotor offset would be equal to zero[17]. The speed of induction motors are defined by the frequency of the AC current powering the motor stator, which is defined by a counterpart inverter converting DC ESS power to AC[16].

While both PM and induction MGs are suitable technologies to apply to HEVs, the PM motor dominates the HEV market today. Induction machines have been used in limited full EV applications including the GM EV-1 and Tesla Roadster[16]. PM MGs are favourable because of their high power densities and slightly higher efficiencies when compared to induction machines. The higher efficiency is derived by the ability of the PM MG to operate at power factors approaching unity[16, 17]. In contrast, induction machines can be more efficient in special high performance vehicles with larger motors since the rotor magnetic field strength can be varied when at part load (PM motor rotor fields are fixed by the permanent magnet properties) which reduces hysteresis losses.

2.2.2.Battery Energy Storage Systems

The ESS forms the central functional component for HEV propulsion. At present there are three types of widely-produced battery chemistries: sealed lead acid (SLA), nickel metal hydride (Ni-MH) and Li-ion batteries. Following the same order are improved performance and energy density, but increased cost. Another energy storage method is ultra-capacitors, which have the benefit of very high power density and cycle-ability with

the drawback of significantly reduced energy density. Comparative functional relationship of these ESS options is shown in Figure 9[18].

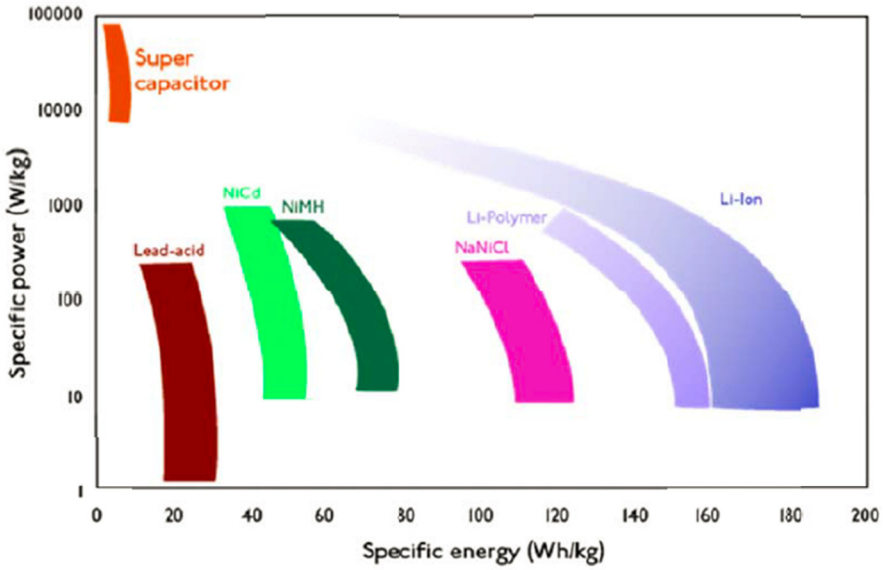

Figure 9: Comparison of ESS Types

(Image sourced from works by Omar et al.[18])

SLA batteries are the most common battery being used in heavy duty applications, mainly due to the low energy unit cost. Additionally, this battery chemistry provides robust operation with great physical cell durability when properly protected. Problems with the SLA battery include low power and energy density and potential environmental impact, where the lead electrodes and electrolyte can cause environmental harm if not disposed properly at a recycling facility. SLA batteries have a limited cycle time (200 cycles for deep discharge), shorter calendar time (4-6 years) and require some level of maintenance[19].

Ni-MH is widely used in HEVs, including the Toyota Prius. The Ni-MH battery has approximately twice the energy density of the SLA battery, allowing for lower overall ESS mass and also demonstrates much longer cycle life. It is also relatively environmentally friendly, as it contains very mild toxic materials that can be easily recycled. The main problems with the Ni-MH battery pack is its higher cost and longer charge time compared to a SLA. Challenges exist with charging due to large heat

production over a charge cycle. Determining exact SOC is also more challenging, requiring the use of more complicated and more expensive chargers.

Li-ion batteries represent the primary battery chemistry used in EVs, including the Nissan Leaf, Chevrolet Spark EV, and Tesla Model S. The batteries are particularly well suited for EV applications due to the high specific energy (150 Wh/kg) and high power density. The main concern regarding using Li-ion battery in HEV/PHEV/EV is over- heating [20]. Lower cost will be developed over time as large investments by major automotive OEMs improve the cost efficiency of manufacturing Li-ion batteries [21].

Ultra-capacitors are electrochemical capacitors with high energy capacity. Energy is stored in the double layer formed at a solid/electrolyte interface [22] . Advances in new materials and new ultra-capacitor designs have considerably improved the energy storage capability and cost of this emerging electrical energy storage device. Compared with conventional capacitors, ultra-capacitors allow for 20 times more energy storage [23]. Other unique characteristics of ultra-capacitors include maintenance-free operation, longer operation cycle life, and insensitivity to environment temperature variation. The energy density of ultra-capacitors is still limited compared with batteries.

2.2.3.Optimization Design via Model-Based-Design

MBD technology and development processes have been championed by the consumer automotive industry to help develop cost effective vehicle prototypes on tight deployment schedules. It allows rapid development and assessment of vehicle control systems in a purely simulated environment prior to physical construction of vehicle prototypes. While this has important safety-critical utility through the use of automated system testing and fault insertion testing, it is also of importance for developing efficient control schemes and testing advanced strategies for improving vehicle fuel efficiency.

HEVs add additional complexity to vehicle control systems in that more powertrain hardware is used in tandem to provide vehicle propulsion in response to driver demands. The higher degree of complexity requires more advanced control schemes to be used for coordinating the system to achieve ideal overall system behaviour. The wider range of possible instantaneous system conditions dramatically increases the amount of system

testing required to validate vehicle control systems. The ability to conduct this testing within a simulated environment is instrumental to on-time delivery of consumer-ready vehicle platforms.

In addition to the functional vehicle development benefits, simulated MBD vehicle testing also allows for optimization of control schemes to minimize fuel consumption. While vehicle testing is a slow process, occurring purely in real-time, with some system conditions being difficult to control to produce meaningful system comparisons, a modeled environment can rapidly test control calibrations to determine ideal set-points. This can be extended for formal global optimization routines used to tune vehicles to particular drive cycles.

The use of MBD techniques to improve overall vehicle performance and efficiency, and tune system component interactions requires high fidelity system models to accurately represent physical system behaviour. The development of these models requires large resource allocation to validate against real-world components in physical test environments. A goal of MBD development is continual refinement of modelled systems so as to create a simulation platform which converges to an ideally controlled accurately represented vehicle system.

2.3. Production Hybrid Vehicle Architecture Variations

North American HEV and PHEV adoption rates within the consumer automotive sector have been increasing since the 1999 introduction of the Honda Insight Hybrid and 2000 introduction of the Toyota Prius. Figure 10[24] and Figure 11[25] display the total U.S. sales by vehicle of plug-in vehicles (PHEV/BEV) and HEVs respectively. HEVs on the market today are available in a wide variety of architecture options, with PHEVs adopting similar designs but with larger ESS capacity.

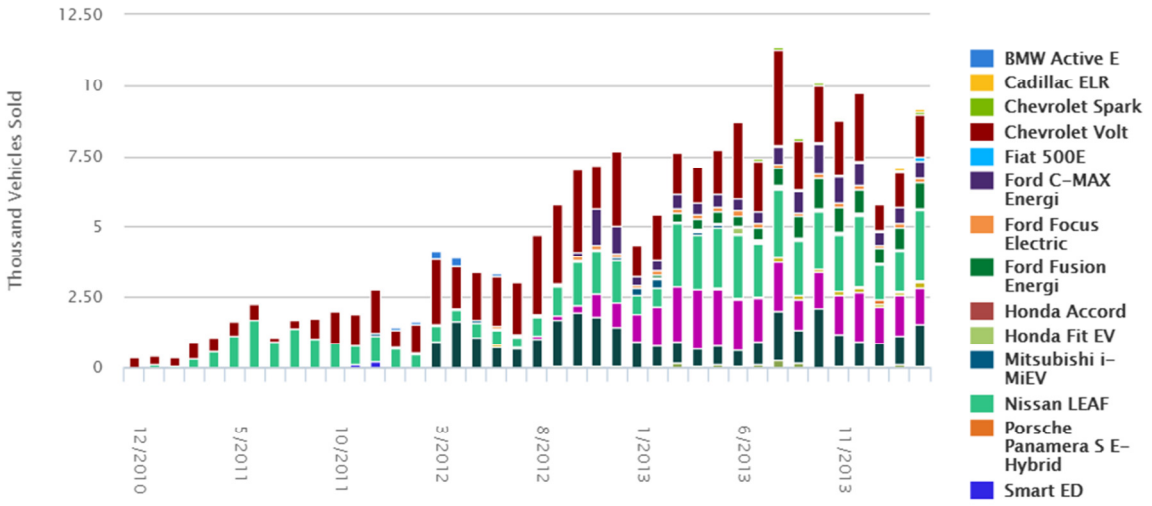

Figure 10: PHEV and EV U.S. Sales

(Image and data from http://afdc.energy.gov/data[24])

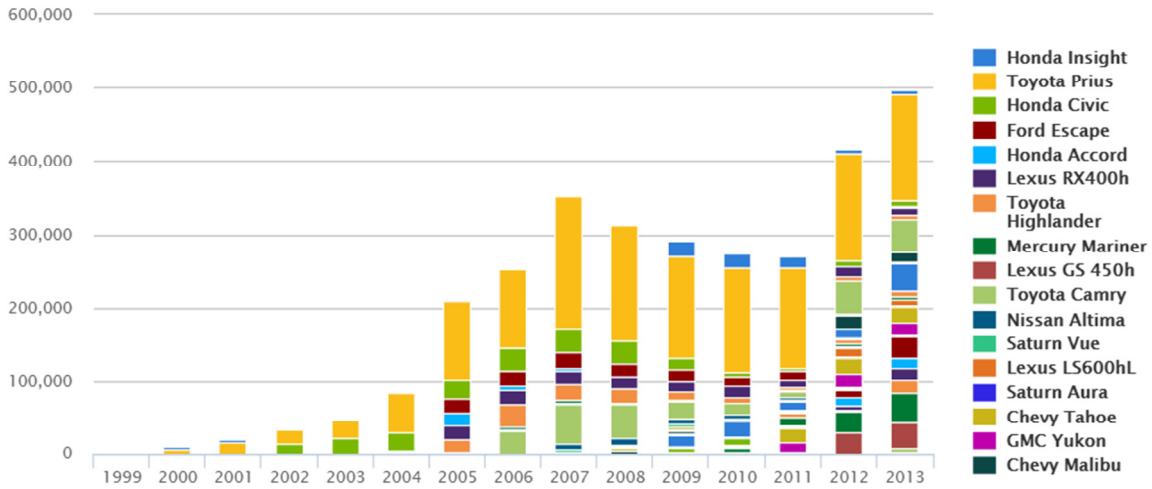

Figure 11: HEV U.S. Sales

(Image and data from http://afdc.energy.gov/data[25])

2.3.1.Mild Hybrid

Mild hybrid architectures employ a slight degree of electrification in the form of a small ESS and low power motor coupled to the ICE. The ICE provides the primary propulsive source for the vehicle, with the electric systems allowing for rapid ICE starting for engine-off stop light functionality, as well as mild amounts of hybrid assist and

regenerative braking. This architecture has no provisions for direct EV propulsion, as the motor power is relatively small at around 15 kW[7].

Mild hybrids are commonly available within the automobile market today. Most common executions are a subset of the parallel hybrid architecture type, distinguished by their lower power electric systems. The GM Belted-alternator-starter (BAS) system is an example of a mild hybrid. The system is employed in several GM vehicles, including the Chevrolet Malibu Eco which provided the base platform for the UVic PHEV architecture.

Figure 12: 2013 Chevrolet Malibu Eco

(Image courtesy of UVic EcoCAR2 team)

It should be noted that many new ICE vehicles, including MINI, Mazda, and BMW, have ICE auto-start/stop systems installed for newer vehicle line-ups which utilize direct combustion to allow rapid restart upon resuming driving[26]. These vehicles are not mild hybrids, as they don't possess hybrid ESSs.

2.3.2. Parallel Hybrid

Parallel HEVs use an ICE in conjunction with an electric motor to propel the vehicle. When one of the drive components is idle, the other assumes the propulsive efforts. In this way, the torque from the two components is added to create a blended output. The motor can act to either add torque or subtract torque, allowing for both assistive torque

and regenerative braking functionality. The architecture is shown in Figure 13. Common examples include the GM mild hybrid BAS systems, and the Honda Insight.

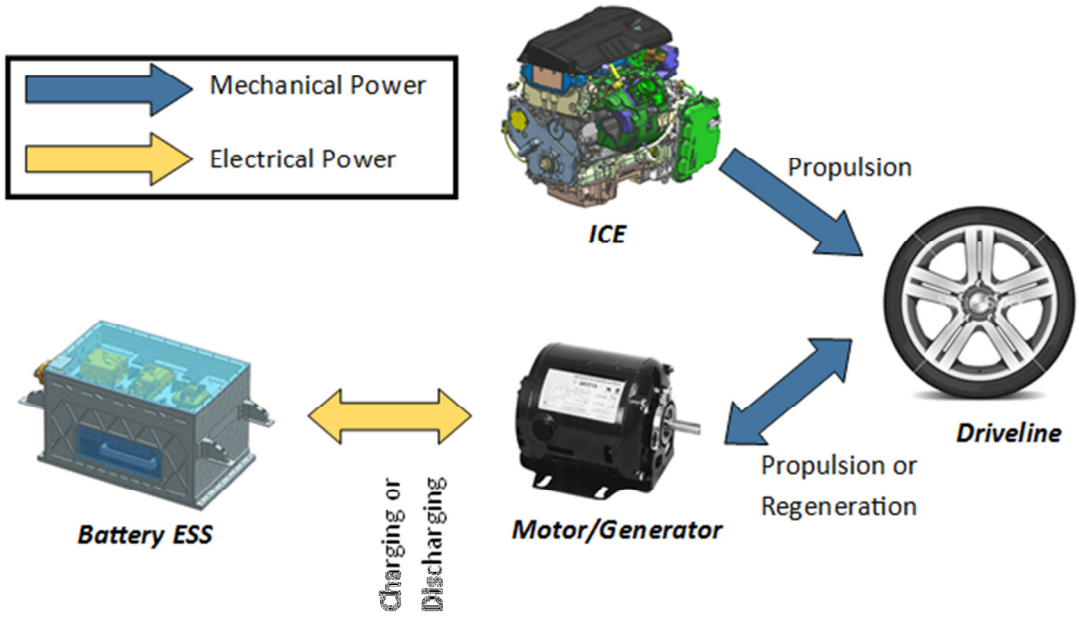

Figure 13: Parallel Hybrid Architecture

A common variation of the parallel HEV is the parallel Through-the-Road (TtR) HEV. The TtR architecture differs in that the ICE and MG are placed on different axles, with the torque interactions between the two drive components acting through the road.

2.3.3.Series Hybrid

Series HEVs use a fully electric propulsion system deriving power from an ESS. The ICE is coupled to a generator which provides for the average power drawn from the ESS to maintain a constant SOC. If the ESS is sufficiently large to support EV operation down to an ESS SOC threshold value, this architecture is also known as an EREV. During CD mode, EREVs can either run as pure EVs or use a blended strategy in which the ESS SOC is drawn down at a reduced rate to prolong the CD range[7]. Series-electric drive systems also exist without the inclusion of ESSs, particularly common in heavy duty applications. A large advantage of having fully electrified propulsion is the ability to

maximize recapture of braking energy by increasing the regenerative power capacity of the drive motors. The series HEV architecture is shown in Figure 14.

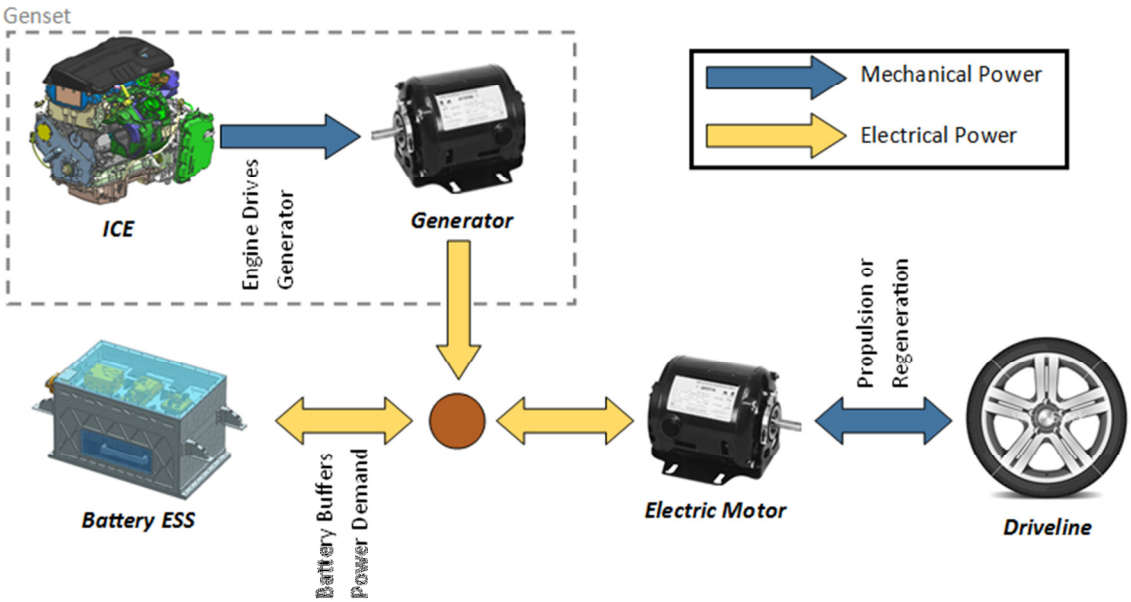

Figure 14: Series Hybrid Architecture

The most notable commercial example of a series HEV is the Chevrolet Volt, utilizing the same powertrain platform is the Cadillac ELR. Both vehicles, while having some capability of having the ICE drive the wheels directly, primarily act in a series configuration except for very specific driving circumstances.

2.3.4.Power-Split Hybrid

Power split hybrids are a specific application subset of the parallel HEV architecture. They use multiple electric motors in conjunction with an ICE and a power-split transmission device to blend power and regeneration capacities of each component to produce the desired propulsion effect. The primary design goal of a power split hybrid is to decouple the user torque demand and vehicle travel speed from the ICE torque production and ICE speed. This allows the power demands on the ICE to be evened out to achieve reduced vehicle fuel consumption[27]. In this way, options for ICE selection and operation points are more flexible, allowing for operation within more efficient

regions of the ICE efficiency map. A generalized power-split hybrid architecture power flow is shown in Figure 15.

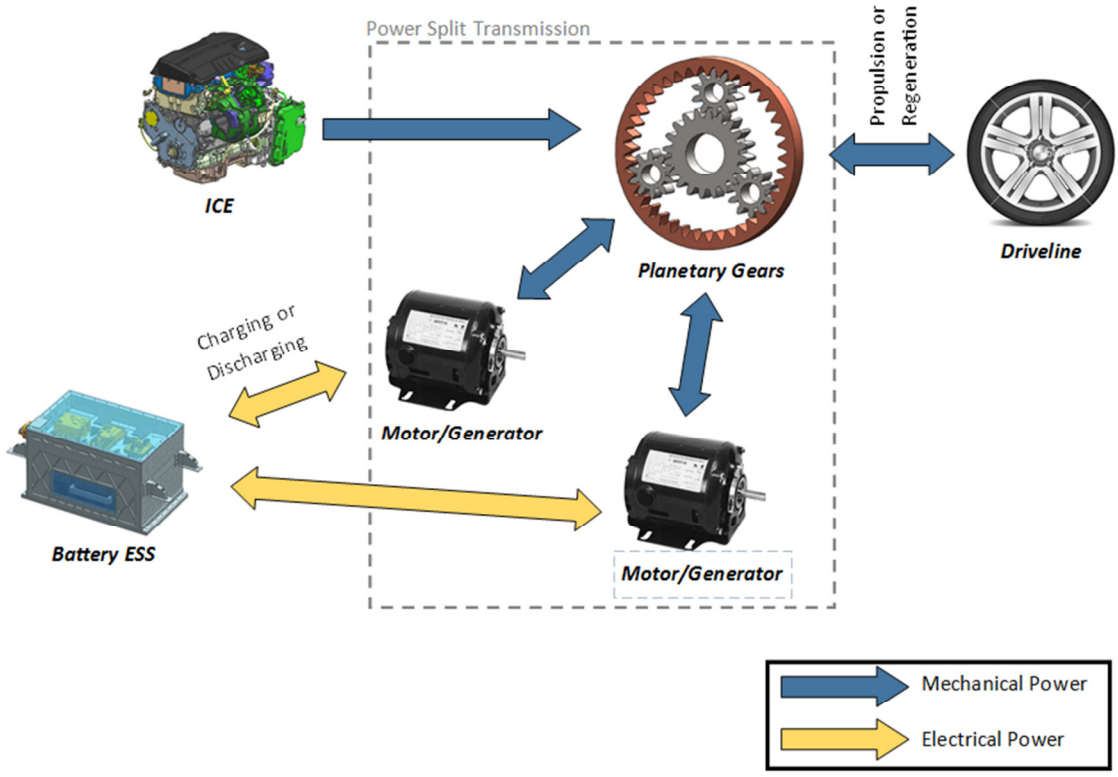

Figure 15: Power-Split Hybrid Architecture

The most common application within the consumer market today is the Toyota Prius. The Prius uses a planetary gear set as the power-split device, which couples together two electric motors and an ICE. The configuration results in one of the motors being in generation mode and the other in assist mode to varying degrees depending on operating point and relative component and vehicle speed. Through controlling the speeds of both motors, the transmission allows maintenance of the ICE speed near a fixed value over a wide range of vehicle speed[27].

Variations employ more complex power-split transmissions with additional fixed and free planetary gear sets, and synchronous clutch systems to open up other operation regimes and produce better performance in high power operation regimes. Variations include the

Toyota Highlander Hybrid which adds an additional planetary to increase the speed of the electric motor and reduce the torque, thus improving overall transmission power density[27]. The GM Two-Mode transmission uses two additional planetary gear sets and 4 synchronous clutches to achieve full electric, blended ICE-electric, and full ICE operation with 4 primary fixed transmission gear ratios[28].

2.3.5. Series-Parallel Hybrid

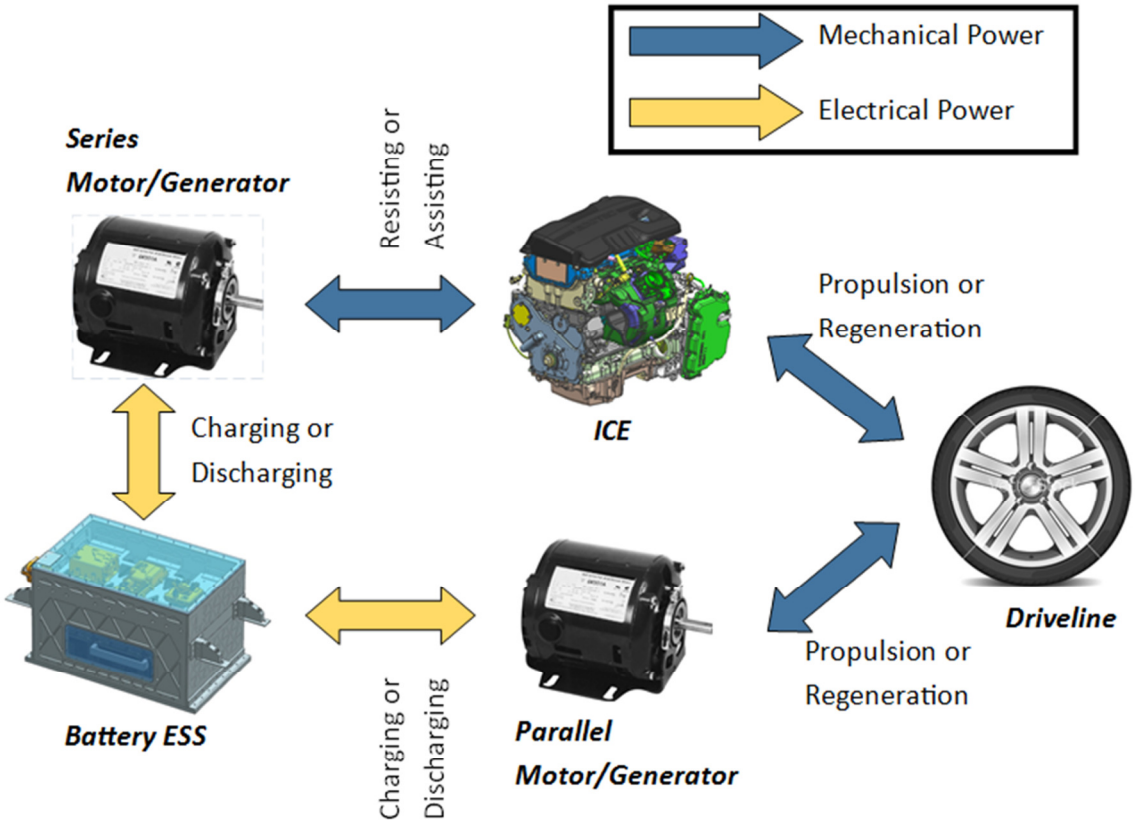

Figure 16: Series-Parallel Hybrid Architecture

A series-parallel HEV is a blend of parallel and series architectures. The presence of a fully independent parallel power path comprised of ICE torque and motor torque provides parallel hybrid functionality. In addition, a MG coupled to the ICE such that it can act to assist or resist ICE torque (motoring or generating) provides series hybrid functionality. These two functions can be implemented as distinct operating modes, or they can be blended together into less distinct operational behaviour. A major pitfall of the

architecture is the high cost of implementation due to the many powertrain components that must be included. Careful consideration must also be paid during component sizing to ensure non-redundant selections. In addition, implementation either requires significant component interfacing to be installed on the front axle in the engine bay (2 MGs, ICE, transmission, couplings), or the parallel MG needs to be installed separately on the rear axle. The latter configuration creates safety concerns due to independently controlled torque sources. For these reasons, commercial application of true series-parallel functionality is not seen. As an architecture deployed in AVTCs, series-parallel PHEVs have been seen in both EcoCAR: The NeXt Challenge, and EcoCAR2: Plugging into the Future. The architecture configuration is shown in Figure 16.

2.4.Hybridization Benefits and Applicability of Advanced Controls to Marine Vessel Powertrains

Recent HEV research at UVic has shifted focus to marine vessel applications. Hybridization of marine vessel powertrains presents different challenges and opportunities when compared with consumer vehicle HEVs. While physical space and component mass are of significantly less concern in a marine vessel design environment, operation is highly constrained by regulations as well as operational constraints associated with large displacement diesel ICEs commonly used in marine vessels. Such constraints present a somewhat similar problem to that of integrating the UVic EcoCAR2 PHEV architecture in that optimal control needs to be constrained to meet operational requirements. Thus similar control strategy development processes can be used via a MBD approach to validate control of various system elements prior to prototype testing. In addition, a strategy-independent controls framework used to control each sub-system and impose respective constraints could also be beneficial in that it would allow constraints to be delineated from strategic optimization of the operation scheme.

2.4.1.Marine Vessel Power System Overview and Hybridization Potential

Marine power systems use on-board energy to produce thrust at the drive propeller. This has traditionally been accomplished with diesel ICEs. A secondary power requirement is electricity for powering the various auxiliary sub-systems of the vessel such as

navigation, special user systems (i.e. defence, laboratories, etc.) and hotel loads. These auxiliary loads are typically met through operation of an ICE coupled to a generator.

With traditional ICE-driven marine powertrain systems, it is possible to reduce the fuel consumption in a variety of classical ways. These include reductions to the load side of the system such as reducing hull drag, improving vessel aerodynamics, creating more efficient auxiliary systems (cabin loads, supplemental systems), and increasing propeller efficiency [29]. It is also possible to improve efficiency of the powertrain itself through improved ICE efficiency and more efficient power transmission components. In addition, vessel operation can be augmented to optimize system efficiency and reduce overall system load. The energy flow for a typical marine powertrain system is shown in Figure 17.

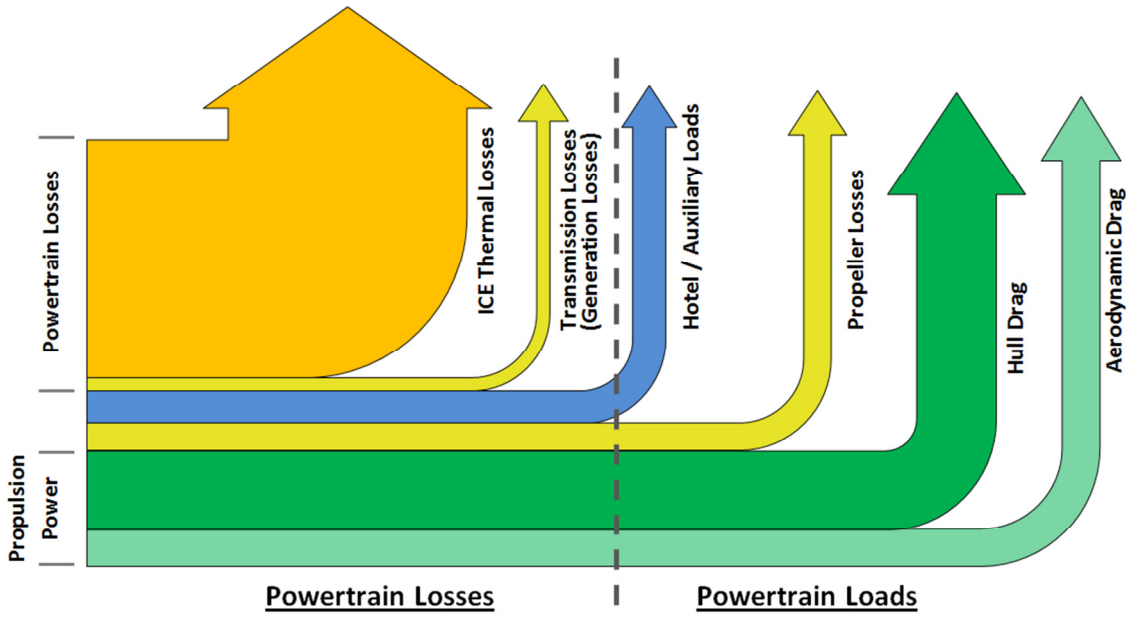

Figure 17: Power Flow and Losses in Marine Powertrain Systems

Once the traditional approaches to improving vessel efficiency are implemented to maximal feasibility, hybridization of marine drive systems provides an avenue for further improvements to overall vessel efficiency. In addition to reducing energy consumption of

the powertrain, hybrid systems also allow for offsetting of fossil fuel use to other more sustainable energy sources such as clean grid electricity and H_2 gas.

Many of the same operational benefits can be found in hybridization of marine powertrain systems when compared to automotive systems, namely efficiency benefits from ICE operational manipulation as well as the implementation of alternative energy storage mechanisms in the form of ESS and fuel cells. In addition, marine vessels provide a suitable platform for the installation of various sustainable energy sources and energy recovery systems, as shown in Figure 18. In addition, improvements related to transient heavy duty diesel ICE emissions production can be achieved.

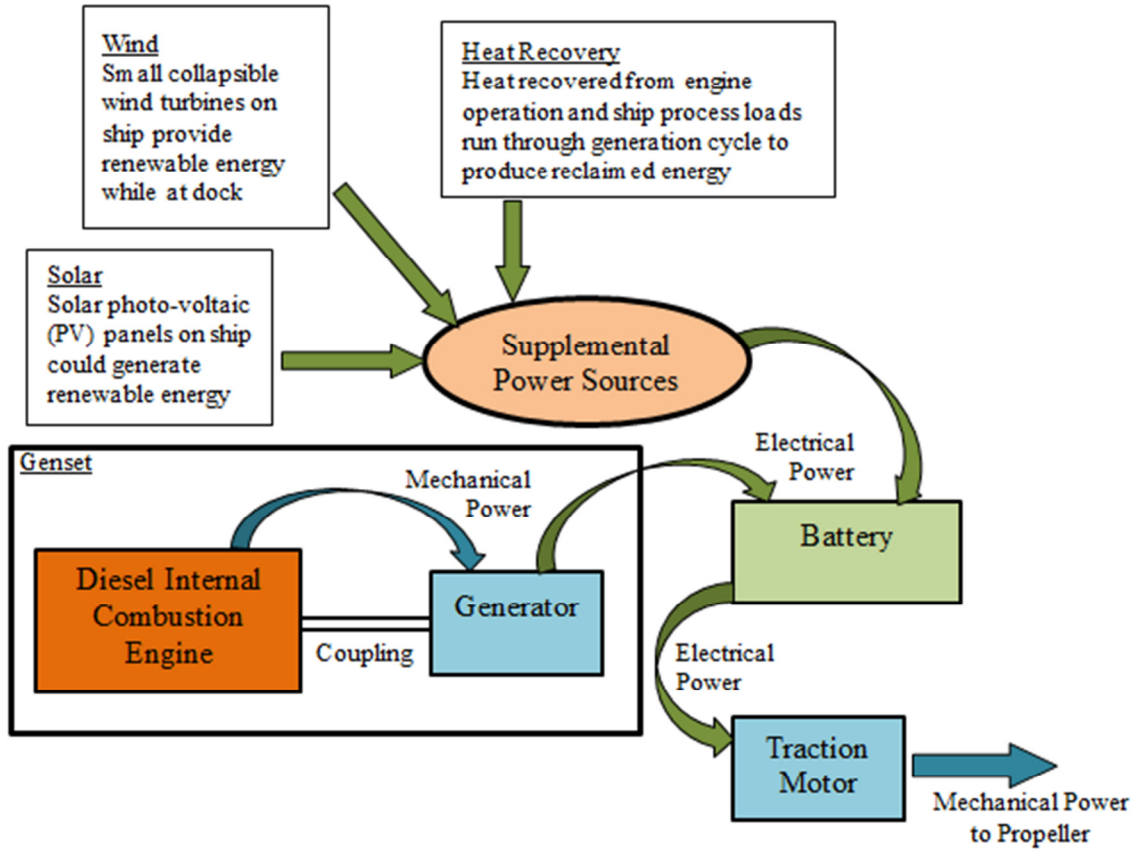

Figure 18: Marine Powertrain System Architecture with Supplemental Power Sources

The application of hybrid powertrains allows for a smaller scale implementation of advanced technologies, without relying on them as sole power sources. Thus hybrid

power systems provide a stepping stone between the conventional systems already employed today and future fossil-fuel independent marine vessels.

2.4.2. Current Marine Vessel Emissions

Worldwide, transportation accounted for 14.5% of carbon dioxide (CO_2) emissions in 2007[30]. Marine transport comprised of 2%. While the overall CO_2 emissions contribution from marine activities is small, other pollutants must be considered.

Most marine vessels use heavy diesel ICEs that run on low grade bunker fuel [31] obtained as by-product from the production of higher grade petroleum products. While this results in significant operational cost savings, it also results in the emission of large quantities of other pollutants including nitrous oxides (NO_x), sulphur dioxide (SO_2), ash, asphaltenes, volatile organic compounds (VOCs), carbon monoxide (CO), and heavy metals [31, 32]. These pollutants are the result of fuel contaminants as well as operational characteristics and dynamic loading issues with heavy diesel ICEs. These pollutants cause marine transportation to be among the highest emission sources for local pollutants and particulate emissions[31]. Heavy marine emissions streams are consequently significantly more toxic than emissions from automotive ICEs.

Internationally, 95% of marine vessels are powered by medium and low speed diesel ICEs, which emit 57kg and 87kg of NO_x per ton of fuel consumed respectively [31]. Marine fuel sulphur content is generally between 1-3% compared to consumer automotive diesel fuels which average 0.0015% [33]. Higher NO_x and SO_2 emission rates per unit of fuel consumed results in marine activities being the dominant source in the Canadian transport sector. Figure 19 shows the sources of SO_2 emissions for Canadian transportation broken down by vehicle type[34]. Continued improvements in emissions controls technology for smaller ICEs and tighter environmental regulation for road based consumer vehicles is anticipated to result in substantial reduction in SO_2 emissions in other sectors, while the marine component is expected to account for an increasingly large percentage of overall emissions due to increased international trade and aging vessel fleets. Emission of these pollutants can have significant environmental effects and

substantially degrade local air quality in coastal regions where marine traffic is heavy such as in major trade ports and straits.

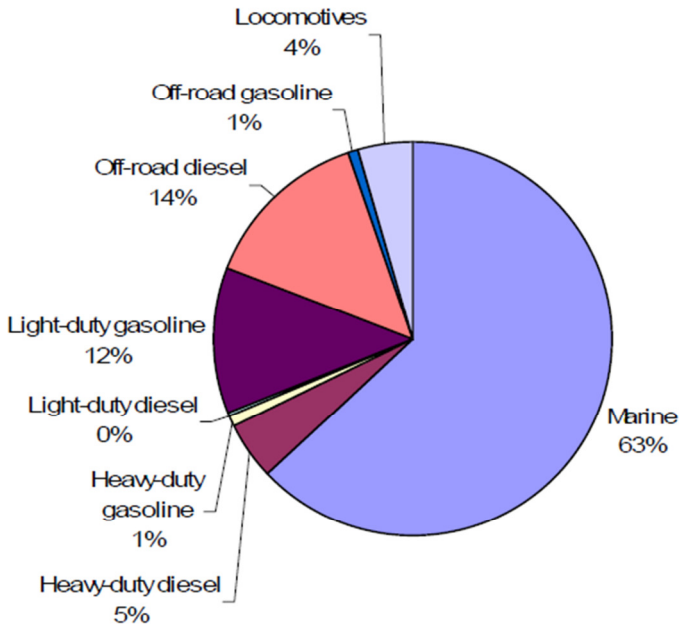

Figure 19: Canadian transportation SO_2 emissions in 2002 by vehicle type

(Data from Transport Canada [34])

The International Maritime Organization (IMO) is responsible for setting international guidelines regarding emissions standards for marine vessel operation. Recently, local effects of heavy marine emissions have become of increased concern in North America, leading to the formation of emission control areas (ECAs) being set up in coastal waters adjacent to shipping routes [34]. Canada is in the process of implementing these industry mandates which will substantially reduce allowable SO_2 and NO_x emission content in exhaust plumes from marine vessels operating in Canadian waters.

A 2006 study commissioned by the California Environmental Protection Agency (EPA) Air Resources Board analyzed the particulate emission sources in the marine ports of Long Beach and Los Angeles, two high traffic ports on the North American West Coast located near large population centres. The study considered all diesel emission sources from port equipment and port related activity. The aggregate distribution of emissions sources is shown in Figure 20. [35]

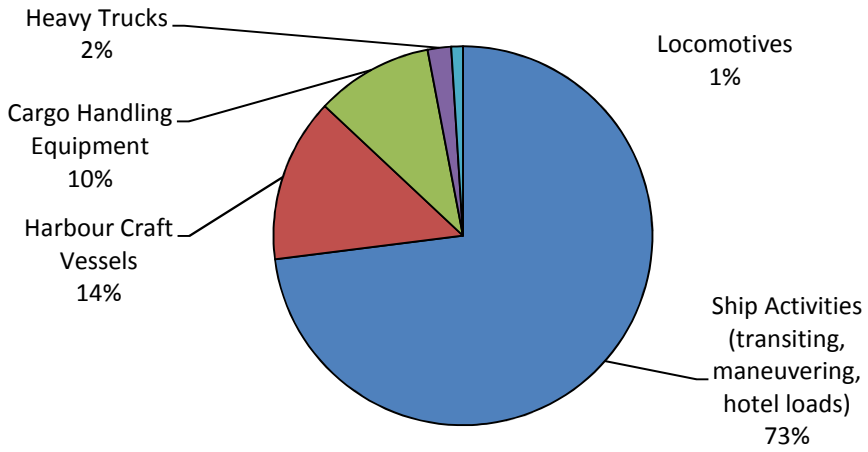

Figure 20: Port Particulate Emission Composition

(Data from California Environment Protection Agency[35])

Hybridization of marine vessels provides a major benefit of not solely relying on diesel power for all ship operations. As shown in Figure 20, port vessel activities, such as transiting, manoeuvring, and hoteling, account for the majority of diesel emissions associated with the operation of ports. With on-board availability of direct-use electrical energy from ESS and fuel cell systems, many low power operations that typically occur around ports can be undertaken without the use of auxiliary diesel ICEs. This effectively eliminates the port-associated emissions contribution of ship activities, as hybrid power systems can effectively power the ship while near populated areas. This is a logical step forward from both technological and regulatory perspectives, as it represents an immense reduction in the human health risk posed by port operations by dramatically reducing overall port emission intensities.

2.4.3. Availability of Hardware

The key technologies required to allow for development of advanced marine vessel hybrid powertrains are suitable drive motors and ESSs.

Batteries have historically been integrated into marine powertrain systems for purposes of propulsion. In the early part of the 20th century, battery-powered boats were used to move people at World's Fair (World Expo). Nevertheless, batteries were rejected as an avenue of technological development effort due to weight, inefficiency, and short period of

economical storage being too problematic for adoption in shipping applications [36]. Since these early efforts, battery technology has made substantial progress in terms of energy and power density. The recent proliferation of consumer HEVs and more recent development of viable plug-in consumer vehicles have generated a large market demand for improved battery technology. Energy and power density, as well as cycle life continues to be a field of intense R&D to satisfy this new market demand. For marine applications, batteries technology is available in the same forms as that for consumer automotive HEVs, but with key differences in capacity requirements and installation constraints. The larger size of marine vessels makes cheaper battery technologies with comparatively lower energy densities more reasonable candidates for integration.

Electric drive systems for marine applications are a readily available and mature technology. Electric propulsion in marine applications has been utilized since the early 20^{th} century in various configurations including hybrid diesel ICE and MG configurations as well as hybrid diesel turbine and electric motor configurations. The U.S. collier Jupiter was a steam turbine electric drive system commissioned in 1913 with a displacement of approximately 20,000 tonnes. The steam turbine powered an AC generator which in turn powered an AC squirrel cage induction motor. The technology was originally developed to overcome disparity between optimal prop speed and optimal turbine speed [36]. Since the original electrification of marine vessel powertrains, there have been many advances in electric generator and drive technology. Improvements in motor efficiency, reliability, safety, and power density have been realized through improvements in design and manufacturing. Modern electric drives for vessels are deployed in a variety of configurations with different operational characteristics and limitations.

A common electric drive configuration in modern large vessels is a diesel-electric drive with a single speed AC induction motor powered with a diesel-electric genset operated to follow the load. Variable thrust is accomplished by varying the drive propeller pitch angle, while maintaining constant motor speed. Another variation employs the use of a variable frequency drive (VFD) to control output shaft rotational velocity. This allows for higher efficiencies in certain operating conditions, such as low speed manoeuvring and transiting. This configuration is made possible by development of very high power VFDs.

An internet search reveals a wide array of companies marketing VFD solutions for marine propulsion drives, with some claiming efficiency gains of up to 40% over traditional single speed configurations [37].

Electric drives can be integrated into a ship propulsion system in two primary mechanical packaging configurations:

- In-board drive mounting has the advantage of maintaining easy access to large electrical components by keeping the electric drive within the ship hull and linking it to the drive prop via a drive shaft.
- Azimuth propulsion drives package the electric drive and propeller in a unitary outboard drive pod, removing all drive components from within the ship hull. This frees up space for installation of ESS or operational cargo.

2.4.4.Challenges Associated with Optimal Design of Marine Hybrid Powertrains

Marine applications present a wide range of loading conditions, diverse working environments, and a different set of design constraints and regulations compared to existing vehicular applications. These new demands, conditions and constraints naturally require different design considerations including

- relaxed weight and packaging volume constraints as compared to automotive,
- high power output,
- extended operation cycles,
- operates independently of infrastructure and support systems (safety concerns),
- highly trained crew,
- on-board maintenance crew capable of mid-mission repairs,
- long vehicle service life.

Developing green marine power systems requires incorporating these considerations into the design process. Many of the same advanced controls methodologies can be employed, but operational constraints must be applied rigidly to the optimized controls targets to guarantee safe and reliable operation. Also, additional user control is acceptable, and even necessary due to the higher degree of operational training possessed by the crew of a vessel.

Efficient application of traditional powertrain technology requires a global optimization approach to the systems. The design and development of hybrid electric powertrains thus demands well-defined user's needs and working conditions. In vehicular applications, the driving and loading cycles of a specific type of vehicles are well defined and generally accepted. For example, the two mostly commonly used automotive driving cycles for fuel economy evaluations are the Urban Dynamometer Driving Schedule (UDDS) and the Highway Fuel Economy Driving Schedule (HWFET), used by US EPA for new cars fuel consumption measurement until year 2011. The EPA has recently updated the method by adding more testing procedures such as the cold and warm starts to better approximate the real world driving conditions [38]. These driving cycles define the minimum powertrain function needs and serve as platform for vehicle performance, fuel economy, and emissions measurement.

For marine applications, the driving and loading patterns of different ships and different vessel applications are vastly different. No national or internationally acceptable standard powertrain load patterns have been published. The operation patterns of different ships vary tremendously, leading to a lot of uncertainties in assessing the power need of a ship and the ESS design of the hybrid power system, and potential failures in delivering the functions of the vessel. In addition, there are other power systems and features such as dynamic position maintenance, hotel loads, and auxiliary systems which must be accounted for in characterizing the overall powertrain duty cycle.

The hybrid electric marine propulsion system for marine vessels, similar to the hybrid powertrain system for automotive, is a complex multi-physics system with various mechanical, electrical, energy storage, power electronics, data acquisition and

communication, and controls subsystems and components. A MBD approach, like the one used as standard practice for the automotive industry, is essential to identify the appropriate, effective and optimal system architecture, component size, and embedded control system algorithms. The mature hybrid powertrain system modeling tools all have built-in high fidelity vehicle dynamics models that allow the performance and fuel economy of a given vehicle for a given driving cycle to be reliably evaluated, thus making comparisons of different hybrid power systems possible.

Implementation of a MBD approach is also more challenging than for vehicle systems due to the increased complexity of determining instantaneous propulsive load for a given system condition. For standard hull ships, water resistance drag on the ship hull can be characterized by resistance sources[39] including flat plate friction effects, surface roughness effects, ship hull form effects on friction, ship hull form effects on pressure distribution, wave pattern generation, and wave pattern breaking.

In addition, further drag will be induced on a vessel by wind resistance, rudder appendages, and propulsion pods or drive screws. There is currently no unified approach to accounting for all of these load effects in a single modeled environment. This can be partially overcome by developing load cycle information from a perspective of powertrain load, rather than developing a multi-physics simulation of the entire ship and powertrain system. This simulated model development platform architecture is shown in Figure 21.

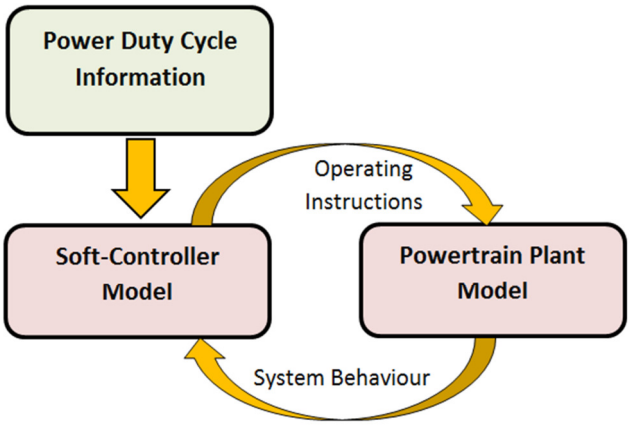

Figure 21: Simplified Powertrain Modelling Configuration

Chapter 3: Vehicle Control System Development

3.1. Vehicle Component Details

The advanced UVic EcoCAR2 vehicle architecture integrates a selection of cutting edge component technologies to achieve its efficiency and performance targets. The vehicle component locations within the vehicle displayed in Figure 22.

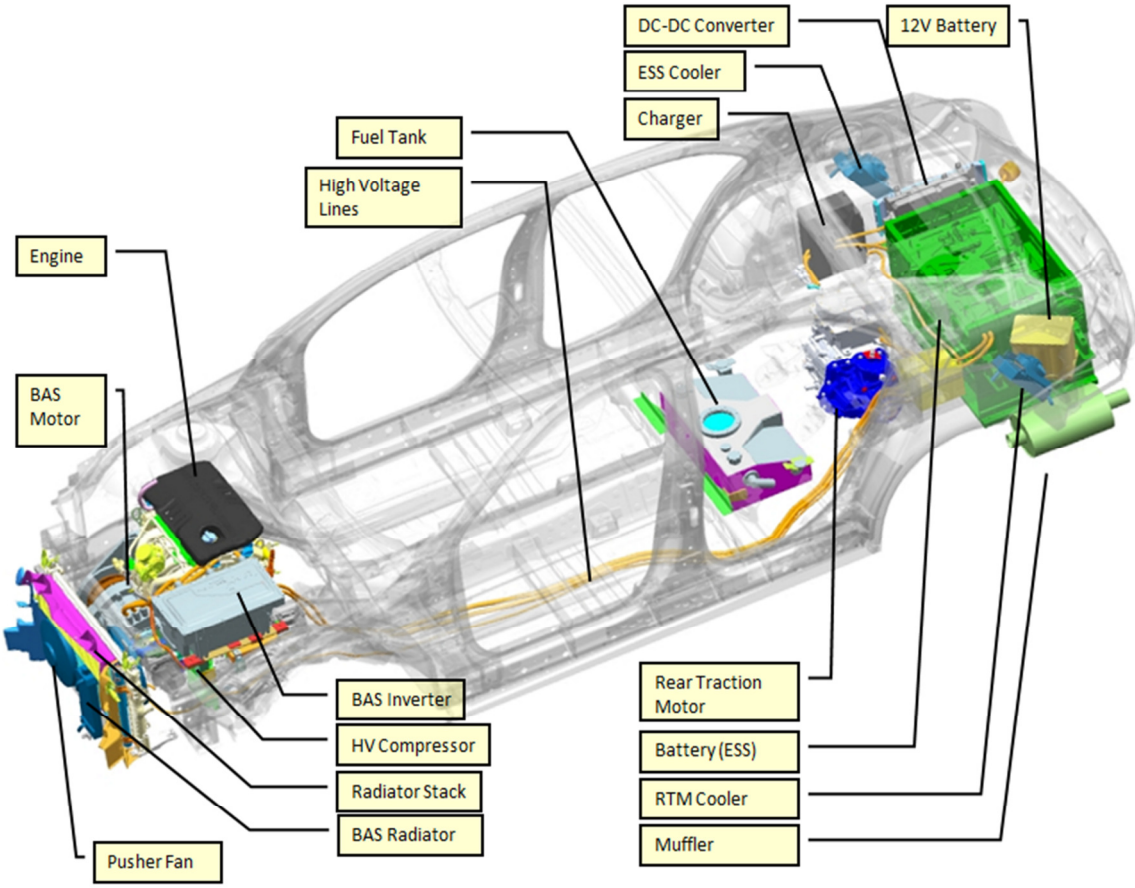

Figure 22: UVic EcoCAR Vehicle Component Layout

The primary powertrain components include the following:

- GM 2.4L EcoTEC ICE
- Magna E-Drive RTM
- TM4 MotiveB BAS Motor
- A123 6s3p15s Li-Ion Battery Energy Storage System

3.1.1.GM 2.4L EcoTEC Engine

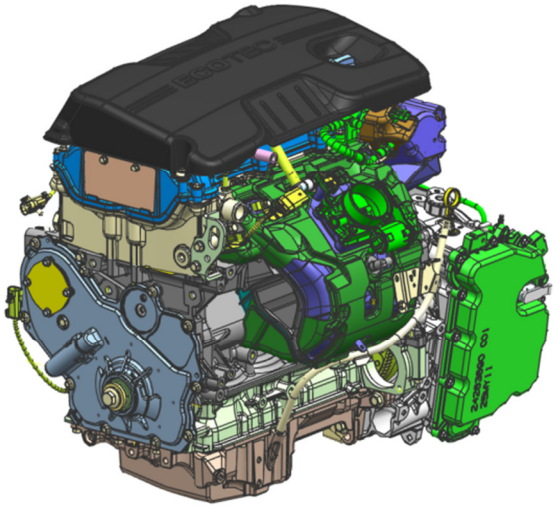

Figure 23: GM LE9 Engine

The ICE used in the UVic EcoCAR2 PHEV is the 2012 2.4L GM EcoTEC LE9 DOHC I4 ICE. It is a flex-fuel capability equipped ICE, and is used in the Chevrolet Malibu and Chevrolet HHR. Maximum power is 170 HP at 6200 rpm and maximum torque is 158 ft-lb at 5200 rpm. The efficiency map of the LE9 ICE is shown in Figure 8[15]. Unique features of the ICE, provided by GM via the EcoCAR2 competition[40] are as follows:

- **Optimized Piston Skirt –** Pistons have a slight barrel shape, enhancing glide through the piston stroke. Pistons use aluminum, reducing reciprocating mass and improving ICE efficiency and NVH characteristics.

- **Dual Overhead Cam (DOHC) with Continuously Variable Valve Timing –** Continuously variable valve timing allows for the optimization of the ICE performance, efficiency, and emissions. Both intake and exhaust cams have hydraulically operated phasers that are managed by a solenoid controlled by the Engine Control Module (ECM).

- **Electronic Throttle Control –** No physical link exists between the driver accelerator pedal interface and the ICE. Sensor inputs are interpreted by the ECM which controls the throttle body and fuel injection system to produce the desired response.

- **E85 Flex Fuel Capability –** Hardware adaptations are limited to the fuel injectors, which have been designed to handle greater flow to compensate for the reduced energy density of E85 fuel.

The electronic throttle control allows for full control of the ICE via Controller Area Network protocol (CAN), digital, and analog inputs and outputs (I/O). CAN and digital signals are used for ICE enabling and starting, as well as diagnostic feedback. Two analog signals are used to provide throttle input into the ECM in place of the stock accelerator pedal input. These two signals combine to represent a percentage accelerator pedal input signal that is interpreted and acted upon by the ECM. There is no explicit capability to define a torque request in physical units. Detailed system I/O configuration is documented in Appendix A.

3.1.2.GM 6T40 Transmission

The UVic EcoCAR2 PHEV front drive systems are connected to the ground via the GM 6T40 automatic transmission. The unit contains a 6-speed automatic gearbox with overdrive and reverse gears, a final drive, an open transaxle differential, and a torque converter. The shift map, taken from ANL Autonomie, is dependent on the accelerator pedal request sent to the ICE, as shown in Figure 24 and Figure 25[41]. The shift line profiles represent the threshold barrier to trigger a shift in the given direction to the next sequential gear, activating the next threshold line. The gear ratios are noted in Table 1.

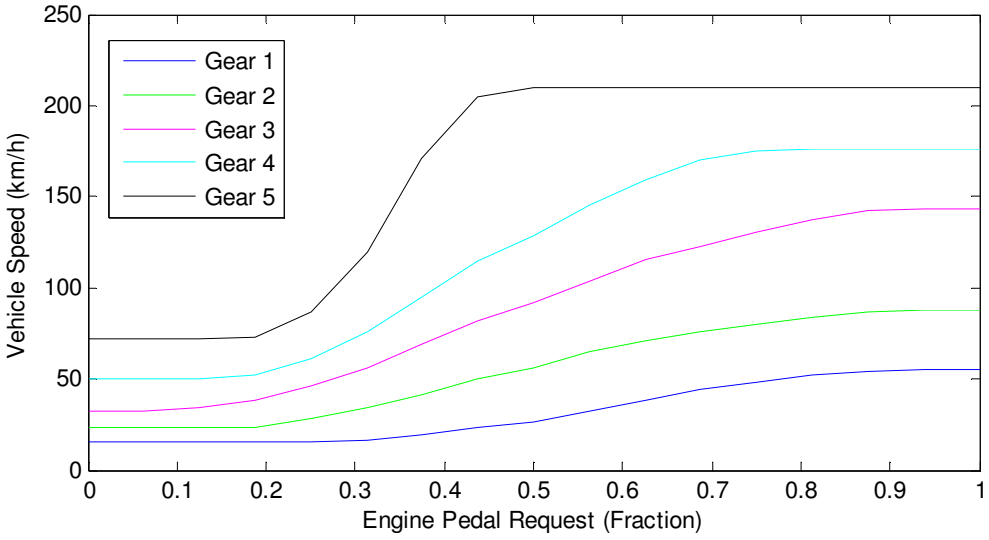

Figure 24: Transmission Upshift Curves

(Data extracted from Autonomie courtesy of EcoCAR2 team[41])

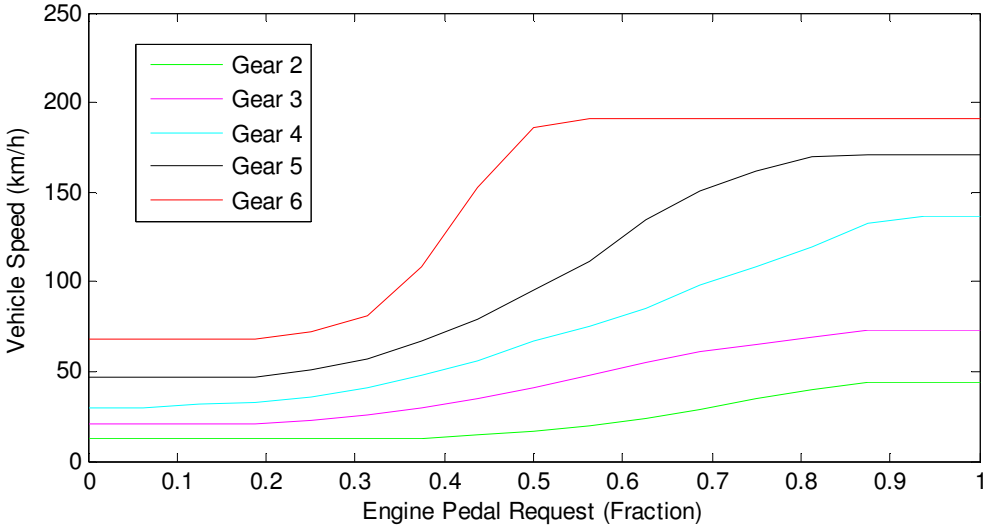

Figure 25: Transmission Downshift Curves

(Data extracted from Autonomie courtesy of EcoCAR2 team[41])

Table 1: 6T40 Transmission Gear Ratios

Specification	Value
Gear 1 Ratio	4.584
Gear 2 Ratio	2.964
Gear 3 Ratio	1.912
Gear 4 Ratio	1.446
Gear 5 Ratio	1.000
Gear 6 Ratio	0.746
Final Drive Ratio	2.89
Reverse Ratio	-2.94

Control of the transmission is limited in the system integration design. Tiptronic manumatic functionality was not used in the vehicle design execution due to the fuzzy nature in which the transmission control module (TCM) interprets commands. As such, control is limited to specifying intended vehicle drive status via the automatic shift lever (PRNDL) as “park”, “reverse”, “neutral”, or “drive”. The automatic transmission makes gear selections based on accelerator pedal requests sent to the ECM and present vehicle speed. When a shift line threshold is crossed, the shift is executed. Upshift and downshift curves are offset from one another to prevent gear selection bounce. Control of the basic functionality is accomplished via the hardware shift lever connection to the transmission and a digital position override interface. CAN communication is used for diagnostic feedback. Detailed system I/O configuration is documented in Appendix A.

3.1.3. Magna E-Drive Rear Traction Motor

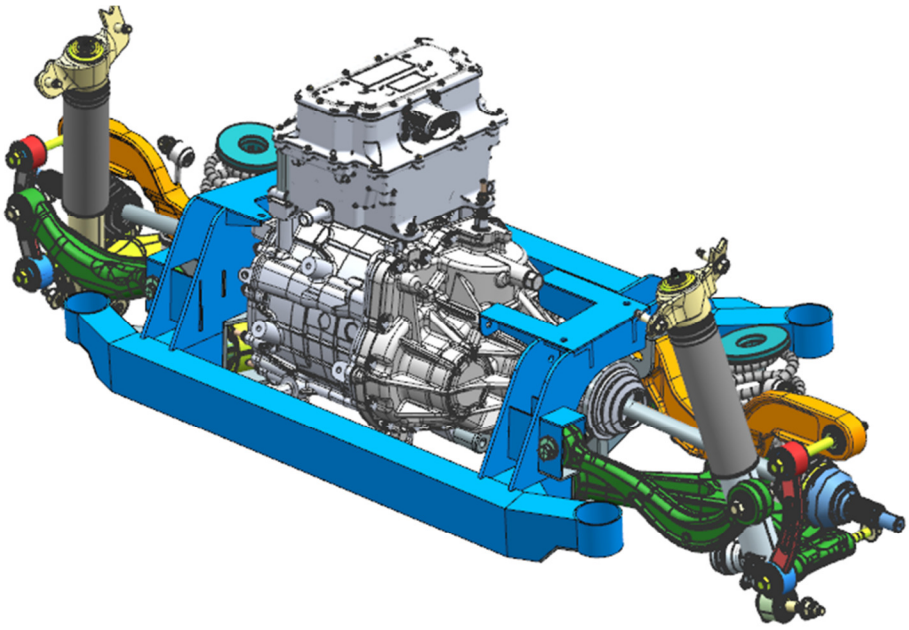

Figure 26: Magna E-Drive Integrated with Rear Sub-Frame

(Image courtesy of the UVic EcoCAR2 team)

The UVic EcoCAR2 PHEV employs the Magna E-Drive as the system RTM. The unit is comprised of a PM motor power plant coupled to a coaxial single stage gearbox and transaxle open differential. Primary specifications are listed in Table 2 as provided by Magna to the UVic EcoCAR2 team. The MG performance and efficiency map are displayed in Figure 27 and Figure 28 as provided by Magna to the UVic EcoCAR2 team

The Magna E-Drive allows for explicit control input of desired torque production and direction via CAN communication. This, combined with the fixed gear ratio, allows for reliable explicit control of the RTM within the greater system. Additional digital inputs are used for enabling the system. Detailed system I/O configuration is documented in Appendix A.

Table 2: Magna E-Drive Specifications

Specification	Value
Maximum Power	83 kW @ 250V, 103kW @ 350V
Voltage Range	250 VDC - 403 VDC
Peak Torque	245 Nm
Peak Current	400 Arms
Continuous Power	45 kW
Continuous Torque	150 Nm
Continuous Current	222 Arms
Maximum Speed	8,833 RPM Powered 10,000 RPM Over Speed 14,200 RPM Burst
Gear Ratio	7.82:1

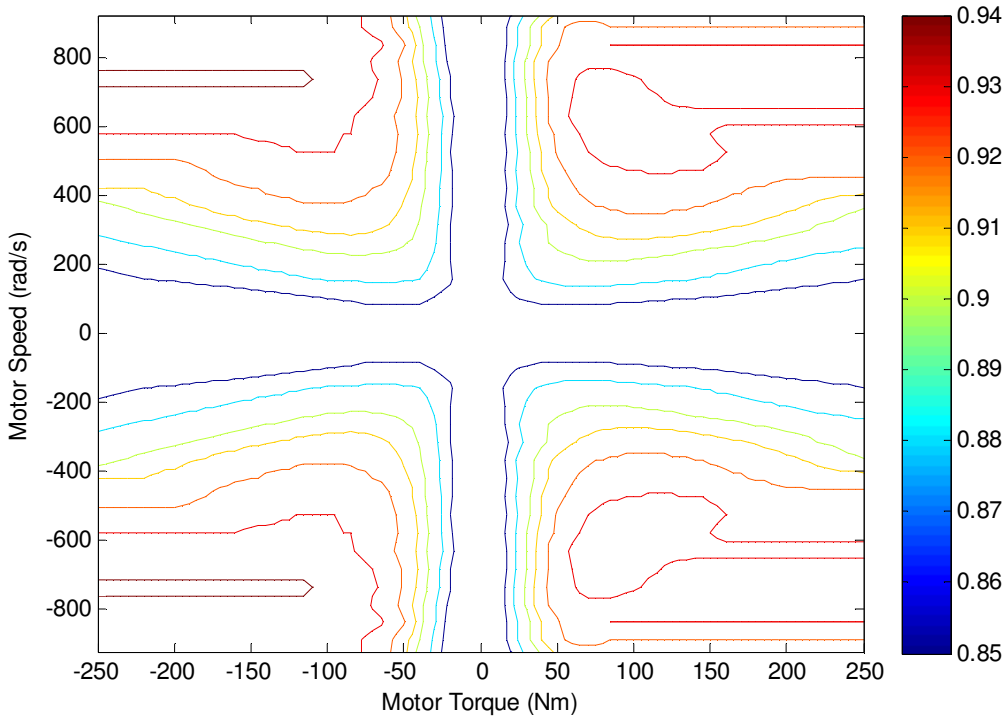

Figure 27: Magna E-Drive Efficiency Map

(Data courtesy of the UVic EcoCAR2 Team)

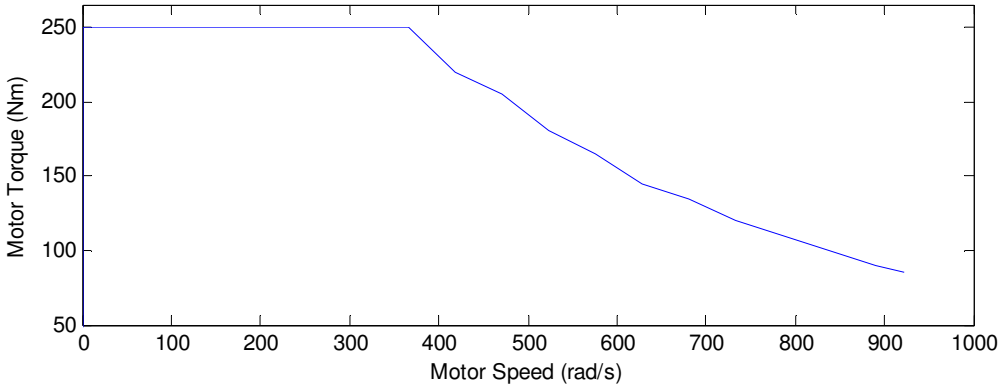

Figure 28: Magna E-Drive Maximum Torque Curve

(Data courtesy of the UVic EcoCAR2 Team)

3.1.4. TM4 Motive B Belted Alternator Starter Motor

Figure 29: TM4 Motive B

(Image courtesy of the UVic EcoCAR2 team)

The UVic EcoCAR2 PHEV employs the TM4 Motive B as the system BAS. The BAS is coupled to the LE9 ICE via a custom belted interface using a Gates Polycarbon Chain Drive complete with tensioning pulley arm, as shown in Figure 30. The MG is a high power density PM motor. Primary specifications are listed in Table 3 as provided by TM4 to the UVic EcoCAR2 team. The MG performance and efficiency map are displayed in Figure 31 and Figure 32 as provided by TM4 to the UVic EcoCAR2 team.

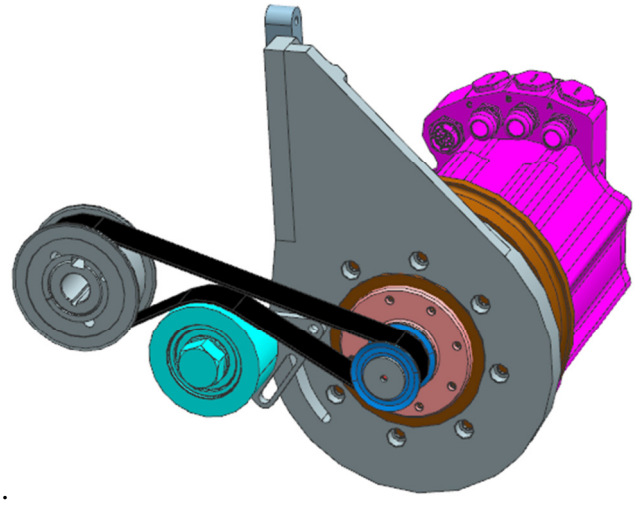

Figure 30: TM4 Belted Interface

(Image courtesy of the UVic EcoCAR2 team)

Table 3: TM4 Motive B Specifications

Specification	Value
Maximum Power	105 kW
Voltage Range	100 VDC - 450 VDC
Peak Current	350A DC
Continuous Power	54 kW
Peak Torque	180 Nm
Continuous Torque	70 Nm
Continuous Current	180A DC
Maximum Speed	11,500 RPM Powered 12,500 RPM Burst
Belt Ratio	1:1.68

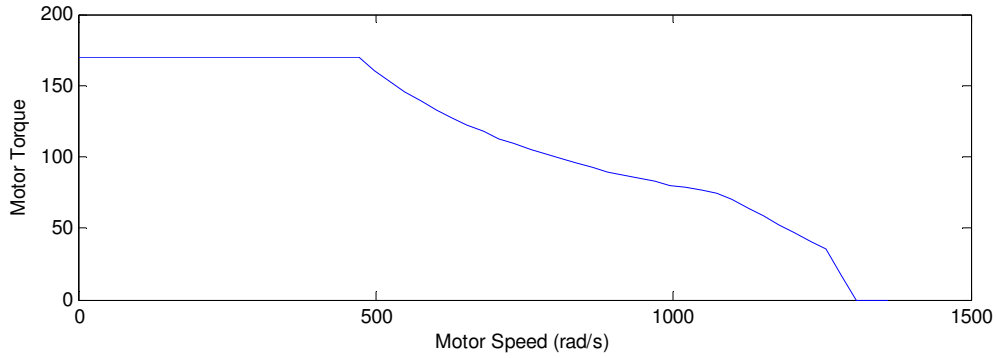

Figure 31: TM4 Motor Maximum Torque Curve

(Data courtesy of the UVic EcoCAR2 Team)

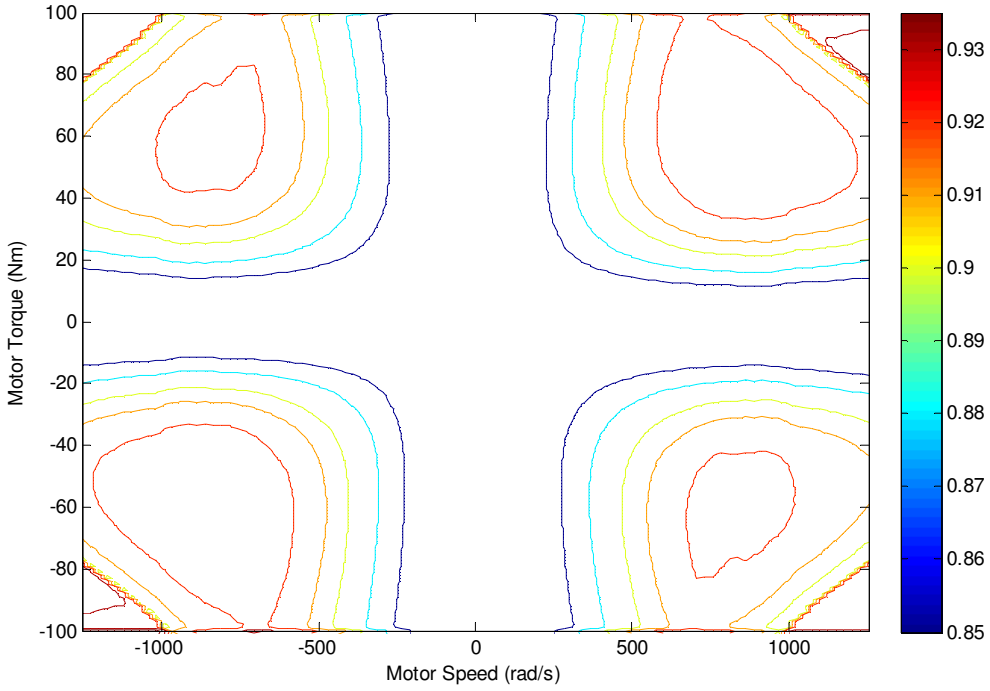

Figure 32: TM4 Motor Efficiency Map

(Data courtesy of the UVic EcoCAR2 Team)

The TM4 Motive B allows for explicit control input of desired MG torque production and direction via CAN communication. Control of the component driveline contribution within the overall system requires accounting of the fixed belt ratio between the BAS and ICE, as well as the variable gear ratio of the 6T40 automatic transmission since it is connected to the wheels via the transmission and ICE. Additional digital inputs are used for enabling the system. Detailed system I/O configuration is documented in Appendix A.

3.1.5.A123 Lithium Ion Battery Pack

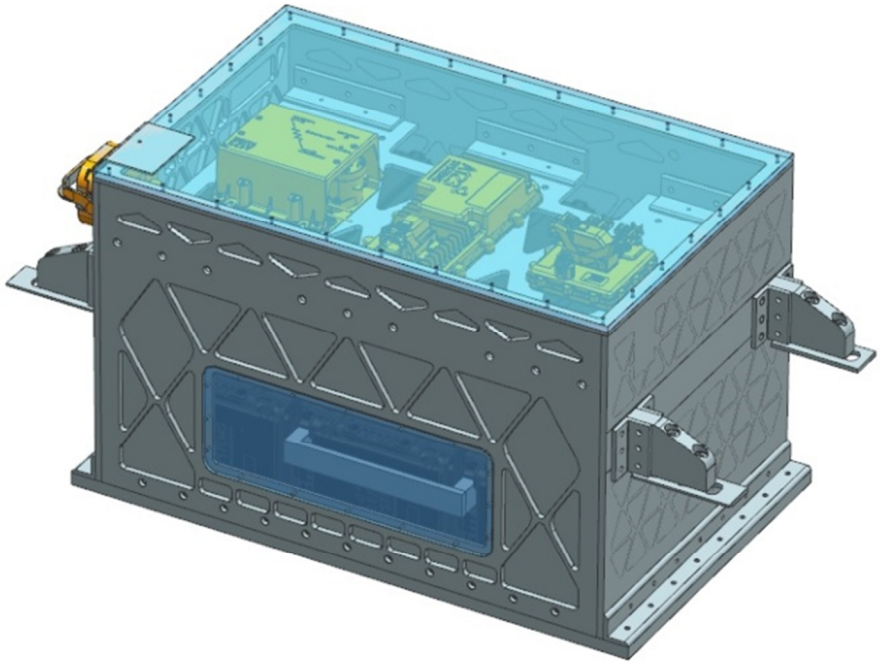

Figure 33: A123 6x15s3p Li-Ion ESS

The UVic EcoCAR2 PHEV employs the A123 6x15s3p Li-Ion battery pack system installed within a custom ESS enclosure as displayed in Figure 33. The pack provides electrical power source to the RTM and BAS MGs, as well as an energy buffer for HEV CS operation. The pack is made up of 6 modules, each with 45 prismatic cells (15 series 3 parallel). In addition to providing the main power plant for the electrical systems, the ESS also provides 12V power during operation via a GM HEV Auxiliary Power Module (APM). The APM is a DC-DC converter which steps the high voltage (HV) DC down to 12V for vehicle accessory power. This is a vital requirement since the vehicle does not have an alternator. Primary specifications are listed in Table 4 as provided by A123 to the

UVic EcoCAR2 team. The ESS open cell voltage (OCV) and cell resistance curves are shown in Figure 34 and Figure 35 as provided by A123 to the UVic EcoCAR2 team.

Table 4: A123 6x15s3p ESS Specifications

Specification	Value
Power	152 kW, 10 seconds 51 kW, continuous
Pack Voltage	324 V Max. 292 V Nominal 225 V Min.
Min. Capacity	58.8 Ah
Min. Power	16.2 kWh

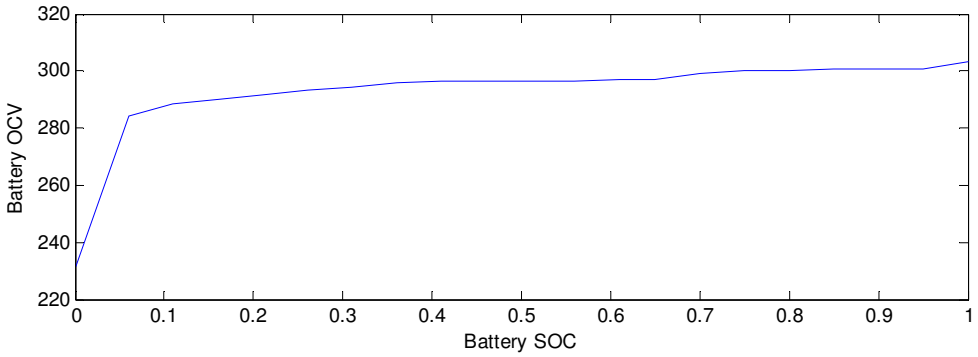

Figure 34: A123 6x15s3p Open Cell Voltage Curve

(Data courtesy of the UVic EcoCAR2 Team)

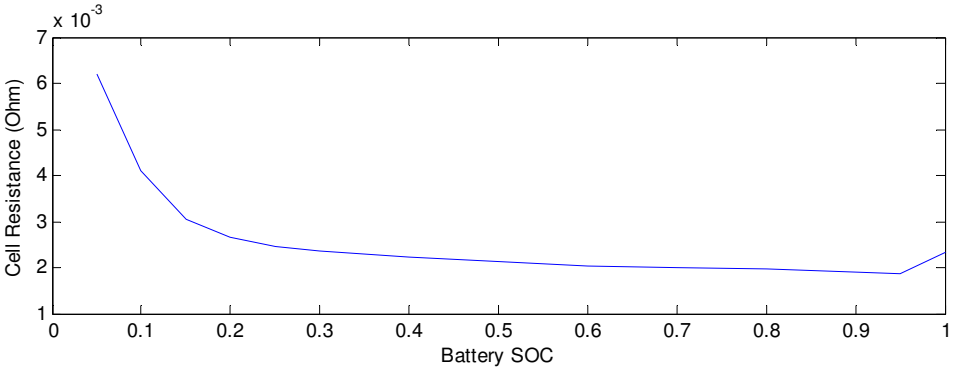

Figure 35: A123 6x15s3p Cell Resistance Curve

(Data courtesy of the UVic EcoCAR2 Team)

Control interfacing is accomplished via digital and CAN I/O. The component control requirements for the ESS are primarily based upon initialization routines. Additionally CAN feedback signals are used for system diagnostics. Detailed system I/O configuration is documented in Appendix A.

3.1.6.Driver Interface

The controller-driver interface is comprised of the accelerator pedal, brake pedal, shift PRNDL, key ignition, and 3 competition override switches. The functions of these inputs within the greater system are described in Table 5. Detailed system I/O configuration is documented in Appendix A.

Table 5: Driver Interface

I/O Element	Description
Accelerator Pedal	2 analog potentiometer signals corresponding to the accelerator pedal depression percentage are interpreted as the driver-desired positive wheel torque generation.
Brake Pedal	1 analog potentiometer signal corresponding to the brake pedal depression percentage is interpreted as the drive desired negative wheel torque generation. Regenerative braking is applied over top of the mechanical hydraulic system.
PRNDL	Shift lever position is communicated via CAN by the TCM and is used to interpret the driver-desired vehicle direction and operation status.
Ignition Key	2 digital signals mapping the 4 potential key positions (off, accessory, on, crank) are used to interpret vehicle start-up requests from the driver.

Fuel Conversion On Switch	Manual override digital switch allows for fixed enabling of the ICE.
Regenerative Braking Off Switch	Manual override digital switch allows for fixed disabling of the regenerative braking capability.
Force CS Mode Switch	Manual override locking the vehicle into CS Mode to demonstrate vehicle operation in both CD and CS regimes on driver demand.

3.2. Operational Performance Targets

The developmental goals of the vehicle were established to align with the performance target requirements and goals of the EcoCAR 2 competition. As such, vehicle fuel efficiency was prioritized as a high scoring component of the competition; however other areas of consideration were acceleration, braking, driveability, dynamic handling, dynamic consumer acceptability, and static consumer acceptability. In addition, specific technical rules regarding the vehicle integration and control system implementation were relevant to the design process and decisions made throughout the competition.

3.2.1.Vehicle Technical Specifications

An emphasis of the competition is vehicle modeling and performance estimation. Throughout the competition, a persistently updated table of Vehicle Technical Specifications (VTS) was used as a design target for validating vehicle performance. These values were updated continuously as a result of modeling updates and improvements to model fidelity and accuracy of results. The UVic Year 3 Competition VTS is shown in Table 6.

Table 6: UVic Vehicle Architecture Vehicle Technical Specifications

Specification	Production 2013 Malibu	Competition Target	Competition Requirement	UVic Target
Acceleration (0-60 mph)	8.2 sec	9.5 sec	11.5 sec	8.5 sec
Acceleration (50-70 mph)	8.0 sec	8.0 sec	10.0 sec	3.8 sec
Braking (60-0 mph)	43.7 m	43.7 m	54.8 m	43.5 m
Grade-ability (20 min @ 60 mph)	10%	3.5%	3.5%	4.2%
Cargo Capacity	16.3 ft^3	16.3 ft^3	7 ft^3	7 ft^3
Passenger Capacity	5	4	2	5
Vehicle Mass	1589.6 kg	2078 kg	2078 kg	2078 kg
Vehicle Range	736 km	322 km	322 km	547 km
Charge Deplete Range	N/A	N/A	N/A	83.8 km
Charge Deplete Mode Energy Consumption	N/A	N/A	N/A	2.59 Lge/100km
Charge Sustaining Fuel Consumption	N/A	N/A	N/A	5.20 Lge/100km
UF-Weighted Fuel Energy Consumption	8.83 Lge/100km	7.12 Lge/100km	N/A	3.37 Lge/100km
UF-Weighted AC Electrical Energy Consumption	N/A	N/A	N/A	10.39 kWh/100km
UF-Weighted WTW PEU	774 Wh PE/km	624 Wh PE/km	N/A	195.6 Wh PE/km
UF-Weighted WTW GHG Emissions	253 g GHG/km	204 g GHG/km	N/A	118.4 g GHG/km
Criteria Emissions	Tier 2 Bin 5	Tier 2 Bin 5	N/A	Tier 2 Bin 5

Compared to the stock vehicle, overall efficiency is much higher than the stock vehicle for both CD and CS operational regimes. As a result, the UF weighted EC values are also much improved from the stock vehicle. Overall greenhouse gas (GHG) emissions and EC have reduced corresponding to the improved efficiency. A large CD range allows for heavy CD weighting with the UF. This leads to additional gains. Vehicle mass increased dramatically due to the addition of the high-power electrical components in the hybrid architecture, namely the ESS. Total vehicle power available has increased across all vehicle speed ranges, allowing for better acceleration in both starting acceleration and highway passing acceleration metrics.

In addition to numerical design targets, vehicle driveability was a prime concern. A highly efficient vehicle may not necessarily drive in an acceptable manner, compromising both ride feel and traffic safety. The competition event assessing this vehicle behaviour utilized industry-grade instrumentation placed strategically around the vehicle to measure response delay, stumble, peak acceleration, surge, kick, jerk, and initial bump. The vehicle control system was designed in a way that addresses these performance metrics to produce smooth and predictable vehicle operations under all operational conditions.

Another competition requirement is that the control strategy be passive. This means the control strategy cannot incorporate additional information input by the user, and must run based on only driver pedal input requests (brake and accelerator) as well as key and shift lever positions.

3.2.2.Operational Flexibility

The UVic vehicle architecture has tremendous operational flexibility. Primary operational regimes possible with the component architecture can be broken down into 3 primary categories, as discussed in the following subsections. Maintaining the operational flexibility is a core design driver for the architecture, allowing the projected efficiency and performance gains in the VTS.

Electric Vehicle Mode Operation

EV operation mode is the simplest regime from a controls perspective. In this mode, the ICE is off, and transmission is in neutral, with all drive power being supplied by the RTM. This regime is active in CD situations where the ESS has surplus charge to use for driving. The power path of this operational mode is shown in Figure 36[42].

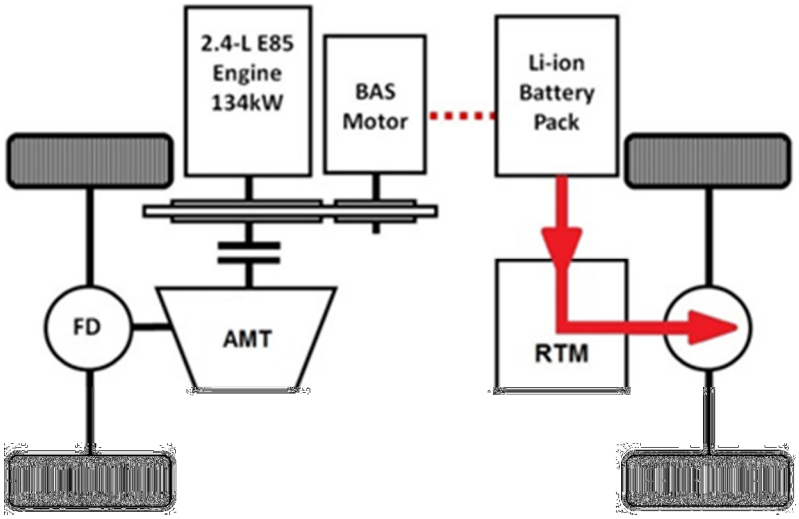

Figure 36: EV Operation Power Path

(Image courtesy of the UVic EcoCAR2 team)

Belted Alternator Starter Conventional Hybrid Mode Operation

BAS conventional hybrid operation is the fundamental regime during CS driving. It is split into two sub-modes: conventional operation mode, and BAS operation mode. During conventional operation only the ICE provides tractive power, with all electrified systems being inactive. During BAS operation, the BAS is engaged and may add or subtract power to the ICE in powering the wheels, allowing for manipulation of the ICE operation point and maintenance of average ESS SOC. In both sub-modes, the BAS is used to start and stop the ICE as needed. Both sub-modes are shown in Figure 37 and Figure 38[42].

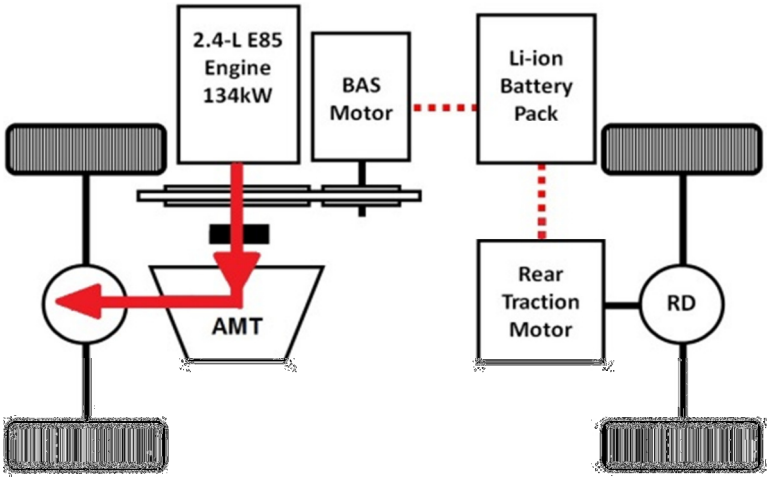

Figure 37: Conventional Operation Power Path

(Image courtesy of the UVic EcoCAR2 team)

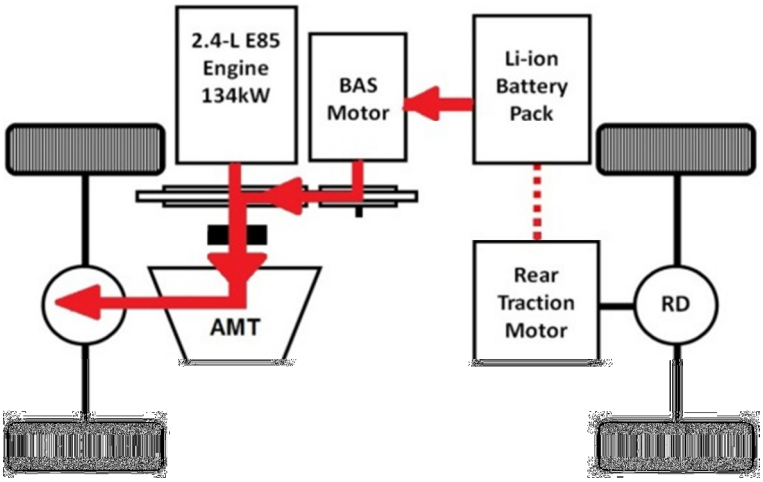

Figure 38: BAS Hybrid Operation Power Path

(Image courtesy of the UVic EcoCAR2 team)

Series-Parallel Hybrid Mode Operation

Series-Parallel hybrid operation is used when determined to be beneficial by the vehicle controller logic. It can be active in either CD or CS driving as needed. It is split into two sub-modes with different typical purposes: Series-Parallel high power operation and Series operation. During Series-Parallel high power operation, AWD functionality is realized through using both the ICE and RTM to power the drive axles. The BAS is also

engaged, and may add or subtract torque from the ICE to manipulate efficiency and maintain ESS SOC. During series operation, the transmission is set to neutral and ICE torque is converted to electrical energy relayed over the HV bus. The RTM is the sole provider of tractive power. ICE power regeneration is set based on average driver power demand to maintain the ESS SOC. This sub-mode is typically beneficial during low power, traffic creeping situations during CS driving. Both sub-modes are shown in Figure 39 and Figure 40[42].

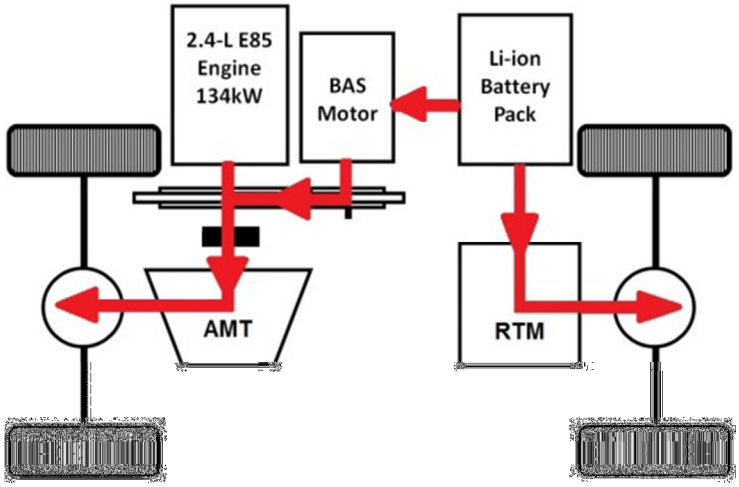

Figure 39: Series-Parallel High Power Operation Power Path

(Image courtesy of the UVic EcoCAR2 team)

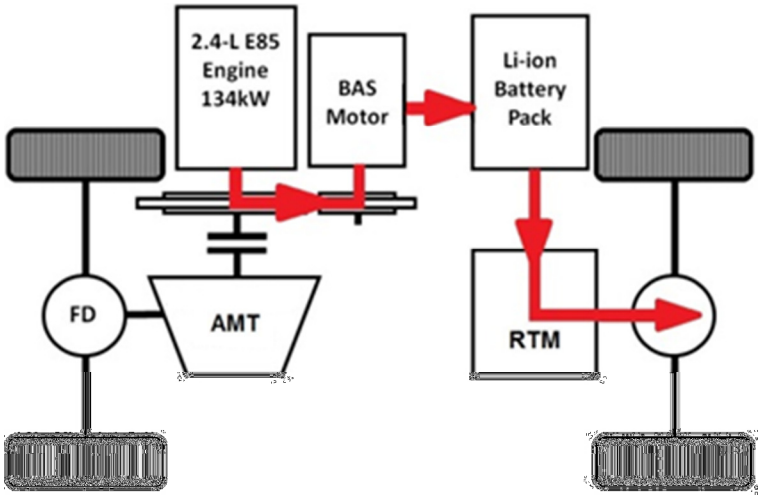

Figure 40: Series Hybrid Operation Power Path

(Image courtesy of the UVic EcoCAR2 team)

Regenerative Braking

In all sub-modes discussed in the preceding subsections, regenerative braking can be applied via the RTM when requirement dictates. Regenerative braking is applied with 2 criteria. The first is a passive regenerative braking applied when the driver torque request is zero, occurring when the accelerator pedal is not depressed. This generates a mild resistance to slow the vehicle down, similar to resistance from coasting in gear for a conventional ICE vehicle. The second is an active regenerative braking which is proportional to the brake pedal depression percentage and is applied over top of the mechanical hydraulic assist braking in the stock vehicle chassis.

3.3.Model-Based-Design Process

MBD allows for the leveraging of continuously developed model simulation platforms to enable development of robust performance-driven systems. It is essential for performance prediction and optimization, and system safety validation during controls development. Development of the vehicle control system was accomplished using a MBD approach and high-fidelity industry component models running in a custom simulation platform.

3.3.1. Development Process Flow

The control system has been developed using an iterative systematic approach, with algorithm and model development preceding incremental testing. A high-level view of the method employed is outlined in the modified V diagram shown in Figure 41[43].

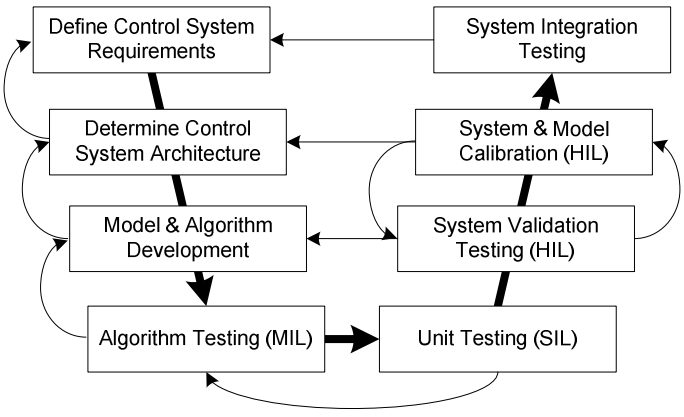

Figure 41: Controls Development V-Diagram

(Image courtesy of the UVic EcoCAR2 Team)

If a development obstacle or design failure is encountered in the descending arm of the V diagram, the previous stage is revisited and corresponding steps repeated. Failure at any stage of the ascending arm of the V results in a return to the related development stage; any revisions always pass through all subsequent development and testing stages up to the level where the failure originated. A step-by-step explanation of the V-diagram follows:

Define Control System Requirements

The vehicle control system functional requirements were determined in year 1 based on the team VTS. All vehicle systems requiring control input were identified, and high level descriptions of required controller inputs and outputs (e.g. vehicle speed input, torque command output) were formulated. Component technical specifications, as well as the expertise of vendors and team mentors were used at this stage.

Determine Control System Architecture

The functional and I/O requirements of the control system were generated to design the sophisticated supervisory hierarchy. The control system architecture was updated and modified several times throughout the 3 year process to facilitate improved functionality and workflow, resulting in an iterative development.

Model and Algorithm Development

High-level Simulink models of the vehicle systems, which reflect the team's selected architecture, were constructed using the dSPACE automotive simulation model (ASM) as a base plant structure. Concurrently, a vehicle supervisory controller (VSU) model was developed in Simulink. The sections of the model that were to be used in the supervisory controller were kept separate from the plant model so the two could be compiled separately into machine code for ease of use later in the development process. Both models are continuously updated as new information relating to the vehicle design becomes available or if any design changes come about.

Algorithm Testing (MIL)

Model-in-Loop (MIL) assessments include vehicle performance tests and examining energy management and control algorithms to uncover errors. In this level of testing, the control algorithms directly command physical responses in the plant model. Messages sent between the control and plant models during this stage use physical units of torque, speed, power, etc. The focus is on overall plant system behaviour given a set of control instructions. Intricacies related to controller area network (CAN) messaging and hardware signals (digital and analog I/O) not included as part of the simulation. Details such as start-up procedures and component initializations are not included, rather components are treated as always ready and directly controllable plant elements,. Individual control algorithms for particular sub-components are developed first in isolation using a MIL procedure prior to system integration and higher order testing procedures as explained below.

Unit Testing (SIL)

Software-in-Loop (SIL) analysis, is performed once the fundamental control algorithms have been tested and validated within a MIL environment. At this step, messages between the models are conditioned to imitate how they will be transmitted on-board the vehicle, however, the analysis is not performed in real time, but rather at the rate determined by the simulation computer CPU capability. All hardware and communication signals are modeled at this stage. For example, throttle position signals were converted to a discretized voltage range corresponding to the output of the physical throttle. VSU software interactions with plant hardware controllers (ECUs) are also fully modeled. For example, component start-up procedures and handshaking requirements are simulated with associated software execution latencies included in the simulation.

System Validation Testing (HIL)

System validation testing and calibration via Hardware-in-Loop (HIL) was performed using a hardware simulator and VSU connected with all analog, digital, and serial I/O replicated per the vehicle real-world interfacing, and system functionality was verified. Some key discoveries at this stage of testing resulted in changes to the CAN architecture of the vehicle, and identified issues with sensor and wiring configurations, allowing

revisions to controller interfacing prior to in-vehicle testing. Since actual vehicle hardware is used in this testing, code run-time, and any unpredictable software interactions resulting from processor response latency can also be identified and corrected appropriately. In HIL testing, the control system is run in real-time with the hardware simulator executing plant simulation at a rate equal to with real vehicle operation. The intention of the implementation is that the VSU is tested with identical inputs and feedback as what it will encounter when deployed in the vehicle. In addition, communication between the vehicle control modules was modified to model CAN messages with dSPACE real-time interface (RTI) CAN and CAN multi-message (CANMM) libraries. All CAN messages are transmitted and received over a test bus connecting the HIL and VSU using message transmission rates as in the real vehicle.

System and Model Calibration Testing (HIL)

As vehicle hardware components became available, they were bench tested in conjunction with the hardware test setup to validate sub-component behaviour. This in turn produced updates to be made to the vehicle plant model soft electronic control units (ECUs) as discrepancies between model and bench test behaviours. To maximize inter-changeability of HIL-interfaced components and integrated plant models, in-model hardware-enabling switches were utilized.

System Integration Testing

The final stage of control development involved full vehicle integration; the ECUs will be hooked up directly to the vehicle possible. Testing progressed through chassis dynamometer testing and road testing. For all safety-critical modifications to control code, previous testing levels were re-validated prior to on-road and in-vehicle testing.

3.3.2. Design Failure Mode Effects Analysis and Test Case Feedback

Design Failure Mode Effects Analysis (DFMEA) is an industry standard tool used to aggregate and assess the effects of particular failures within an engineered system. An aggregate rating is determined through attempts at quantifying 3 criteria ratings: a rating for failure frequency, a rating for difficulty of system detection of failure, and a rating for the severity of the failure outcome[44]. Failures with high overall aggregate ratings must

be prioritized in the design process to determine and implement appropriate mitigation techniques, either passively or actively via the vehicle control system.

Together, DFMEA and the desired general system functionality determine the overall control system requirements. Control system requirements are used to develop algorithms, which are tested and integrated into the overall vehicle system. Test feedback from each stage of development is used to feed back into the algorithm development. This process is shown in Figure 42[45].

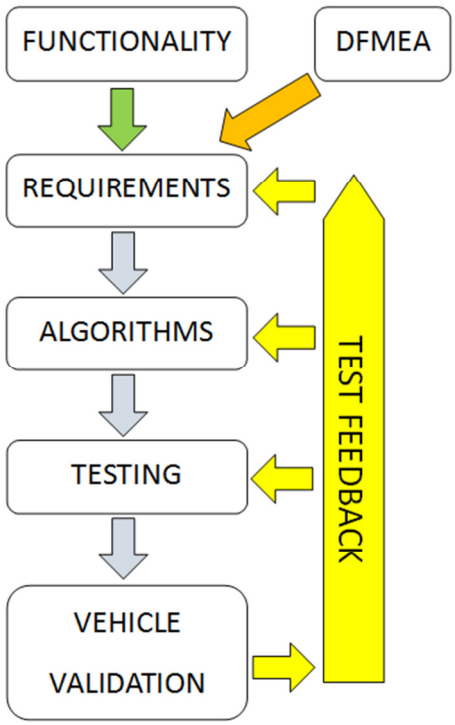

Figure 42: Controller Requirement Feedback

DFMEA drove safety critical control requirements and associated system test cases for the Controls team. A separate DFMEA was developed for each major vehicle subsystem in order to explore different failure effects for the overall system. It was assumed that GM and other component manufacturers have already utilized DFMEA to mitigate issues internal to their components or subsystems, and therefore emphasis was placed on newly integrated vehicle components, as well as component interactions with the system.

The VSU plays a critical role in mitigating potential safety concerns. Feedback from various system components and comprehensive diagnostic routines allow for mitigation action to be applied in the case of a potentially hazardous failure or system state. These diagnostics are the direct response to the DFMEA, and are tested for functionality through the V-diagram.

Unexpected vehicle behaviour posing a safety concern noted at all levels of testing (SIL, HIL, vehicle) is investigated and mapped back to new requirements for additional safety control requirements, which result in the development of additional algorithms to mitigate the new concerns. While apparent failure modes were anticipated early in the development cycle to give a basis of safety critical functionality to start with, continuous testing results in an iterative process which expands requirements.

3.3.3.Automated Testing

The development pace for the vehicle control system was fast throughout the development process. The high system complexity and high risk danger ramifications of testing the vehicle control system on-road result in necessary automated system testing procedures being integrated into the system validation process. Automated testing was conducted on two levels: safety critical operation testing and performance driven optimization testing.

Safety Critical Automated Testing

Regression testing is used to validate code functionality against developed test cases on a periodic basis moving forward with development. Test cases are stored in a test case library, which constitutes all the functional tests required to validate the system behaviour. This provides confidence that the system functions with newly implemented code throughout development cycles. Regression testing is often an iterative process during a testing cycle. Automated testing will usually be executed after the system integration testing phase and any errors which are introduced will result in implemented code being regressed.

Development and deployment of a regression test platform for controller development was a primary goal of the modeling and simulation activities conducted throughout the

EcoCAR2 VDP. Safety critical algorithm test cases were identified and treated as most critical to integrate into the regression automated testing platform. These algorithms were prioritized due to the life safety ramifications for vehicle testing.

Testing of individual controller functionalities go through multiple stages which fall in-line with the development of the algorithm and implementation of the V-diagram. Successful testing of an algorithm allows the generation of an automated test routine to allow for a regression platform which continuously evolves and advances with the controller development process as more functionality passes through the V-diagram development process. This process flow is shown in Figure 43[45].

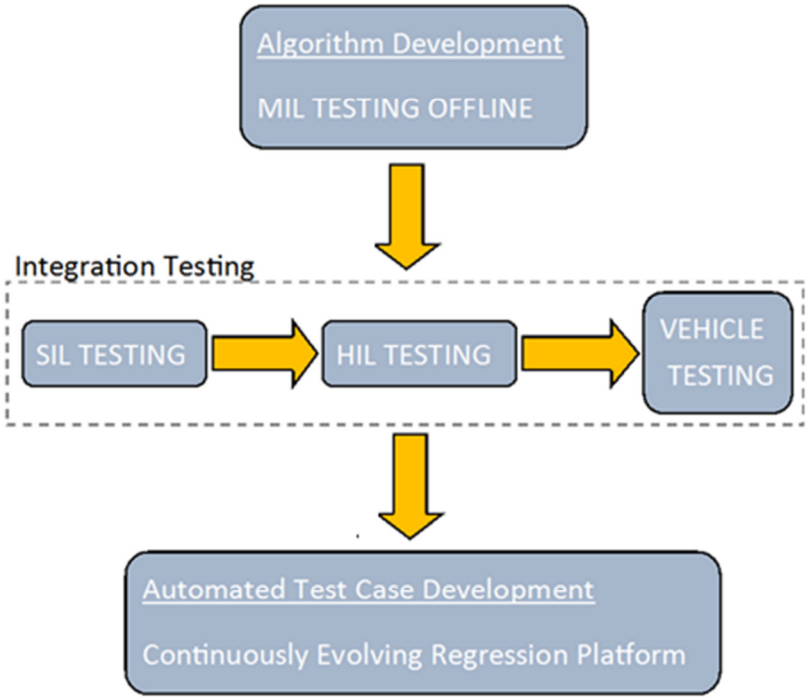

Figure 43: Process Flow from Algorithm Development to Automated Regression Test Platform Integration

Safety critical automated testing was conducted using dSPACE AutomationDesk interfaced with the UVic vehicle plant model simulation. Variables in the plant were manipulated using AutomationDesk to provide input coverage for a given algorithm while driving, with the controller output behaviour resulting in either a pass or a fail. An example of test output is shown in Figure 44 courtesy of the UVic EcoCAR2 team[45].

The test shows a successful pass state granted to a safety critical accelerator pedal diagnostic algorithm which detects an out of range value on one of the two accelerator pedal potentiometer sensors, and passes on only the valid input, rather than trying to average the two inputs as would be the typical control action[45].

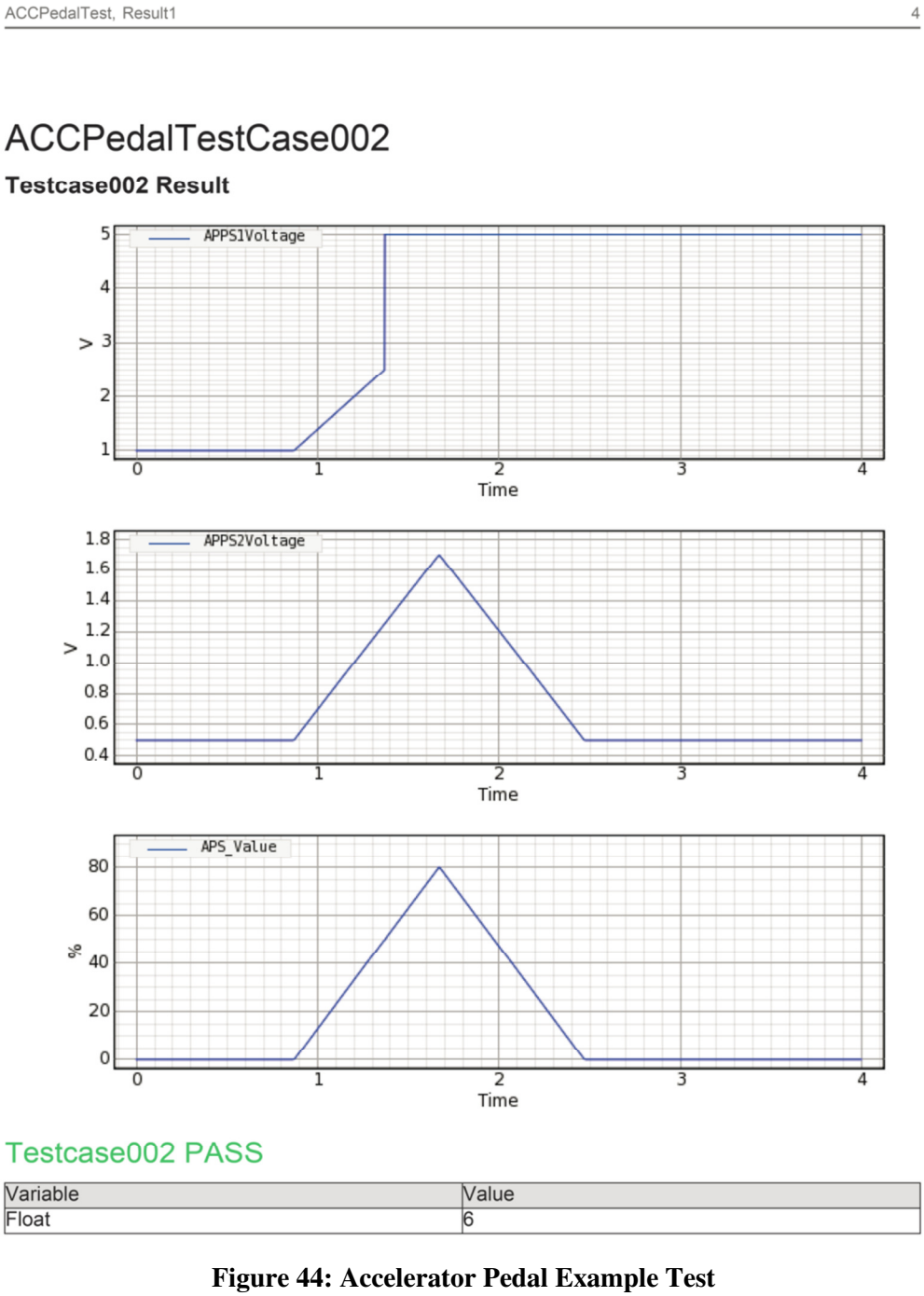

Figure 44: Accelerator Pedal Example Test

(Image courtesy of the UVic EcoCAR2 Team: Automated test by Herbert Zhu)

Performance Automated Testing and Optimization

The flexibility of the UVic EcoCAR2 PHEV vehicle architecture allows for significant optimization potential through manipulating operation regime functionality, and optimizing selection of various operation modes available to propel the vehicle. Optimization requires consistent metrics for evaluation. In the case of optimization of the vehicle control system over a given drive cycle, it is important to have an automated test process for following drive cycles for various control tuning set-points.

All of the vehicle simulation platforms used in the vehicle development process were built with the capacity for automated drive cycle evaluation. This was accomplished through the use of a driver model which seeks to track the desired vehicle speed curve of the drive cycle through application of the accelerator and brake pedal. This action was simulated using separately tuned P-I control for each pedal. The control system logic was constructed with tuning variables to allow variance of control function while running a given cycle. This provides the fundamental framework for vehicle performance evaluation as well as active tuning optimization, as will be discussed in Chapter 5.

3.3.4.Process Documentation and Development Team Organization

Each controller algorithm is defined by a requirement for functionality and a counterpart list of test cases for validation. Given the team effort required to integrate the control system, process documentation was required to track the efforts of each developer. Test cases were tracked throughout the development process using the ‘Master Test Case Summary’ document, an excerpt of which is shown in Table 7. In addition, each algorithm test is documented in a separate ‘Test Case Document’ used to track progress in implementing and testing algorithms through the V-diagram process. A sample test case document is also shown in Figure 45.

Table 7: Master Test Case Summary Document Excerpt

Ring	Test Case ID	Algorithm Functionality	MIL	SIL	HIL	VIL	Automation Ready
System Moding	SU01	**Functionality Driven Requirement** Initialization of MABX, ESS, APM, RTM, BAS, Transmission, ICE upon key start to their correct operational states.	Pass	Pass	Pass	Blocked	Yes
System Moding	ENA01	**Safety Driven Requirement** Loss of CAN at VSU results in shutdown of vehicle energy sources and disabling of torque production. MIL and SIL testing is not applicable to this algorithm, as it is only meaningful in hardware platforms.	N/A	N/A	Not Started	Not Started	No
System Moding	SD01	**Functionality Driven Requirement** Shutdown of MABX, ESS, APM, RTM, BAS, Transmission, ICE upon vehicle shutdown by driver	Pass	Pass	Pass	Not Started	No

TEST: BAS05

BAS Temperature Derating Diagnostics

EcoCAR2 PLUGGING IN TO THE FUTURE

University of Victoria British Columbia • Canada

Control Algorithm Functionality:

This algorithm provides logic for derating the performance of the BAS motor depending on temperature.

If the temperature of the motor is above an initial threshold, the performance of the motor will start to decrease. At an upper threshold, the motor will provide 0 torque output. BAS_epo will be sent if this upper threshold is reached, since the cooling system must have been malfunctioning in order to occur.

Test Level Applicability: MIL, SIL, HIL, in-Vehicle

In-Vehicle Test Notes: There is a percent derating signal in the BAS controller code that will be monitored in Control Desk as the vehicle is driving.

MIL	SIL	HIL	Vehicle	Automated
Not Started	Not Started	Not Started	Not Started	N/A
				N/A

Test Result Notes and Recommendations:

Figure 45: Sample Test Case Document

The Test Case Summary Sheet provides a central resource for the controls team that contains the test level validation for each test case and algorithm in the controller. The information contained includes

- the control subsystem containing the algorithm tested by test case,
- a brief description of the algorithm functionality being tested by the test case,
- definition as either a safety critical or functionality driven algorithm test case,
- an algorithm ID (Test Case ID) used for categorizing and tracking control model changes throughout development that references the Test Case Document,
- MIL algorithm validation status,

- SIL algorithm validation status,
- HIL algorithm validation status,
- vehicle validation status,
- development status of an automated test routine in the regression test platform.

Each algorithm listed in the Test Case Summary is described in detail in a Test Case Document. Each Test Case Document includes

- test case ID and description,
- test case definition and objectives,
- pre-condition(s),
- required system inputs,
- required system outputs,
- test procedure steps,
- expected result at given simulation time,
- actual result data,
- revision (change-log) table.

Algorithms are developed once the driving requirements are established. Algorithm development is conducted by a controls developer who is responsible for a given controller component or particular sub-system functionality. This includes MIL testing to ensure algorithm functionality in isolation from the overall vehicle system.

Integration testing is conducted by controls developers who are responsible for the vehicle controller at a system level. Requirements are passed on from the algorithm developer or sub-system manager along with algorithm code to be integrated into the system as necessary. Testing is conducted manually with the entire vehicle model to ensure appropriate behaviour matches that of the MIL testing.

Automation testing is conducted by a controls automated tester. The tester is given information regarding the particular integration format of the algorithm to be tested, along with a description of the desired system response and uses this data to construct an automated test case to be added to the continuously evolving automated test regression platform.

This responsibility breakout ensures algorithm intent is preserved through the testing process. Documentation of test results in both the 'Test Case Document' and 'Master Test Case Summary' document allowed for the control team to track progress to safely release algorithms for in-vehicle testing and subsequent use.

3.3.5. Multi-Platform Controls Development

Multiple controls development platforms were employed in tandem to develop the control system for the UVic EcoCAR2 vehicle. This was done to facilitate more effective parallel development paths, but also was used in the strategy optimization process. The interface between the control strategy and the rest of the model was kept consistent between the two platforms to facilitate migration of optimized strategies from the simplified model to the SIL platform model; however the underlying plant models and controller-plant interfaces are very different. A summary of major differences is shown in Table 8.

The general reason behind the extreme level of complexity, and associated computational overhead, of the SIL platform model is that the simulation needs to capture all of the software and communication interactions occurring within the vehicle during operation to allow troubleshooting of low-level problems before in-vehicle testing. In contrast, the simplified MIL platform model is used to assess high level aggregate model performance and conceptual behaviour while running drive cycles with various control strategy

implementations. As a result, the chain of events resulting in a component response, which would be modelled in full detail on the SIL platform, can be cut down to the minimum level of detail required to capture the system behaviour on a high level.

Table 8: Comparison of Model Features for SIL and MIL Models

SIL Development Model	MIL Development Model
High fidelity with the capability to validate low level controls operation details	Low fidelity, with the capability of assessing aggregate performance metrics
Utilizes industry-level subsystem models from dSPACE ASM libraries for ICE, drivetrain, vehicle body, ESS	Uses SimDriveLine vehicle dynamics block and static power loss tables for powertrain components
1.5 seconds runtime per simulated second (on research computer)	0.07 seconds per simulated second (on research computer)

Both simulation model platforms used in tandem allow for parallel development and testing of the energy management strategy and detailed control system implementation. More computationally expensive processes such as optimization work is conducted on the MIL model and then the results are ported to the SIL model for detailed testing and validation.

Software-in-Loop (SIL) platform

The SIL development platform is an integrated simulated environment including both a detailed plant model and the controller code structure. Communication between the controller and plant is modelled to be a realistic representation of actual vehicle controls communication. Digital, analog, and CAN communication is configured to accurately represent the individual component-controller interactions that exist in the real system. Thus, plant component models also include simulated ECU behaviour to communicate with the controller realistically. Controller commands are received by the component

soft-ECU simulation which responds accordingly to actuate the physical component model. Readings from the physical component model are sensed by the soft-ECU and relayed realistically to the vehicle controller as CAN feedback signals. This configuration is shown in Figure 46.

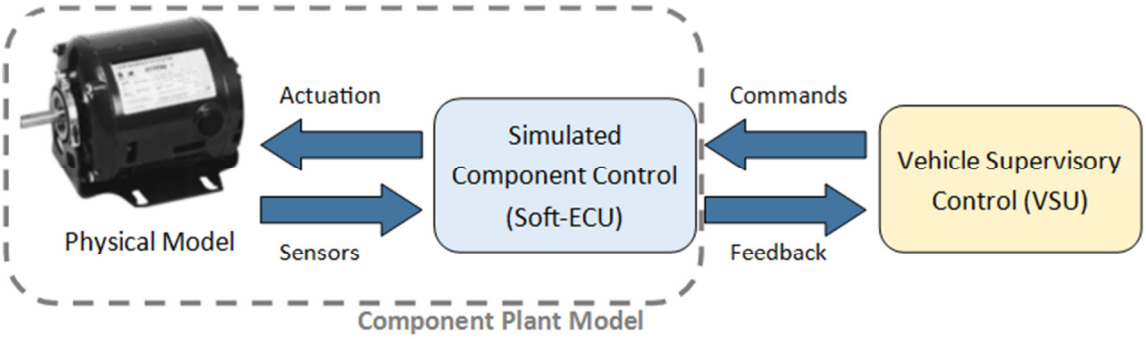

Figure 46: SIL Platform Soft-ECU Interaction

The plant physical component models are high fidelity, allowing the capability of detailed system validation and fault prediction. Detailed physical models combined with soft-ECU representation allows for validation of communication and initialization configurations. This level of detail is required for developing diagnostic algorithms and safety critical robust operation.

Physical component model detail varies by component. Some system components are modelled as part of the dSPACE ASM package, which provides very high fidelity modeled results. Other models were provided by manufacturers and allow for less insight into their inner workings. Both scenarios above yield models that should allow for great confidence in detailed results due to the high level of industry effort which has been devoted to their generation. Table 9 shows some summary information regarding the inner workings of each modeled component within the SIL simulation platform.

Table 9: SIL Component Model Summary Information

Component	Model Source	Simulated Operation
ICE	dSPACE ASM Gasoline ICE Model	Industry-tuned ICE model with physical simulation of air system, fuel system, piston ICE mechanics, fuel combustion kinematics (homogenous and stratified), exhaust-gas recirculation. Custom soft-ECU developed representing observed controller behaviour for diagnostic feedback and operational signals from ICE.
ESS	A123-developed physical and ECU model	Industry-tuned battery model with physical simulation of capacitance, resistance, inductance, ion diffusion, thermal behaviour. Provided detailed soft-ECU of A123 pack communication behaviour.
RTM	Magna E-Drive product data	Power-loss model based on manufacturer documentation with maximum power, torque, speed limitations. Custom soft-ECU developed representing recorded signal feedback during component start-up and operation including fault monitoring.
BAS	TM4-developed physical and ECU model	TM4 provided MG model with obscured underlying operation. Custom soft-ECU developed representing recorded signal feedback during component start-up and operation including fault monitoring.

Transmission	dSPACE ASM automatic transmission model	Industry-developed transmission model with physical representation of defined gear ratios, torque converter, clutch pack slip. Custom soft-ECU developed representing recorded signal feedback during operation.
Driveline	dSPACE ASM driveline models	Basic gear ratio multipliers for torque and speed throughput to drive axle.
Vehicle Loads	dSPACE ASM vehicle loss models	dSPACE longitudinal vehicle dynamics with tuning for Chevrolet Malibu drag behaviour and UVic HEV mass.
Driver	P-I Simulink control with dSPACE tuning	Basic P-I tuning developed by dSPACE to represent driver behaviour while following a drive cycle.

The major drawback for the platform is that the maximum runtime speed for a typical workstation is quite slow as shown in Table 8. This makes it unsuitable for conducting iterative optimization. Its increased complexity makes it undesirable for developing advanced controls energy management strategies.

Simplified Model-in-Loop (MIL) Platform and Validation

The simplified MIL platform is comprised of a SimDriveLine based vehicle model, component power loss models, and an interfaced energy management strategy. Since powertrain components are modeled simply as power loss tables, detailed component transient effects are not captured. Additionally, component ECU behaviour is not simulated, so supervisory controller inputs directly result in output response from components, accounting for any physical component performance limitations.

Model detail is kept simple in the MIL model to speed up computation. Manufacturer-provided data was used to construct quasi-static models built on component power loss lookup tables. Table 10 shows some summary information regarding the inner workings of each modeled component within the simplified MIL simulation platform.

Table 10: Simplified MIL Component Model Summary Information

Component	Model Source	Simulated Operation
ICE	ANL Autonomie LE9 static model data	Power loss component model with maximum torque limits, static fuel map.
ESS	A123 product data	Power loss component model with terminal voltage curve, cell internal resistance losses.
RTM	Magna E-Drive product data	Power-loss model based on manufacturer documentation with maximum power, torque, speed limitations and static efficiency map.
BAS	TM4 product data	Power-loss model based on manufacturer documentation with maximum power, torque, speed limitations and static efficiency map.
Transmission	SimDriveLine variable gear ratio model block	Variable gear-ratio SimDriveLine block with transmission gear ratios entered.
Driveline	SimDriveLine connector blocks	Basic gear ratio multipliers for torque and speed throughput to drive axle.
Vehicle Loads	SimDriveLine 2-D vehicle dynamics blocks	SimDriveLine longitudinal vehicle dynamics with tuning for Chevrolet Malibu drag behaviour and UVic HEV mass.
Driver	P-I Simulink control with dSPACE tuning	Basic P-I tuning per dSPACE ASM model suite to represent driver behaviour while following a drive cycle.

The low level of fidelity makes the MIL platform unsuitable for development of lower level component interface algorithms and drive tuning algorithms. The quick run-time, as noted in Table 8, and relative simplicity make it a good platform for developing energy management strategies in a manageably isolated, yet relevant simulation framework.

The simplified MIL model may be validated by comparing their relative output over a set drive cycle. Since the procedural intent is to use the pair of platforms for expedited energy management optimization, power and EC are the most relevant metrics for validating model co-relevance.

A US06 City cycle was used (displayed in Figure 75 in detail) for both models and both electrical and fuel power and energy uses were compared using an identical control scheme as described in detail in Chapter 4. The results are shown in Figure 47 through Figure 50.

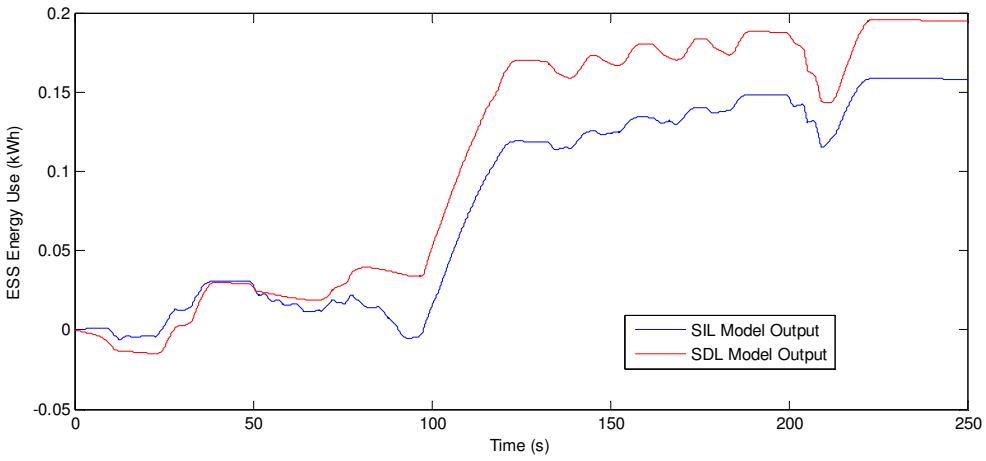

Figure 47: SIL and MIL Model Comparison – ESS Energy Consumed

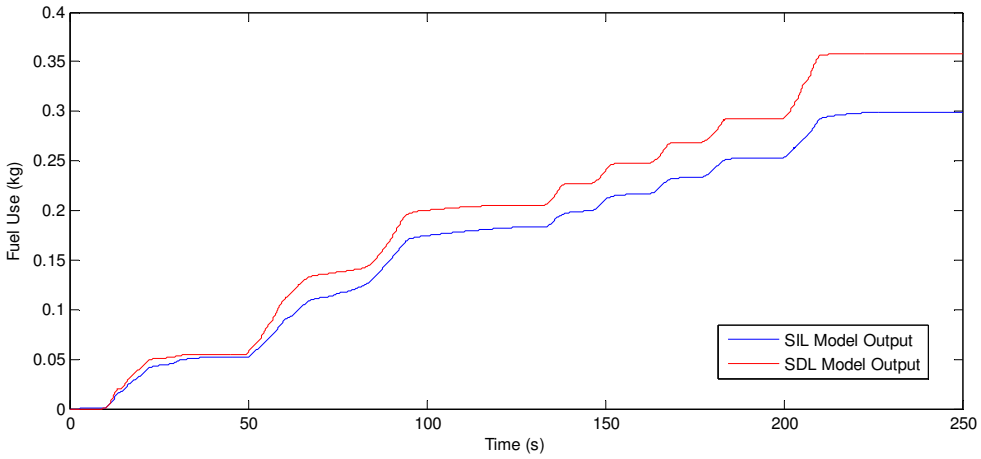

Figure 48: SIL and MIL Model Comparison – Fuel Consumed

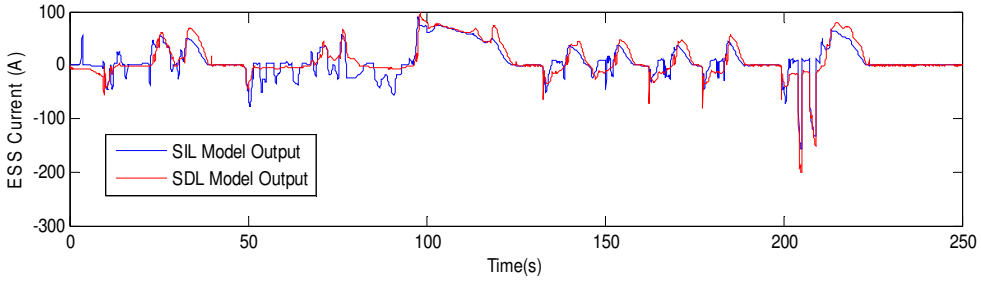

Figure 49: SIL and MIL Model Comparison – ESS Current

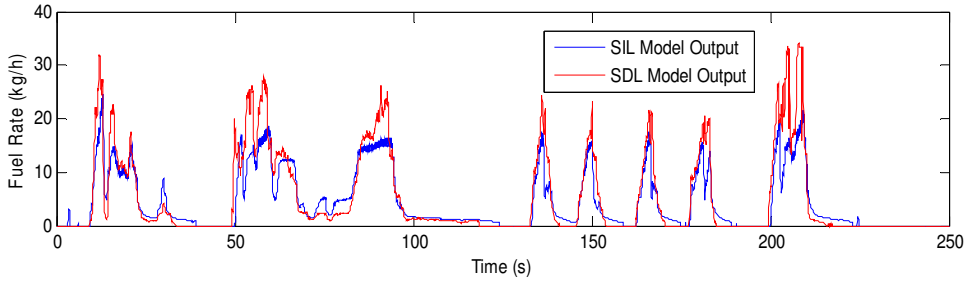

Figure 50: SIL and MIL Model Comparison – Fuel Rate

While there are visible differences in some transient behaviour response seen in the power use comparison plots, energy use over the cycle is characteristically similar. The normalized root mean square error (NRMSE) between the instantaneous power usage for each model is shown in Table 11 and calculated as follows[46]:

$$NRMSE = \frac{\sqrt{\sum_{cycle}(P_{MIL} - P_{SIL})^2}}{\sqrt{n}(P_{SIL}^{MAX} - P_{SIL}^{MIN})} \quad (3)$$

where:

P represents the power use metric used (fuel use, current, power, etc.)

n represents the number of data points collected during the cycle

Table 11: Normalized Root Meet Square Error of SIL and MIL Model Platforms

Metric	NRMSE
ESS Current (A)	0.0616
ESS Power (W)	0.0617
Fuel Rate (kg/h)	0.1449

3.3.6. SIL to HIL to Vehicle Validation

Progression through the V-diagram involves iterative feedback to regressed stages of development. As such, testing platforms must be set up for efficient transfer of various code algorithms between the different levels of testing validation.

The UVic plant model was configured for seamless transition between SIL and HIL simulation platforms. This was accomplished through the use of Simulink switches which change the plant simulation interface source from the embedded SIL Simulink controller code, to physical input dSPACE library blocks interfaced with the HIL simulator digital and analog I/O. In order for this to function properly, The SIL and HIL controller code and vehicle simulations were required to be identically configured. This was made possible through use of Simulink code libraries for major subsystem functionality, which interface to the vehicle simulation plant model through I/O configuration mapping blocks, translating the controller logic into representations of the I/O messages and signals. Thus, the vehicle simulation can either accept inputs from the vehicle controller hardware (HIL), or from the virtual controller code (SIL). Since the vehicle simulation

model running on both platforms is identical, transition between the two platforms is primarily useful for testing of hardware interactions and real I/O. The configuration of both test platforms is shown in Figure 51 and Figure 52[43].

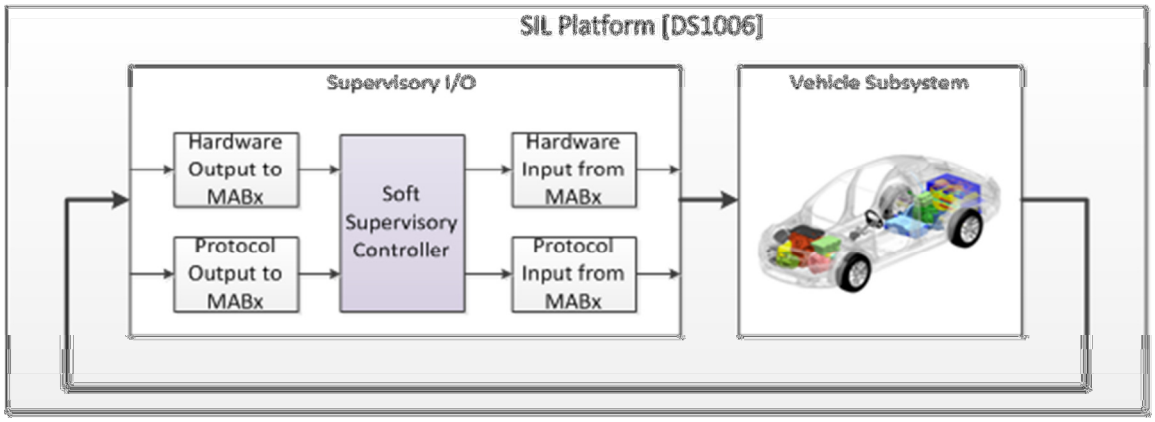

Figure 51: SIL Platform Configuration

(Image courtesy of David Killy and the UVic EcoCAR2 Team)

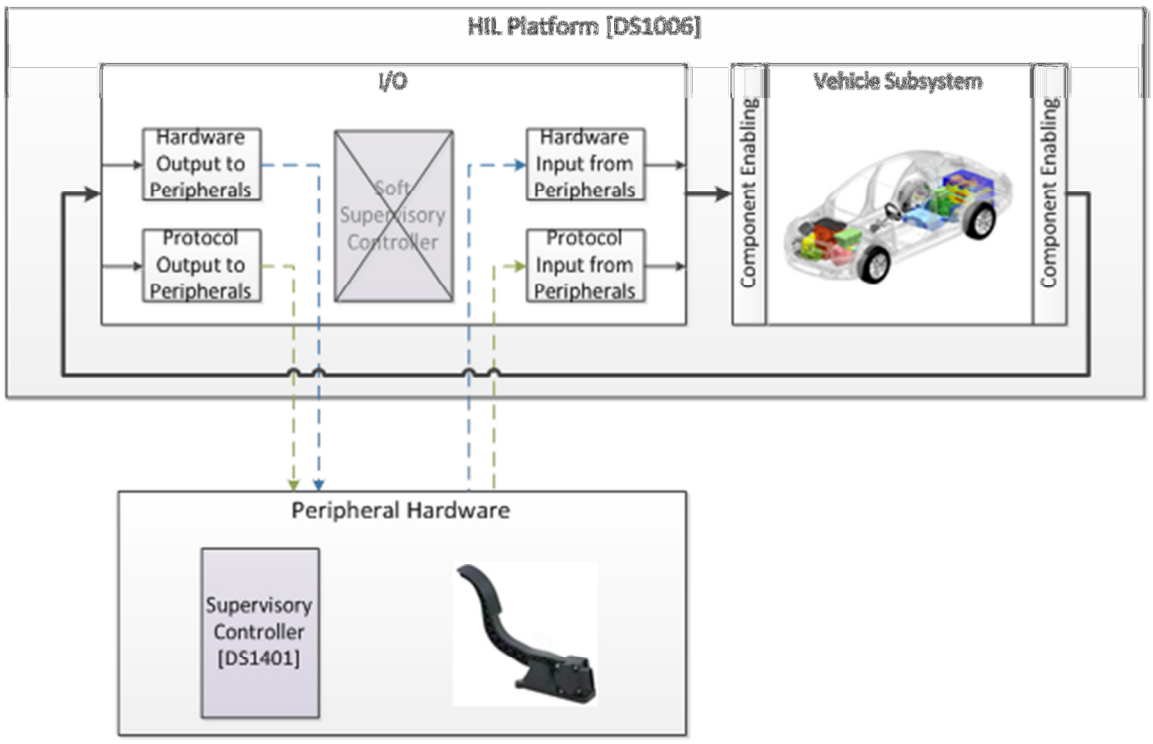

Figure 52: HIL Platform Configuration

(Image courtesy of David Killy and the UVic EcoCAR2 Team)

Transition between HIL validation and in-vehicle testing was possible through harmonization of the HIL platform wiring connection harness, and the in-vehicle VSU harness. Ensuring the controller I/O configuration of the HIL platform is identical to the vehicle component I/O enables seamless transfer of current controller code between the simulation platform and the vehicle. Some minor differences in I/O configuration are summarized in Appendix A.

3.3.7. Linear Vehicle Dynamics

Real vehicles driving in real-world conditions see highly dynamic loads which can be broken down into several components: lateral, vertical, longitudinal. While lateral and vertical dynamics are very important for vehicle dynamics handling, longitudinal dynamics capture the primary considerations for vehicle powertrain efficiency testing.

Longitudinal vehicle dynamics may be simplified greatly without too great an impact on end aggregate results. The free body diagram of the simplified longitudinal system is shown in Figure 53[47].

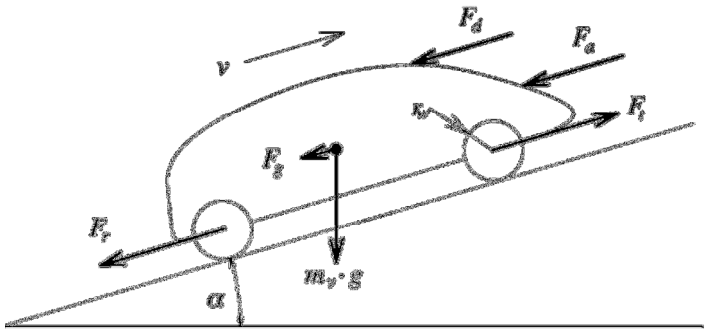

Figure 53: Vehicle Glider Free Body Diagram

(Image from Vehicle Propulsion Systems, Lino Guzzella[47])

The instantaneous vehicle power demand placed on the powertrain systems while driving can thus be expressed as[47]:

$$P_{req} = \left(m_v \frac{dv}{dt} + F_{roadload}(t) + m_v g sin(\alpha)\right) v(t) \tag{4}$$

$$F_{roadload}(t) = A + Bv(t) + Cv(t)^2 \tag{5}$$

Coefficients A and B represent constant and mass-related viscous drag on the vehicle powertrain, and C represents aerodynamic drag. In vehicle baseline consumption modeling and performance estimation, level ground is generally considered, removing the gravity component of propulsive force required. This component is nevertheless important for assessing grade climbing ability, typically considered in the context of uphill towing capacity at a given speed and grade. The SimDriveLine model and dSPACE ASM model accept drag coefficient and frontal area information (provided by GM) for coefficient C and simulate coefficients A and B with tire drag and driveline component losses. These were left as provided by dSPACE (Malibu ASM model). It is likely that A and B changed somewhat with the inclusion of the RTM in the vehicle architecture. A vehicle coast-down test would be required to validate the model inputs accurately.

3.4. Control System Development Summary

The control system development process was generally a joint effort amongst the UVic EcoCAR2 team throughout the 3 year vehicle development cycle. Physical models were constructed by the controls development sub-team in order to develop performance measures of the proposed architecture as presented in the VTS. In addition, some of the basic interfacing and design processes were developed in direct response to the requirements of the competition. Architecture selection was completed as part of the competition process using model results as justification for selection criteria.

The controls development and testing plans employing a dual simulation platform algorithm validation procedure was developed specifically to support strategy-independent vehicle subsystem validation. Individual algorithm functionality for low-level subsystem control was defined and developed by the control development team within the framework discussed in this Chapter. Model comparison validation and related work effort to ensure cross-platform compatibility and equivalent results are integral to allow the vehicle simulation model research platform to satisfy its purpose of allowing interchange-ability in the strategy component of the controller, which is discussed in detail in Chapter 4.

Chapter 4: Vehicle Control System Logic and Strategy

The UVic vehicle control system uses a multi-level logic hierarchy which allows for control responses to cascade through the different layers, each of which manages varying system considerations. This provides a framework which can readily accept varying high level energy management strategies, irrespective of exact operation, making it an ideal platform for conducting advanced HEV optimization research. A description of the different levels and an overview of the functionality contained within each layer are discussed in the following subsections with key topics as follows:

- the model hierarchical command structure developed to facilitate a strategy-independent control platform
- safety critical diagnostic functions for low level subsystem component control, driver input fault handling, system level fault handling, and system level status diagnostic functions
- system level algorithm structure developed to accept generic energy management command inputs and translate into working system level commands
- the functionality of the rule-based strategy that was developed to test and validate the control system and provide an initial basis for global optimization of the energy management strategy

4.1. High Level Controller Logic Hierarchy

The control logic hierarchy devised to implement the control system requirements is shown in Figure 54. The different levels of logic interaction allow for delineation of different functional elements within the software structure, and correspondingly delineation of different levels of testing processes.

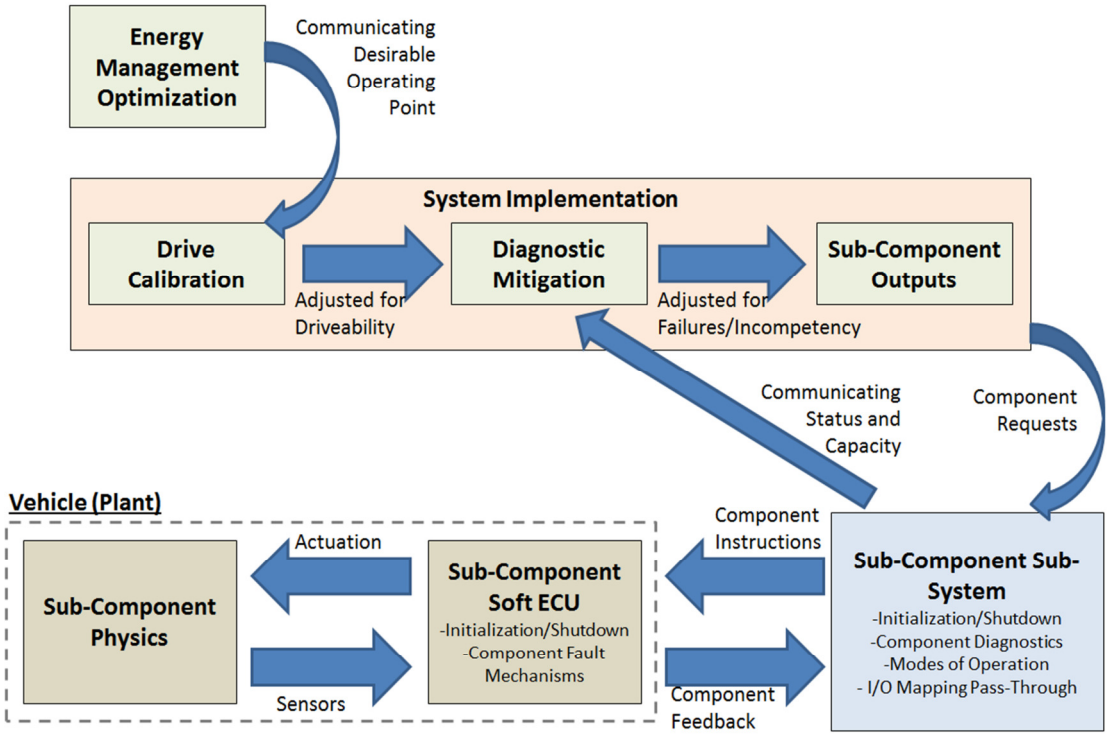

Figure 54: Control Logic Hierarchy Interactions

The control logic is implemented in 3 hierarchical levels: energy management, system implementation, and sub-component control.

The energy management level of the control system uses basic feedback real-time data from various vehicle systems required to make high level controls decisions, including ESS SOC, vehicle speed, and user torque request (driver interfaces). The decisions made at this level affect primary operation and strategy decision making. Outputs are confined to simple wheel torque requests to each powertrain component, as well as a definition of operation mode type to allow for downstream torque filtering and mode transitioning.

The system implementation level of the control system receives primary torque requests from the energy management level and applies system level driveability filtering and manipulations before passing final requests down to the sub-component control level. Feedback from component level control includes instantaneous component torque limits and operational status of each component. These are used to impose constraints and

overrides on the energy management level torque request outputs and transfer commanded torque burden accordingly. Instantaneous drive ratios are also applied here based on current transmission gear and final drive ratio to compute the correct sub-component torques. Mode transitions being signalled by the energy management level are also identified and mode transition protocols activated. Mode transitions are called each time a new primary operation mode is signalled. During these temporary transition sub-modes, component torque requests are overridden to facilitate smooth transition. Overall, these functions allow coordination between energy management level commands and sub-component level constraints. Additionally, non-strategic torque requests such as regenerative braking and creep torque are overlaid on top of the strategic component torque requests.

The sub-component level of the control system is responsible for all low-level interaction between the supervisory controller and the individual sub-component ECU. This includes start-up and shutdown algorithms and handshaking, as well as failure detection. Real-time operational data is translated to functional values to be passed up through the logic hierarchy for decision making. In addition, low level diagnostic mitigation is invoked to accomplish actions such as switching on cooling systems or limiting component torque.

4.2.Safety Critical System Design

Control system development for HEVs needs to take into special account the safety of the end system prior to completing any on-road in-vehicle validation processes. This is accomplished at both the subsystem and system level to ensure an overall safely operating vehicle with behaviour as the driver intends.

4.2.1. Subsystem Level Requirements Handling

Subsystem-specific commands and component feedback aggregation are handled in a dedicated and separate sphere of controls code, as shown in Figure 54. This allows for component-specific limitations to be compared against real-time outbound commands prior to transmission over the CAN network to the respective ECUs. Component specific limitations can be either specified by the controls developer, or they can be the result of real-time feedback coming from the respective component.

An example of a situation in which this provides safety critical operational benefits is in torque limitation handling in the RTM. The Magna E-Drive sends real-time critical data including torque production, current, voltage, temperature, and limit flags back to the VSU over the CAN network. Aggregation of this feedback via limit checks and truth table logic allows for the application of torque limits to be imposed over top of the commands coming from the energy management system. Since this occurs at the bottom level of the controller logic hierarchy, the decision to limit torque is irrespective of commands flowing downstream through the logic process.

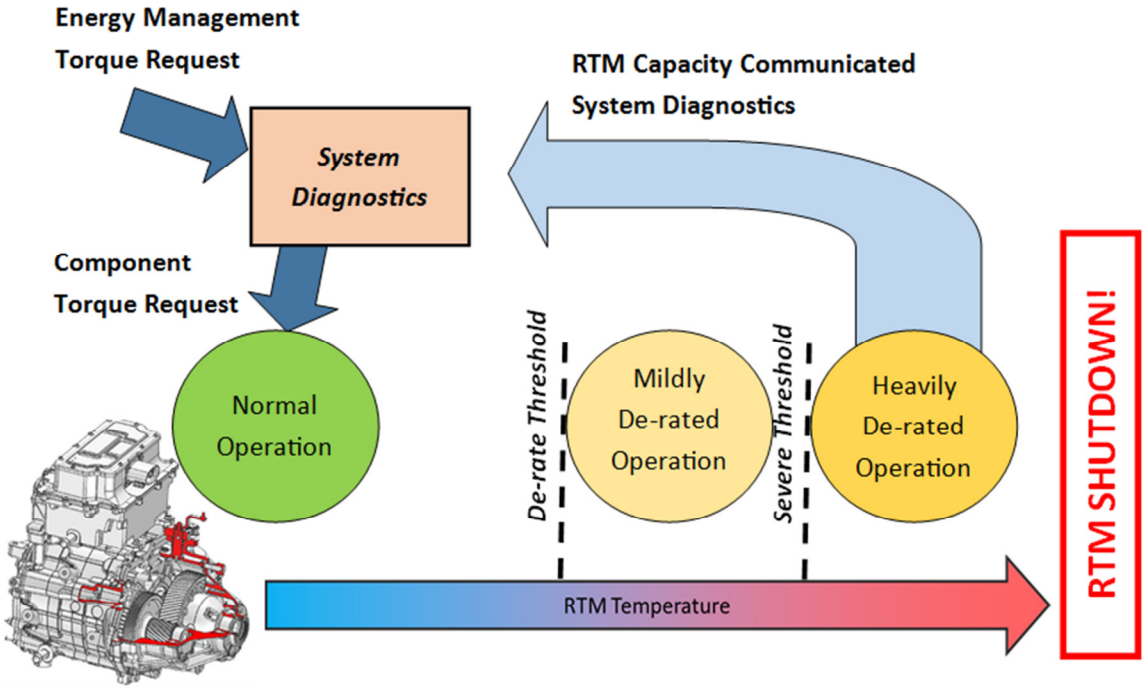

Figure 55: RTM De-rating Process Overheating

The de-rating process can is allowed to occur isolated within the subsystem control level of the system up until the point where the conditions become a failure. At this point, the subsystem level communicates back to the system level so that a controller mode switch can be made to mitigate failure of the respective drive component. This process is illustrated in Figure 55.

4.2.2. System Driver Torque Request Handling

During driving, the primary driver input is the system torque request. As this command flows through the controller logic hierarchy, computations applied to the initial value as it is distributed across the drive components are safety-critical in nature. It is of critical importance that the powertrain does not produce unintended positive or negative torque, as unintended acceleration or deceleration can cause driver accidents.

A multi-level approach is applied to ensure torque requests being received at the sub-system level match up to the original intent of the driver as communicated by the accelerator pedal position. This process accounts for both physical failures at the accelerator pedal input level, as well as logic failures throughout the control system information hierarchy. The various diagnostic steps are illustrated in Figure 56, and listed as follows:

- Accelerator pedal sensor inputs (2 analog signals) are compared against known ranges and checked for consistency. Rates of change are assessed and conditions are applied for detecting floating values resulting from bad wiring connections. Analog signals are combined and averaged to produce a percentage describing the intended torque production.

- Vehicle speed and torque percentage is input into a 2-D lookup table to produce an overall system wheel torque request, which is passed to the energy management level of the controller.

- Overall vehicle wheel torque request is distributed across the drive components according to the strategy employed at the energy management level of the controller. Known drive ratios are applied to calculate component torque request.

- Subsystem level controller spheres receive the individual component torque requests. Component level signal filtering and rate-limiting is applied, and final torque command value is sent back to the system level of the controller for validation.

- System level diagnostics receive subcomponent torques and current drive ratios. Summation of wheel torque is calculated and compared against the original torque request produced by the driver. If signals are equivalent, the sub-system controller spheres are allowed to communicate torque requests to the respective component ECUs.

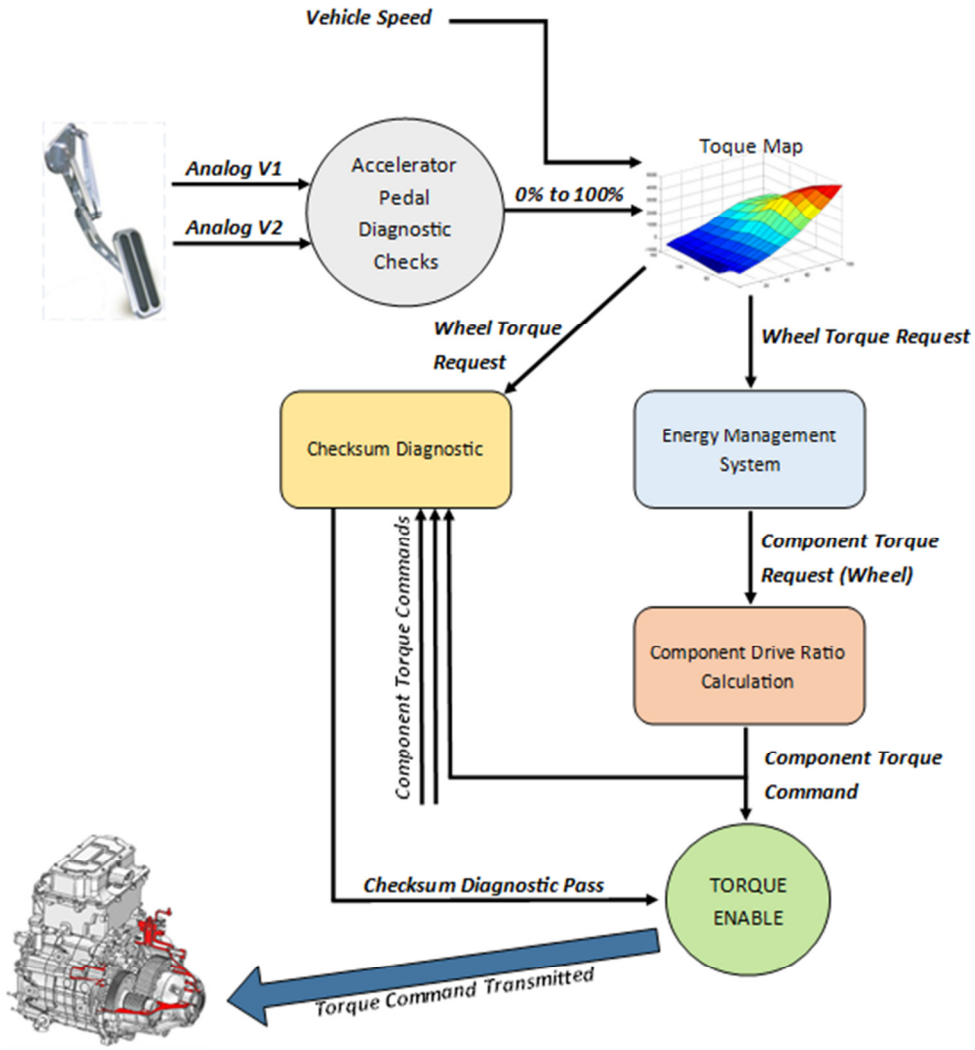

Figure 56: Driver Torque Distribution Safety Diagnostics

4.2.3. System Level Failure Mitigation Algorithms

At the system level, the potential for failures or operability interrupting faults at the component level need to be mitigated with diagnostic algorithms which detect and respond to the failure. This is essential for failures in drive systems, as failure resulting in unintended acceleration or loss of power could result in an accident.

One significant safety risk in the case of failure is a mechanical failure of the belt interface bridging the ICE and BAS. Since the BAS is often acting as a generator, failure of this interface could result in unintended acceleration as a result of the ICE torque surplus not being taken up by the BAS regeneration. Diagnostic mitigation was developed to facilitate a mode switch in the case of such failure.

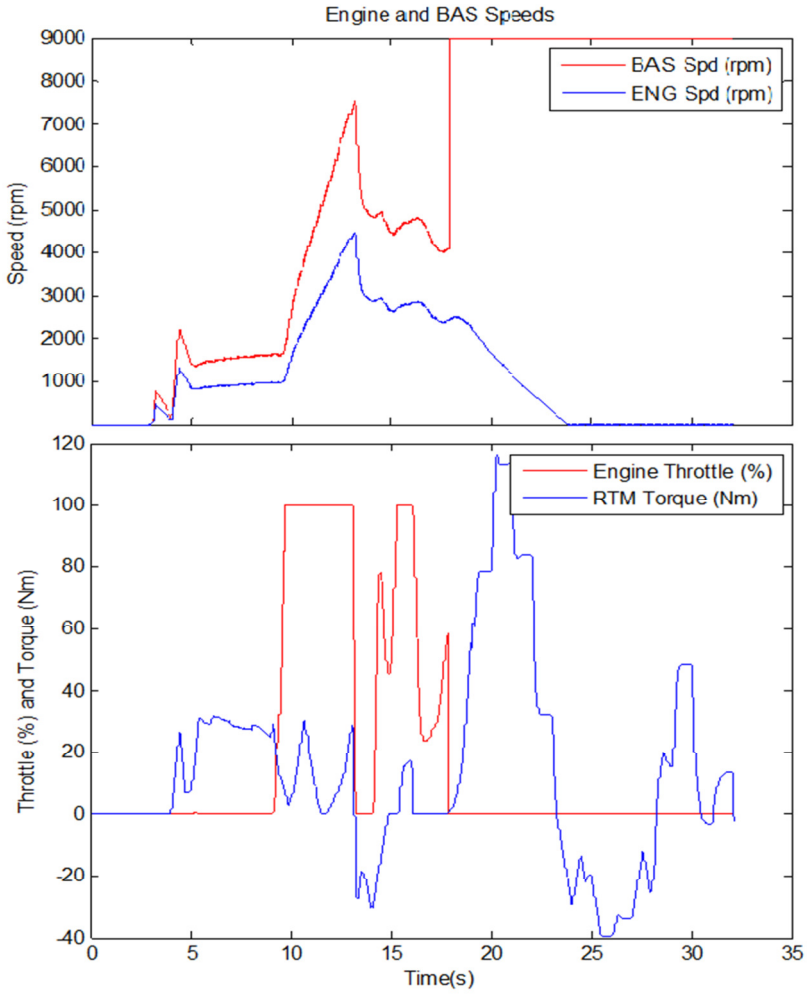

Figure 57: BAS Failure Simulated System Response

The relative rotational speed of the BAS and ICE are continuously monitored to detect a divergence of the values. Since the belt interface is at a fixed ratio, values can be error checked to a tight instantaneous range. The response of the mitigation diagnostic algorithm is shown in Figure 57. When a divergence in relative rotational velocity is detected, the control system responds by switching to EV mode operation and shuts down the front drive systems.

4.2.4.System Level Operation State Diagnostics

The operation of the control system is fundamentally managed with a central logic interlock which monitors the readiness of all driveline components and responds to emergency failure conditions transmitted by each component. At this system level sphere of the controller, vehicle enabling is controlled, and the operation state of the vehicle is defined.

The two primary feedback messages defining vehicle operation status are component "Ready Set Go" (RSG) flags and component "Emergency Power Off" (EPO) flags. Together these flags define the ability of the overall vehicle system to operate. This interplay is shown in Figure 58.

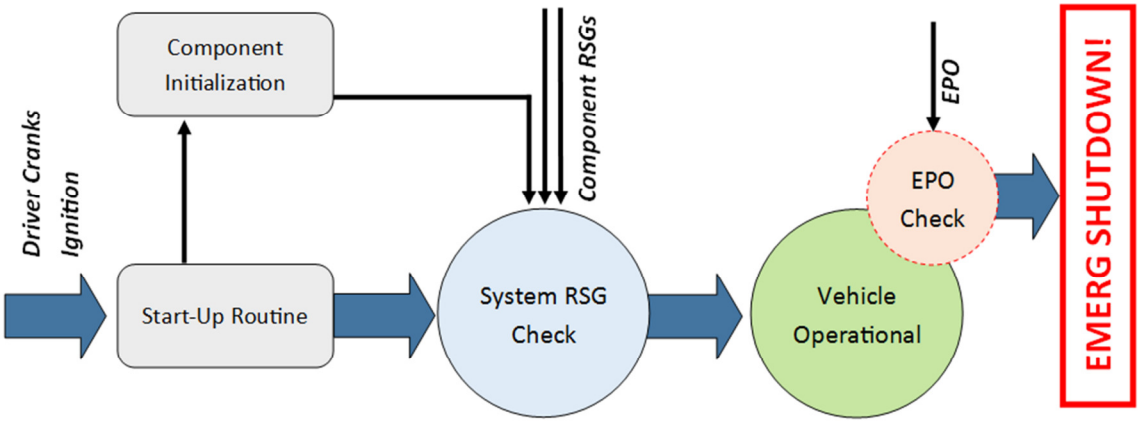

Figure 58: System Operation Status Diagnostics

Vehicle operation upon start-up is locked out until all drive system component subsystem controller spheres report back that the component is operational and ready to drive, which is communicated as the RSG signal. As such, previous failures mitigated during the last drive resulting in a non-operational component will translate to a non-operational vehicle. Upon a critical component failure while driving requiring shutdown of the vehicle, the respective component communicates the EPO signal, which results in termination of vehicle operability and shutdown of all drive systems.

4.3. Strategy Override Tactics for Strategy-Independent Controls

In order to allow robust vehicle operation independent from the particularities of the vehicle energy management strategy, a system of algorithm overrides were developed to facilitate switching between modes and minimize disturbance to the driver. They are activated by a mode-switch manager which takes an input from the energy management output signalling which mode is presently active. When the mode-switch manager detects a change in this value, it initializes the appropriate override transition to facilitate the switch. This process is shown in Figure 59.

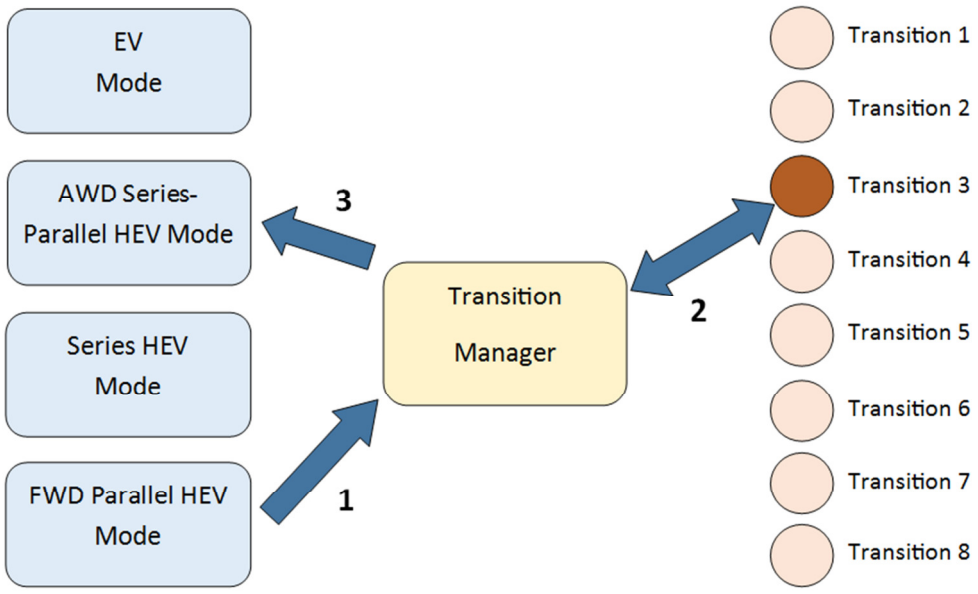

Figure 59: Mode Switch Overrides

This controls scheme allows for the vehicle platform to accept any high level energy management strategy while ensuring robust and safe operation. The only caveat requirement is that the strategy must identify present operation mode as one of the modes in Table 12.

Table 12: Strategic Operation Mode Definitions for Control Platform

Mode	Components Engaged	Description
EV Mode	ESS, RTM	-RTM generates driver torque
Series HEV Mode	ESS, RTM, BAS, ICE	-RTM generates driver torque -ICE/BAS maintain ESS SOC
Parallel HEV front-wheel-drive (FWD) Mode	ESS, BAS, ICE, Transmission	-ICE/BAS generate driver torque -BAS maintains ESS SOC -BAS optimizes ICE efficiency
Series-Parallel HEV AWD Mode	ESS, RTM, BAS, ICE, Transmission	-ICE/RTM generate driver torque -BAS maintains ESS SOC -BAS optimizes ICE efficiency

4.3.1. ICE Starting While Driving

Mode changes between EV operation and HEV operation require on-the-fly ICE starts. Since this could occur in a wide range of vehicle operating conditions and driver torque requests, a robust algorithm which overrides any strategic set-points must be used to facilitate and confirm successful ICE start-up.

Another concern for ICE start-up on-the-fly is torque disturbance resultant from engaging the transmission. Consequently, ICE revolution matching is required to some extent in order to more smoothly manage engagement of the ICE via the transmission. A complication with achieving this result is that the transmission gear selection occurs automatically within the TCM. Gear selection is accomplished according to a function of ICE torque and transmission output speed.

Since control of the transmission gear is not explicit, the transmission ratio needs to be estimated based on vehicle speed. The transmission shift maps shown in Figure 24 and Figure 25 were used to construct a curve from which a reasonable estimate for the selected gear ratio upon transmission engagement based on present vehicle speed. A relatively low throttle position was selected for determining this curve, as higher throttle positions result in significantly more aggressive ICE speeds. The rationality and methodology for constructing this curve is discussed in detail in Appendix B. This is used to set a target speed of the ICE, and the BAS is used to spin up the ICE to target speed prior to transmission engagement. A flowchart of the ICE start process is shown in Figure 60.

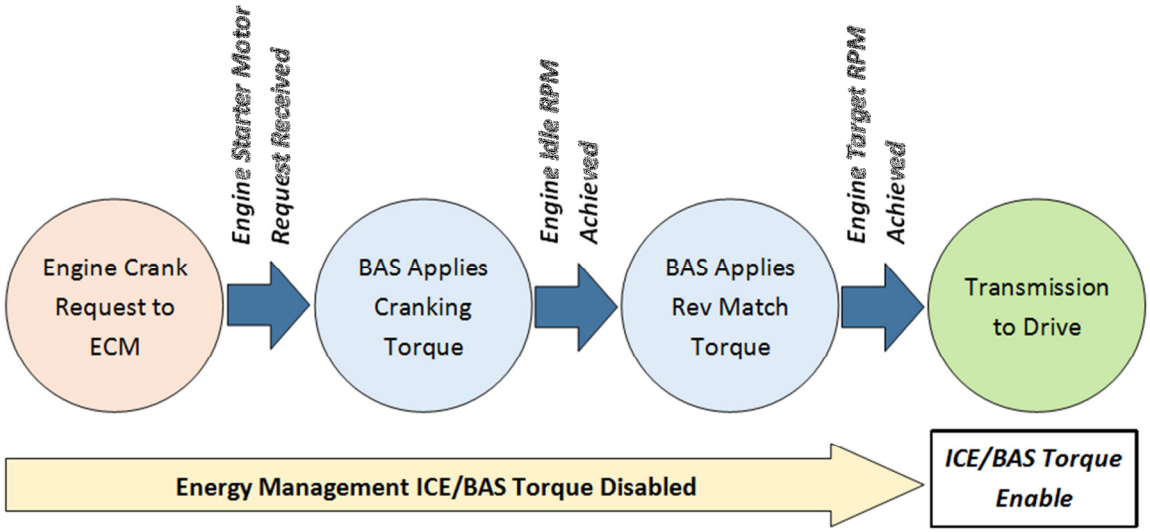

Figure 60: On-the-Fly ICE Start-Up Procedure

The resultant process creates an operational delay in mode switches requiring the ICE to switch on. During this delay, the strategic rules of the previous mode are used to meet the driver torque demand. This delay is shown in Figure 61.

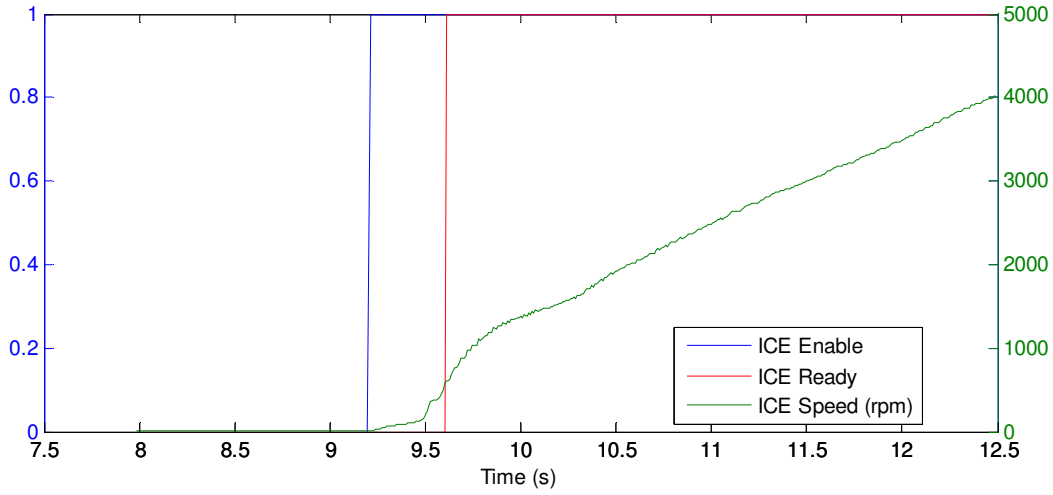

Figure 61: On-the-Fly ICE Start-Up Results

4.3.2.Component Torque Transition Overrides

The efficient operation of the UVic EcoCAR2 architecture is dependent on the availability and acceptability of highly frequent mode transition. A jump from one mode to another can be accompanied by a point jump in torque request to several components, resulting in poor vehicle driving characteristics as a result of discontinuous vehicle acceleration and jerk. While a high level control strategy which uses total component torque checksums to ensure constant total vehicle output torque at the wheel is a possible approach, the response of various components are subject to differing physical constraints, and thus the net result in the vehicle will not be smooth operation. Varying vehicle acceleration on fixed user torque request is acceptable to a level to which the user can reasonably adjust the accelerator pedal position to compensate, and is generally expected in conventional automatic vehicles on gear switches, however a control mechanism is required to limit the discontinuities and their effect on acceleration behaviour.

Point jumps in component torque requests as a result of mode transitions are handled by applying torque request overrides with consistent transition functions used to move between previous and target torque values. Ideally, these transition functions should create a continuous torque request, continuous resultant jerk, and limit maximum jerk. A function which is suitable for such an operation is the Gauss Error Function described as follows [48]:

$$erf(x) = \frac{2}{\sqrt{\pi}} \int_0^x e^{-t^2} \tag{6}$$

The quick convergence to zero on both sides of the function and the continuous nature of its first and second derivatives makes the error function suitable for transitioning between point jumps in component torque demand resulting from transitions. The error function is relatively computationally expensive and subject to numerical error due to the numerical integration required to compute its trajectory[48]. This is of concern while running time-sensitive real-time operations in-vehicle. As such, the hyperbolic tangent function allows for a reasonable approximation while being far cheaper to execute[48]. The two functions are plotted in Figure 62.

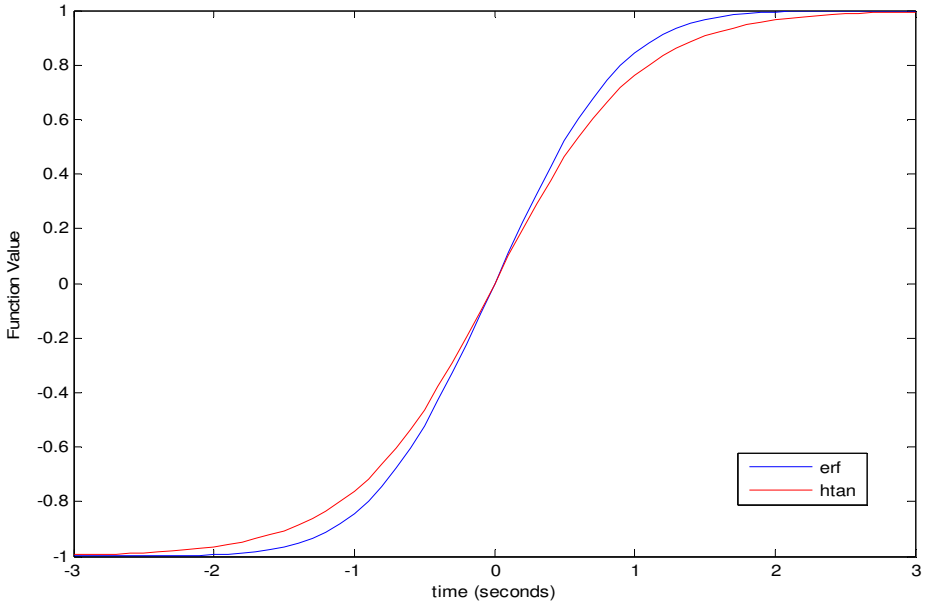

Figure 62: Gaussian Error Function versus Hyperbolic Tangent

The hyperbolic tangent function was applied for mode transitions and scaled to apply a maximum reasonable bound on vehicle jerk. The result is a smooth transition between point jumps in component torque requests. The energy management level output and post-override output for a transition between two vehicle modes is shown in the following figures.

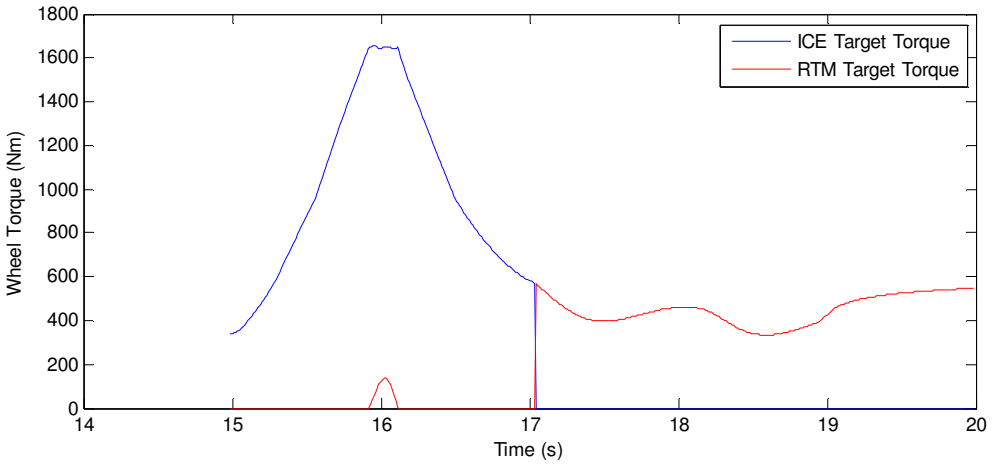

Figure 63: AWD Series-Parallel to EV Transition Strategy Target Values

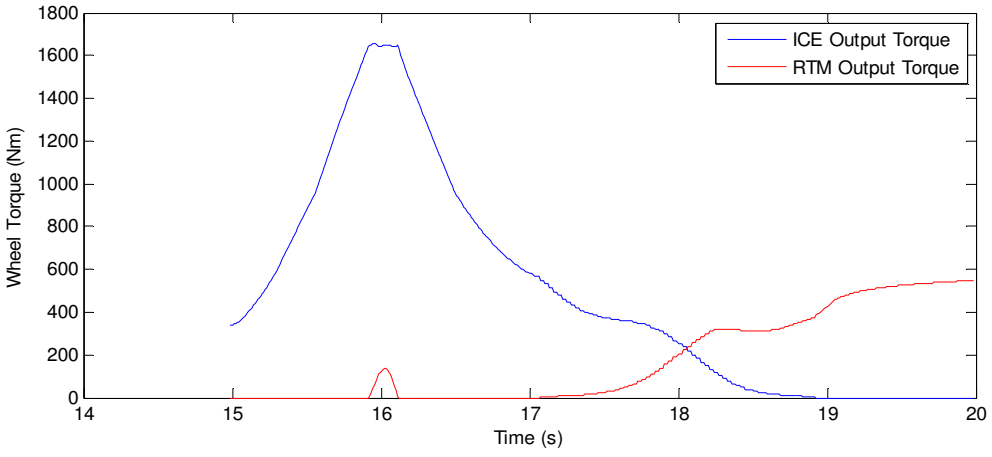

Figure 64: AWD Series-Parallel to EV Transition Output Values

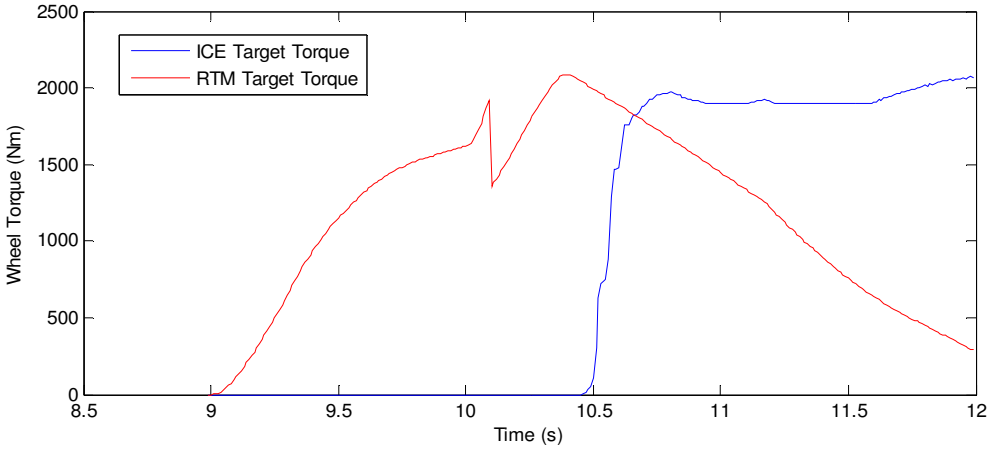

Figure 65: EV to AWD Series-Parallel Transition Strategy Target Values

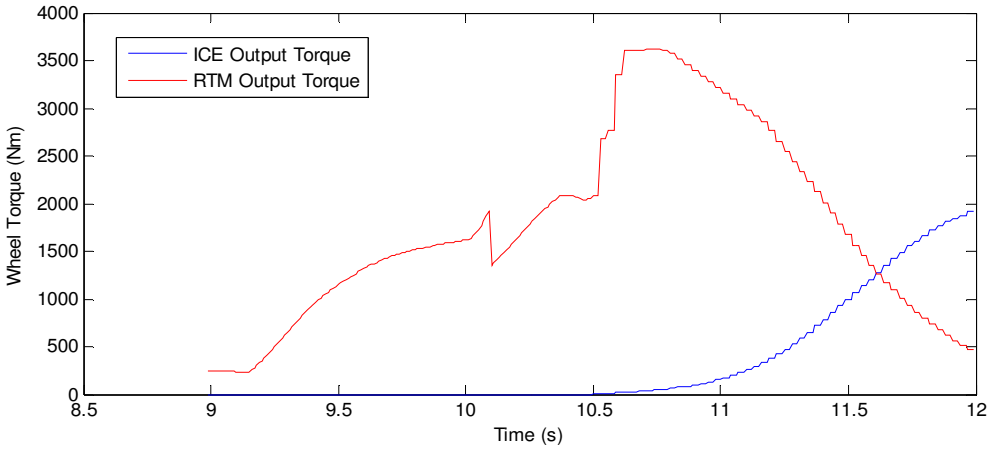

Figure 66: EV to AWD Series-Parallel Transition Output Values

4.4. Rule-Based Control Strategy Employed for Validation

While the vehicle control system hierarchy was developed with the intention of being compatible with a real-time optimization strategy, validation of its functionality is possible using a rule-based control strategy. Additionally, testing of a real-time optimizer strategy in-vehicle requires substantial protocols for SIL and HIL testing prior to running in-vehicle. The control logic and development process has been validated using a rule-based control strategy as discussed in the following subsections.

4.4.1.Energy Management Logic and Rationale

The rule-based control strategy tested in the UVic Series-Parallel HEV uses nested parallel state-machine logic to switch between modes and compute torque to each of the powertrain sub-components, with the following states and calculations as described in Figure 67:

- **Charge State:** CS and CD constitute two primary states of operation. Transition between these states is determined based on the ESS SOC being above or below the threshold value.

- **Charge Sustain Mode Select:** The two sub-states within the CS mode state (vehicle modes) are parallel FWD and series-parallel AWD. The FWD mode is active when the user torque request is lower than the optimal ICE torque for the speed expected. AWD mode is active when this value is surpassed. This generally results in AWD being active when power demand is higher and FWD being active when power demand is lower.

- **Charge Deplete Mode Select:** The two sub-states within the CD mode state (vehicle modes) are series-parallel AWD and EV. EV mode is active when user torque demand is less than the maximum torque available from the RTM, while AWD mode is activated when user torque is higher than EV mode can achieve. The general intent is that EV mode is maintained for most driving operations to allow full utilization of the ESS charge.

- **FWD Parallel Hybrid Mode Operation:** The strategy requires the torque request to the ICE be above a minimum torque threshold to avoid the lower thermal efficiency at low toque output. The ICE torque is bound by the instantaneous optimal torque for the given ICE speed. Surplus torque is taken up by the BAS via regeneration and stored in the ESS.

- **AWD Series-Parallel Hybrid Mode Operation:** Since this strategy is primarily employed during high power requests from the user, ICE torque request is kept at

the optimal torque for the given speed. Any torque deficit is made up by supplemental power from the RTM.

- **EV Operation:** EV mode user torque requests are translated to the RTM only to create pure EV operation.

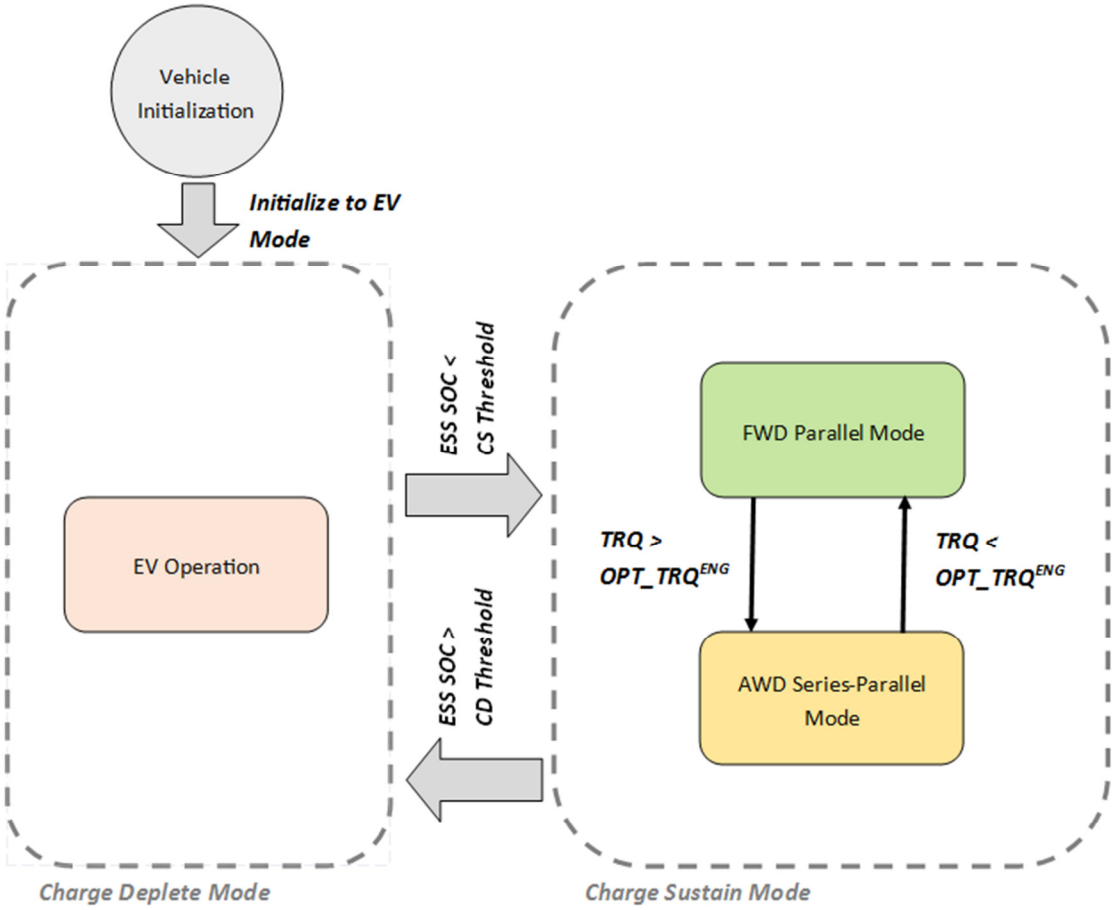

Figure 67: Rule-Based Controller State Logic

4.4.2.Road-Tuned Variables

Additional algorithms tuned through on-road testing to create acceptable drive feel and familiar vehicle response were developed to work in conjunction with the primary strategy. These are mode-independent algorithms, as they are not applied with any strategic energy management goals or feedback.

User Throttle Response Tuning: The driver throttle request to torque request translation uses an overall vehicle system torque approach. The sum of each torque-producing component output contribution at the wheels should equal the system torque request from the driver. Known gear ratios between the BAS and ICE and the RTM and rear wheels, and estimated gear ratio at the automatic transmission are then used to calculate respective component torques per the strategy employed. The system torque response was initially tuned with a 2D map as a function of vehicle speed and pedal request percentage, as shown in Figure 68. This was then tuned by an additional scalar and 1D curve to allow on-the-fly tuning on-road. The shape of the vehicle system torque response reflects the higher amount of system torque required to drive at fixed velocity at higher vehicle speeds by correspondingly ramping up system response sensitivity with vehicle speed. It also accounts for the reduced leverage ratio the ICE and BAS have over the vehicle wheels as the transmission shifts up through its map, which prevents the system from erroneously requesting very high component torques, which are calculated by applying the instantaneous gear ratio. At higher vehicle speeds and low pedal requests there is negative torque applied to allow for passive regenerative braking. The uncorrected system torque response map is shown in Figure 68 with gear ratio corrected system torque map shown in Figure 69.

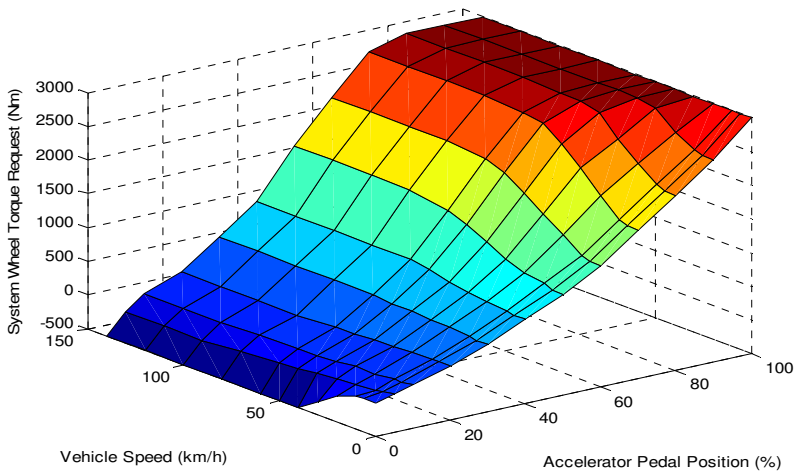

Figure 68: Uncorrected System Torque Response Map

(Map developed with help from Ted Alley and the UVic EcoCAR2 Team)

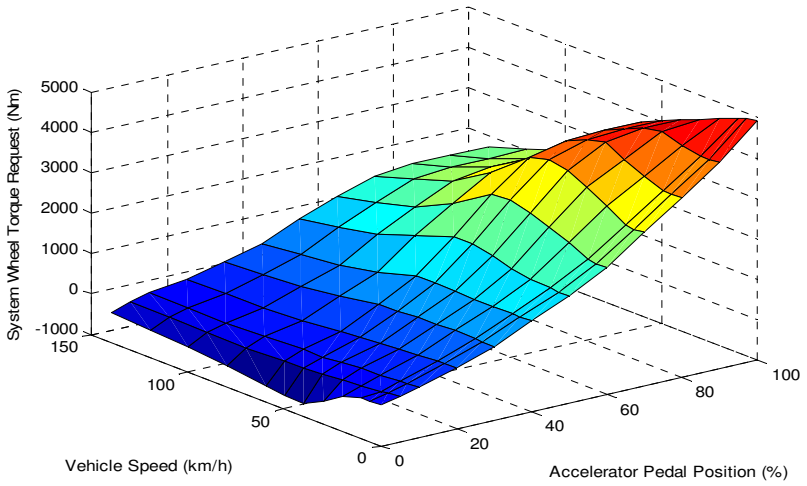

Figure 69: Corrected System Torque Response Map

Creep Torque: Torque is applied by the RTM to allow vehicle creep when the user releases the brake pedal. This allows for the driver to operate the vehicle in a familiar manner while in traffic. Creep torque is applied as a decreasing function of vehicle speed as shown in Figure 70. The RTM torque output is set to the greater of the creep torque and the strategy torque set-point for the RTM.

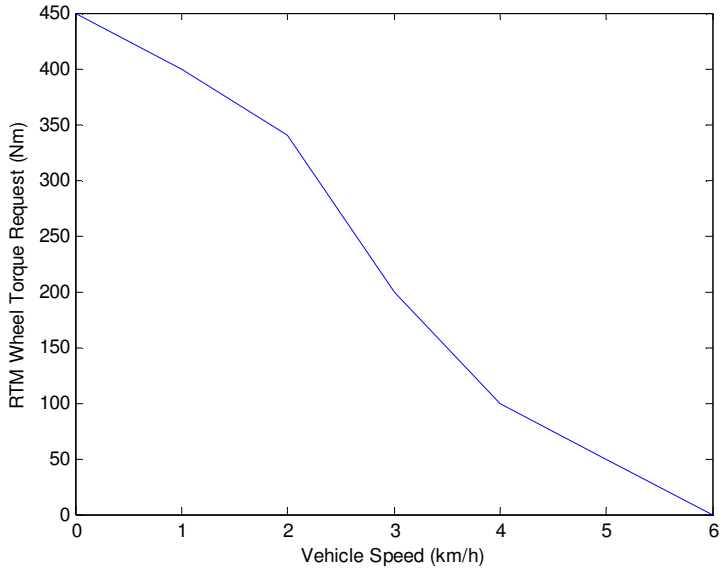

Figure 70: Vehicle Creep Torque Curve

Minimum ICE Torque Application Smoothing: The FWD Parallel HEV operation mode minimum ICE torque value results instantaneous ICE torque request changes from zero to the threshold value. While the algorithm provides for the summation of component torque contributions being smooth and continuous, point jumps in the ICE, with its relatively large time constant response, would create some unpredictable transient behaviour. As a result, a scaling linear multiplier is applied as a function of both accelerator pedal position and ICE speed to prevent harsh system response. The resultant multiplication map applied to the minimum ICE torque set-point is shown in Figure 71.

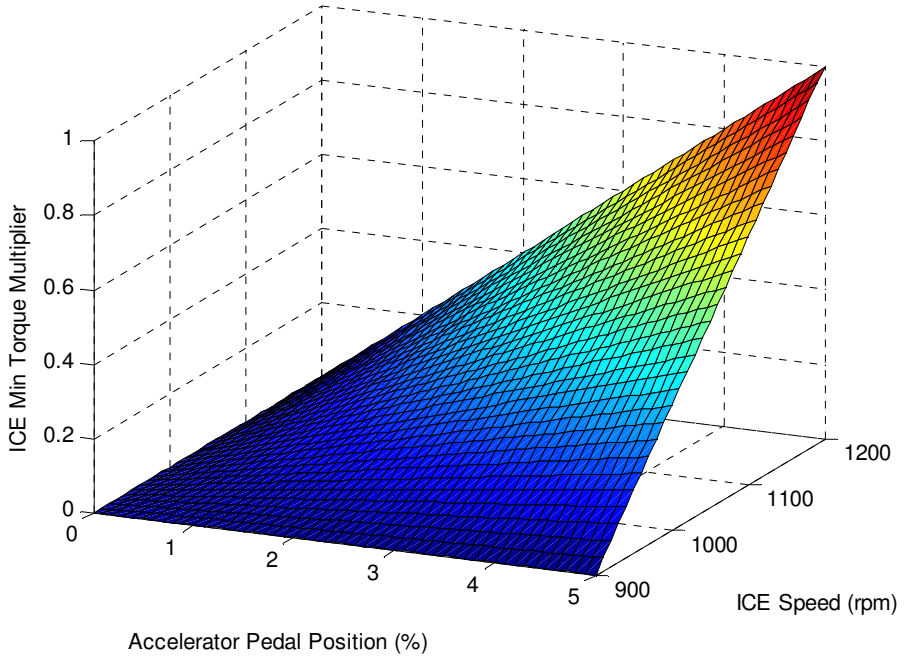

Figure 71: ICE Minimum Torque Application Multiplier

4.4.3.Drive-Cycle Tuned Variables

Tuning variables used to augment the behaviour of the rule-based strategy were applied to allow for offline global optimization. These variables allow for automated optimization test simulations on a given drive cycle to optimize the cumulative efficiency effects of the

tuning variables. As these affect the operation of the rule-based strategy, they can be used to find an optimal operation profile within the framework of the developed rule-based control.

- **Minimum Engine Torque Value:** The ICE thermal efficiency is at its worst at low ICE output torque as shown in Figure 8. The rapid reduction in efficiency occurs at a relatively constant torque range for the given vehicle speed, so it is sensible to place a lower limit on ICE torque. Since surplus ICE power will be stored in the ESS, the value of this minimum ICE torque threshold has profound effect on the operation of the rule-based control strategy over the course of a drive cycle, and must be tuned using offline optimization to arrive at an ideal result.

- **Optimal Engine Torque Point Modifier:** FWD Parallel HEV mode tends to be charge-accumulating, while AWD Parallel-Series HEV mode tends to be charge-depleting. Since the optimal ICE torque at a given moment defines the transition between these two modes, it is desirable to have functional control over this operation to allow for maintenance of a target ESS SOC. This has further SOC target maintenance effect by increasing the RTM share of torque responsibility in AWD Parallel-Series HEV mode. The linear equation used to augment this input into the rule-based control strategy is:

$$OPT_{TRQ}{}^{ICE}_{MOD} = OPT_{TRQ}{}^{ICE}_{ACTUAL}(RPM_{ICE}) - \Delta SOC_{TARGET} * ICE\_OPT_{OFFSET} \quad (7)$$

- **BAS Torque Bias Charge Sustain Algorithm:** In an effort to maintain ESS SOC, an additive torque value is applied at the BAS as a percentage of ICE instantaneous torque to add or subtract charge bias from the system. As this value is calculated as a fraction of ICE torque, it acts to remove or supplement ICE torque. Since the value is a function of ESS SOC drift, this value changes very slowly, so the algorithm is able to depend on the user to adjust their pedal request

to accommodate operation. To ensure the algorithm function remains manageable for the driver, it is bound by limits. The cubic equation used is:

$$TRQ_{CS}^{BAS} = \begin{cases} (\Delta SOC_{TARGET})^3 * A_{CS}^{+} + \Delta SOC_{TARGET} * B_{CS}^{+}, & \Delta SOC_{TARGET} > 0 \\ (\Delta SOC_{TARGET})^3 * A_{CS}^{-} + \Delta SOC_{TARGET} * B_{CS}^{-}, & \Delta SOC_{TARGET} < 0 \end{cases} \quad (8)$$

These drive-cycle-optimized tuning variables form the basis of modifiable inputs for global optimization results derived in the following chapter. A summary of these optimization variables is presented in Table 13.

Table 13: Drive-Cycle Strategy Tuning Variables for Optimization

Variable	Initial Value	Description
MIN_TRQ_{ICE}	45	Sets the minimum ICE torque to be requested to maintain operation in a more efficient region
$OPT\_TRQ_{MOD}^{ICE}$	12	Biases the system towards or against using the AWD Series-Parallel Mode based on SOC drift to try to maintain SOC target
A_{CS}^{+}	0.005	Coefficient A of cubic BAS torque add function with SOC surplus
B_{CS}^{+}	0.02	Coefficient B of cubic BAS torque add function with SOC surplus
A_{CS}^{-}	0.0166	Coefficient A of cubic BAS torque add function with SOC deficit
B_{CS}^{-}	0.0334	Coefficient B of cubic BAS torque add function with SOC deficit

4.4.4.Operational Limitations

Some operational limits were set within the rule-based control strategy to ensure safe and predictable vehicle operation under the full set of driving possibilities.

- **Mode Switch Delay Criteria:** While the UVic PHEV architecture relies on frequent mode-switching, this frequency must practically be limited in some way to prevent highly intermittent driving situations from resulting in erroneous mode changes. This is accomplished through using a two-step timed criteria-driven delay in the mode switch process. The first delay is a minimum runtime in any given mode. This is kept on the order of several seconds, varying for different modes, to prevent unwanted operation within a non-ideal mode. The second delay is a requirement that the criteria for a mode switch be met for a set amount of time prior to the switch occurring. Any intermittent failure to meet the mode switch criteria restarts the timer. This timer is set on the order of 0.5 to 2 seconds depending on the mode switch in question. A flowchart of this timer logic is shown in Figure 72.

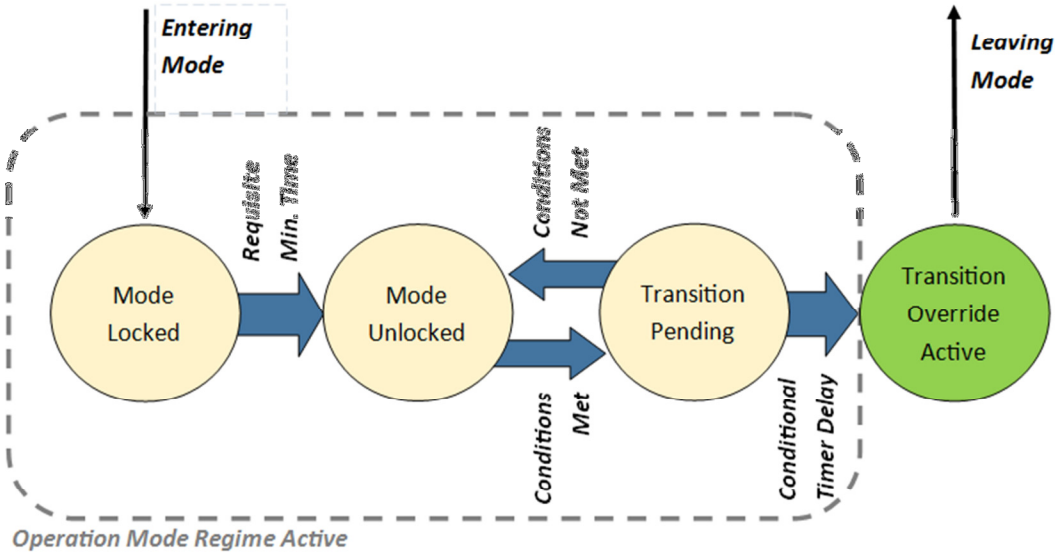

Figure 72: Mode Switch Criteria Timer Delays Operation

- **BAS Operational Torque Limit:** Repeat mechanical failures in the interface between the ICE and BAS resulted in the need to apply an operational constraint on the torque available from the BAS. This value was set based on mechanical design calculations performed on the interfacing component, while applying a reasonable safety factor. The limit was set to 55 Nm. This limit is restrictive on the operation of the control strategy in some operation modes.

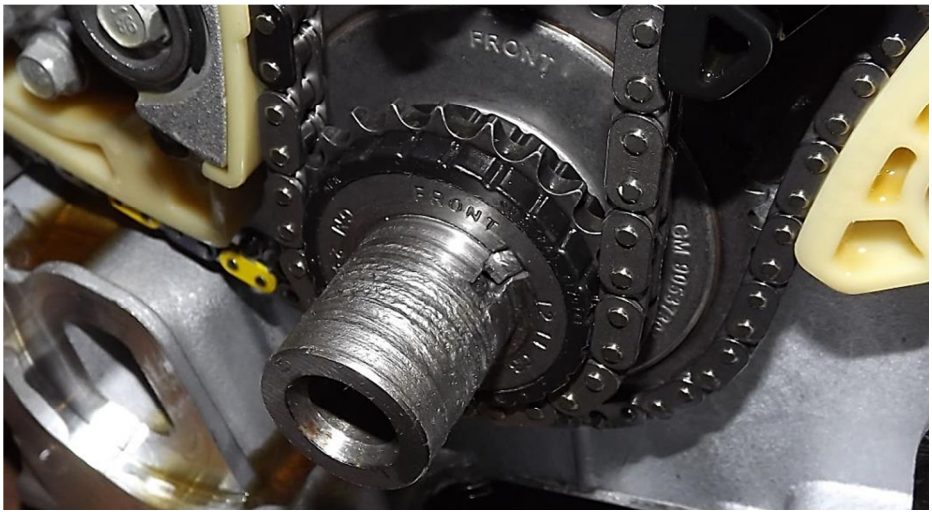

Figure 73: BAS-ICE Interface Mechanical Failure at Engine Crankshaft

(Image courtesy of UVic EcoCAR2 team)

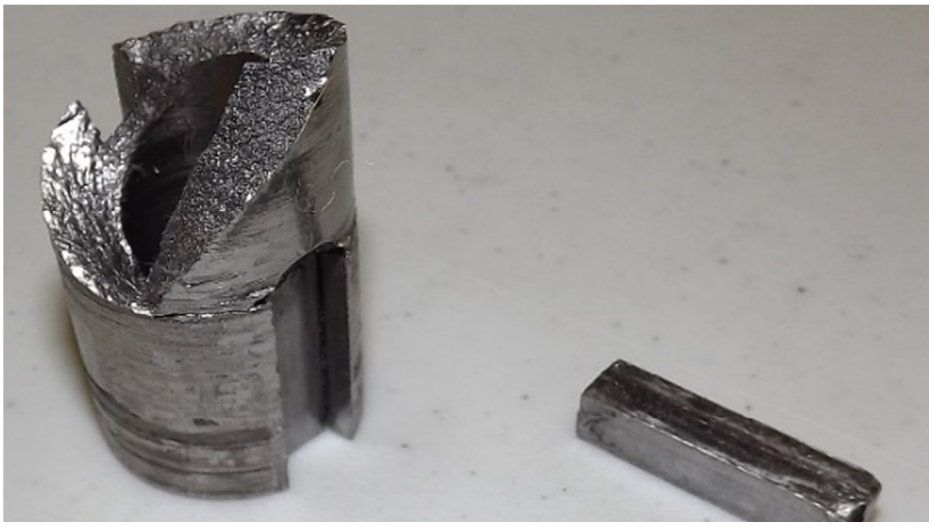

Figure 74: Broken Crankshaft Snout and Sheared Key

(Image courtesy of UVic EcoCAR2 team)

4.5. System Logic Development Summary

An overarching control system logic hierarchy was conceived to support the proposed research objectives. In the lower levels of the controls hierarchy, individual component subsystem routines and diagnostic mitigation routines were developed and validated through a joint effort of the controls development team. This process was carefully managed in order to support the intent of the overarching logic hierarchy and prevent unintended operation which would undermine the capability of the platform to support generalized input energy management strategies. At the core of its functionality, the developed logic hierarchy depends on operational transitions between driving modes which are vitally important to realising a strategy-independent robust controls platform. At an implementation level, additional calibration was applied at the system integration level and subcomponent operation level of the control hierarchy. Developmental contributions from the overall control team were managed extensively to ensure preservation of the future research intentions for the vehicle platform and simulation platforms.

Chapter 5: Assessments of Performance of Control System Architecture

The UVic hybrid architecture control system was developed to serve as a platform for powertrain optimization research work. In this chapter, the performance of the resultant system is assessed while simulated on the simplified MIL development platform before and after applying a global optimization of the rule-based control strategy tuning variables to assess the possible efficiency gains within the system. Additionally, optimal tuning variable set-points are transferred to the SIL control development platform to assess the design optimization methodology used during the competition. Subsection topics include

- an overview of the global optimization methodology used and the metrics used in determining the vehicle equivalent fuel consumption,
- a statistical analysis of the standardized drive cycles used to assess and optimize vehicle performance,
- the non-optimized benchmark performance of the rule-based control strategy,
- the optimization results and performance assessment of the optimized system using the simplified MIL development platform model,
- an assessment of the generated optimized system tuning when transferred to the SIL controls development model platform,
- a discussion of the detailed SIL model behaviour exhibited while optimally calibrated for two specific drive cycles.

5.1. Methodology and Metrics for Assessment

In order to facilitate objective assessment of performance and optimization of operation, standardized metrics are required. Consumption for simulated automated standardized vehicle test cycles was measured and compared to allow for global optimization of the control strategy.

5.1.1. Global Optimization Algorithm and Method

Global optimization of the control strategy inputs listed in Table 13 was conducted using automated drive-cycle testing of the simplified MIL SimDriveLine power loss model in conjunction with a Genetic Algorithm optimization process.

Genetic algorithms (GA) are general purpose search and optimization routines and have widespread applicability on engineering applications. They are a sub-type of evolutionary algorithms, based on the analogy of evolution.

A starting population is initialized in an algorithm-specific procedure. Through the application of mutation, the search population evolves over time. For each iteration step, individuals are assessed for their optimality and are either terminated or reproduced accordingly, with a higher weighting of reproduction given from individuals with highest optimality. In this way, the population gradually evolves towards optimal traits until a final solution is found. Final solution conditions are identified through a termination criterion, which may include a generational limit on the simulation. Major components of GA can be divided into eight main steps:

- **Population Representation –** The problem solutions are encoded into information strings, representing the chromosomes of the population of individuals. Inputs are commonly encoded in binary, but can also be evaluated based on ternary, integer, or real values. Population size is important, with larger populations resulting in more informed searches.

- **Initialization –** The population is initialized across the search space. This can be done randomly, uniformly, or using an informed methodology. Sometimes prior knowledge of the search space is applied to narrow the search field through manipulation of the initialization space.

- **Objective Functions (Fitness Functions) –** At each generation, each individual is evaluated for its relative fitness. A transformation of the objective function (linear scaling, factoring, or powers relations) results in a fitness assessment being applied to the individual.

- **Selection –** A selection algorithm is applied to determine reproduction quantity for each individual, with higher fitness individuals producing more offspring. This is typically stochastic in nature, but can be adjusted to reduce statistical likelihood of a few individuals dominating.

- **Crossover –** Information from two or more parental individuals is swapped to produce offspring of different combinations.

- **Mutation –** Individuals' information is randomly changed upon initialization of the next generation. Typically the probability of mutation is kept very low. This allows a more complete coverage of the search space.

- **Reinsertion –** Offspring are inserted into the population. Population size is maintained, requiring an elimination protocol for the existing individuals. This can be done many ways, but most typical is removal of the oldest individuals.

- **Termination –** After a set number of generations, members of the search population are evaluated to check for adequate solutions. At this point, the algorithm can be restarted or a new search initiated. Typical convergence criteria cannot be applied, as stagnation through several generations is possible prior to domination of more fit individuals.

In the optimization of the vehicle control system, the fitness function is defined as the equivalent fuel consumption over the given cycle being optimized for. The number of individuals within the population was set based on best practices at 30 (5 individuals for each degree of freedom), and the number of generations was set at 50. It was noted that convergence was achieved before 50 generations for all optimization attempts.

A major drawback of GA is that it is impossible to conclusively determine that a global optimum has been achieved. In the context of this optimization process, this is acceptable, as absolute global optimal is not important given the apparent differences between the simplified and SIL model platforms. Performance improvements and associated carry-over between platforms is the desired result of the exercise.

5.1.2. Calculation of Performance Metrics

Vehicle efficiency was assessed using standardized metrics for EC over a series of drive cycle tests. Gasoline consumption and ESS charge depletion were tracked and average consumption rate over the known drive cycle distance was computed.

The UF, used to weight the relative consumption rate of CD and CS for a given drive cycle as described in Section 2.1.2, was used where appropriate to synthesize consumption in both CD and CS modes[1]:

$$EC_{UF} = EC_{CD} * UF + EC_{CS} * (UF - 1) \quad (9)$$

where:

$$EC = Energy\ Consumed$$

5.1.3. Equivalency Factor

The mixed energy source nature of PHEVs requires a methodology for blending the consumptions into a meaningful metric. The first item that must be captured is the relative energy density of each fuel. Energy contents of various vehicle fuel options are shown in Table 14[1].

Table 14: Fuel Energy Density Comparison

	Gasoline	E10	E85	B20
Fuel Specific Energy (kWh/kg)	11.73	11.44	7.96	11.55
Fuel Density (kg/L)	0.7583	0.746	0.7871	0.8552
Fuel Energy Density (kWh/L)	8.895	8.534	6.265	9.878

Thus total EC can be used to calculate the equivalent fuel consumption:

$$L_{ge}/100km = \frac{\left(L_g + kWh_{elec}/8.895\right)}{d} \tag{10}$$

where:

L_{ge} is equivalent gasoline consumed

L_g is actual gasoline consumed

kWh_{elec} is actual electrical energy consumed

d is the drive cycle distance

The above calculation does not take into account the relative efficiencies of the associated drive systems. An additional fuel-electricity equivalency factor (EF) can be used to more fully capture the relative effect of consumption of the two fuel sources:

$$L_{ge}/100km = \frac{\left(L_g + E_{gas}^{elec} * kWh_{elec}/8.895\right)}{d} \tag{11}$$

where:

E_{gas}^{elec} is the electricity-gas equivalency

The selection of an appropriate EF is important, as it changes the way total consumption is assessed. Since the electric system (ESS, PM) has a higher system efficiency when compared to the fuel-based systems (ICE)[10, 11], it is appropriate to set the EF as greater than 1. This reflects the fact that equal amounts of stored fuel and electrical energy are capable of performing different quantities of real work in terms of vehicle propulsion. As a result, extra residual ESS capacity left over at the end of a CS mode drive cycle can be made to count for more fuel consumption offset than its fuel volume equivalent when only considering chemical energy. This will tend to favour systems for biasing towards charge accumulation during CS mode. This biasing effect has been used to achieve the desired functionality of the CS regime in former research at UVic.

Waldner used a scaling EF which adjusted up and down a polynomial curve in response to ESS SOC drift away from the desired CS target[3]. This scaling EF allowed for efficient maintenance of the ESS SOC target.

As the global optimization results presented in the following sections are offline, EF is used retroactively to account for surplus or deficient charge in the ESS at the end of the cycle. For the purposes of the EcoCAR2 competition, surplus ESS charge is not given credit at the end of a cycle to count in favour for the vehicle consumption. Additionally, shortfall SOC is made up using the on-board systems to manually charge until the target SOC is achieved. As this does not have physical justification (though it may have operational justification) it is not a useful accounting method for conversion into an optimization metric. As a baseline means of comparison, strict energy consumption is used to determine equivalent fuel consumption in CS mode. Thus, the EF is established as equal to 1. This essentially results in a test metric which promotes very tight ESS SOC management during CS operation with cycle completion resulting in very near to target SOC.

5.1.4. Driver Model Tuning Effects

Automated drive cycle testing uses driver model inputs to keep the vehicle at the desired speed throughout the cycle. Since the driver model operates as a P-I control trying to maintain a vehicle speed set-point, and acts on the vehicle through respective accelerator pedal and brake pedal inputs, the tuning of this model could have substantial effect on the transient operation of the vehicle. This is representative of the counterpart situation in a real vehicle on road in that different driver behaviours can have effects on outcomes.

While this inescapable source of inconsistencies is present in the simulation and in real life, it has been mitigated in the tests conducted by maintaining identical driver P-I block tuning throughout the various simulations and optimization procedures conducted. It was also maintained as consistent between the simplified model and the SIL mode.

5.2. Drive Cycle Schedules Used for Assessment

Five standard drive cycles were used for the purpose of testing the vehicle controller performance in simulation, and optimizing the controller tuning variables. The cycles selected were chosen for their applicability to the EcoCAR 2 competition, since the vehicle was developed with the intention of ideal performance at the competition.

5.2.1. US06 City Cycle

The US06 City drive cycle is a high acceleration, high aggression drive cycle intended to mimic aggressive driving in a city environment. The cycle is characterized by a low average speed, with frequent aggressive accelerations and stops.

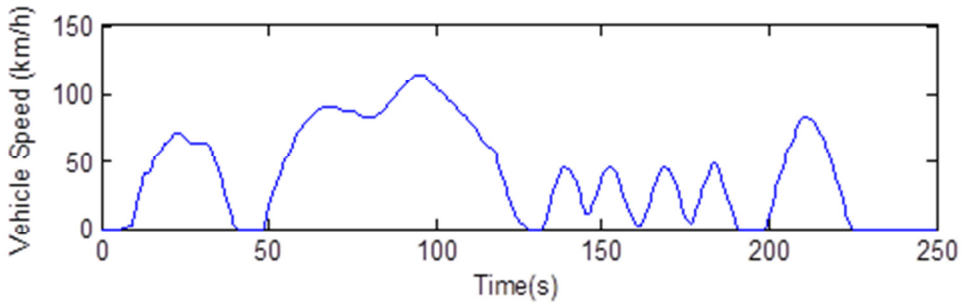

Figure 75: US06 City Drive Cycle

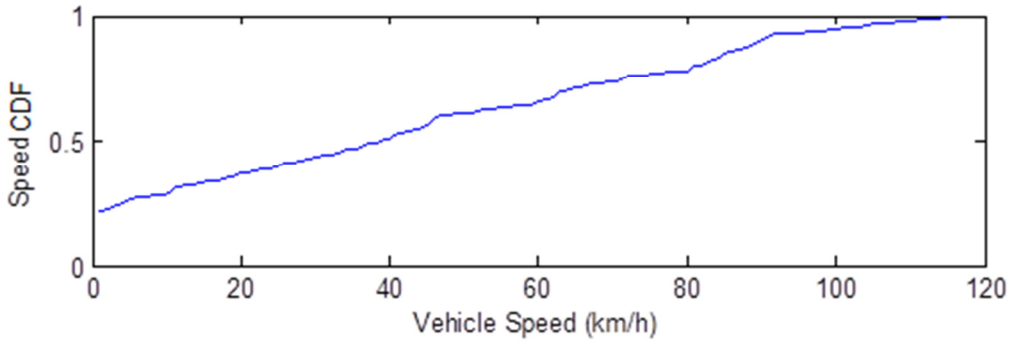

Figure 76: US06 City Speed Distribution

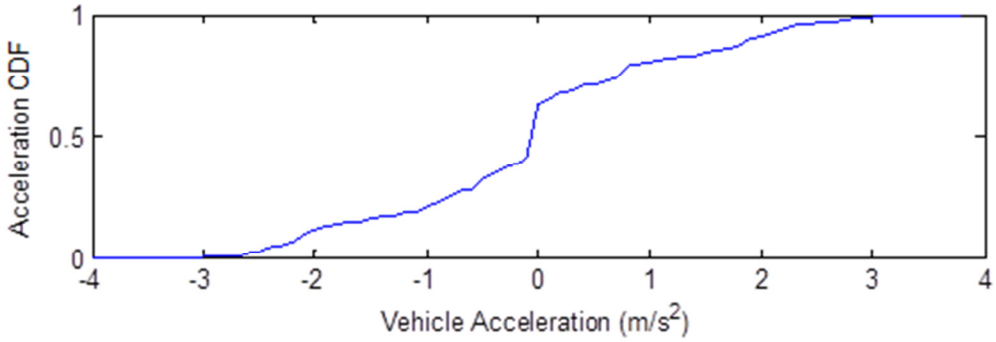

Figure 77: US06 City Acceleration Distribution

5.2.2.US06 Highway Cycle

The US06 Highway drive cycle is a high acceleration high aggression drive cycle intended to mimic aggressive driving in a highway environment. The cycle is characterized by high average speed with high intensity on-road accelerations and decelerations.

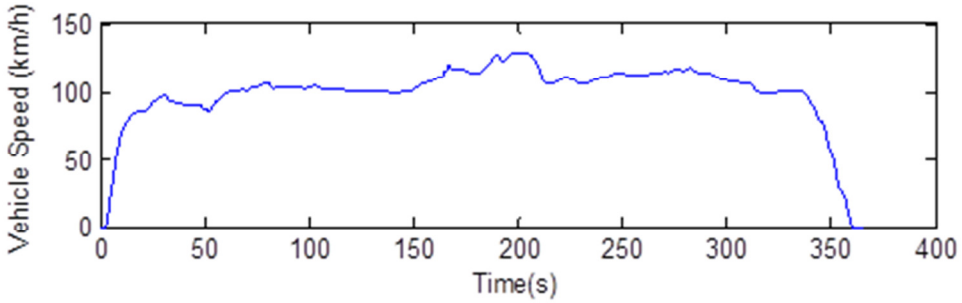

Figure 78: US06 Highway Drive Cycle

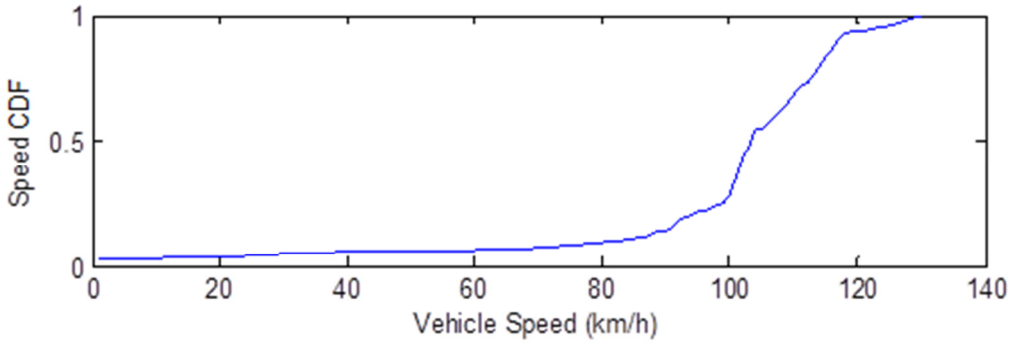

Figure 79: US06 Highway Speed Distribution

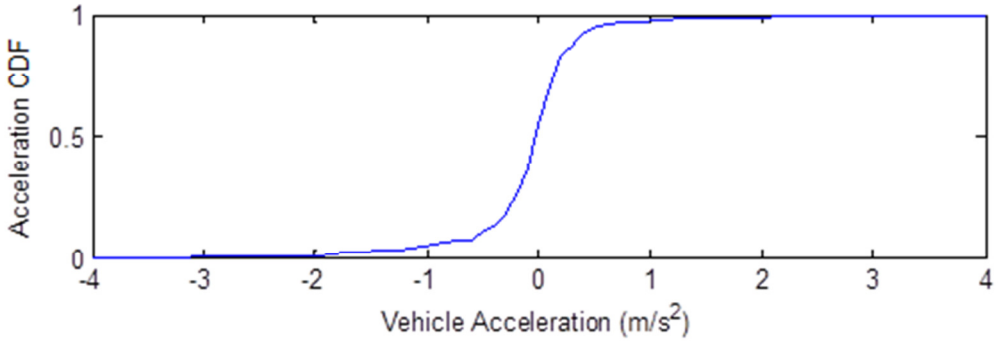

Figure 80: US06 Highway Acceleration Distribution

5.2.3.HWFET Cycle

The HWFET is intended to mimic typical highway driving conditions under speeds of 100km/h.

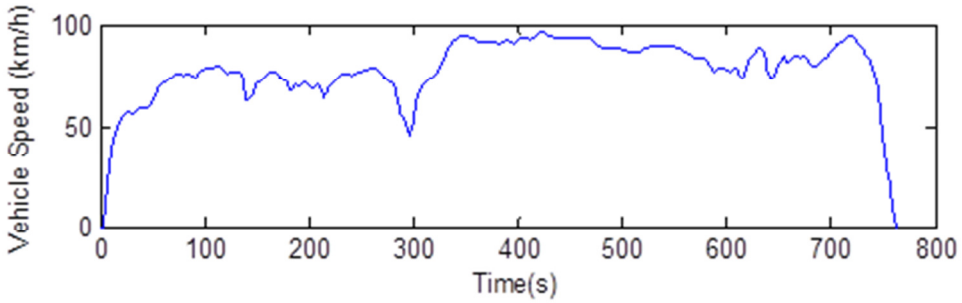

Figure 81: HWFET Drive Cycle

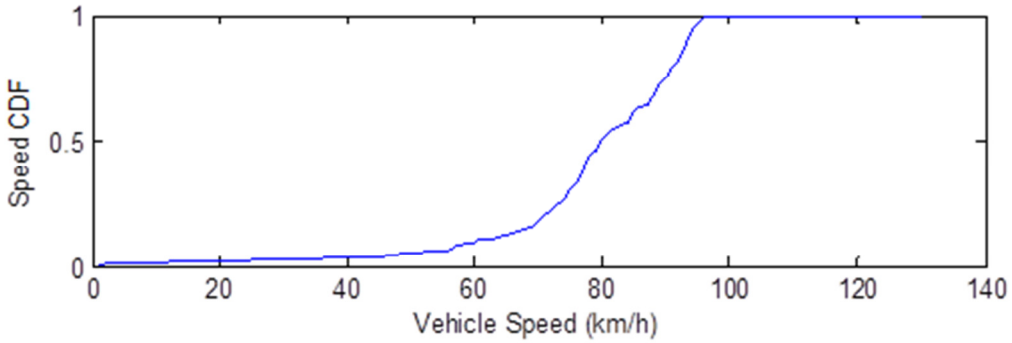

Figure 82: HWFET Speed Distribution

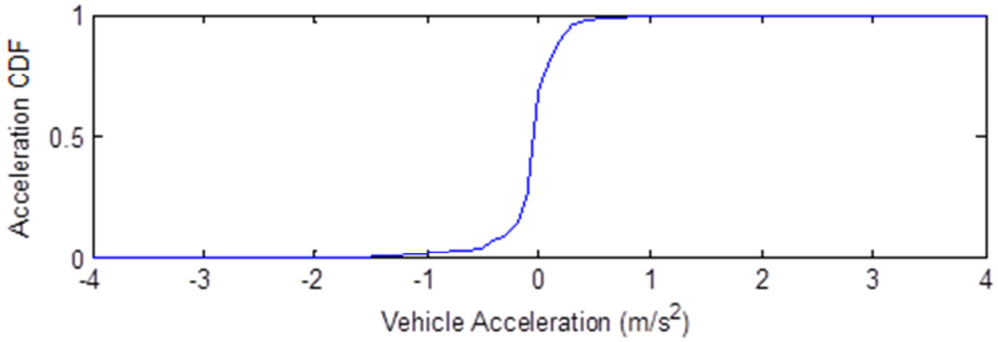

Figure 83: HWFET Acceleration Distribution

5.2.4.FU505 Cycle

The FU505 drive cycle is made up of the first 505 seconds of the UDDS drive cycle. The UDDS was developed by the EPA to conduct dynamometer testing of light-duty vehicles in a simulated city environment. The FU505 is a truncated version to allow for more rapid iterative testing.

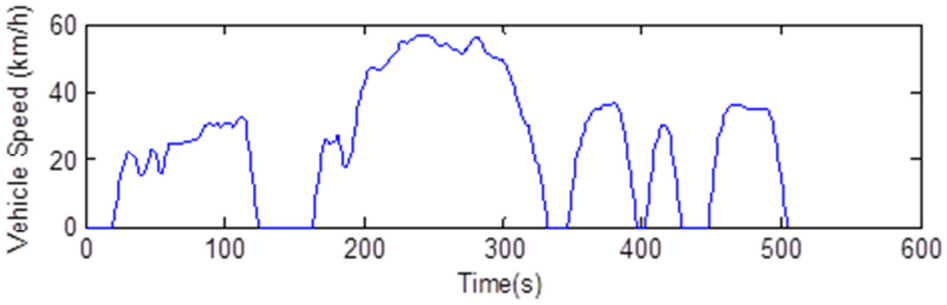

Figure 84: FU505 Drive Cycle

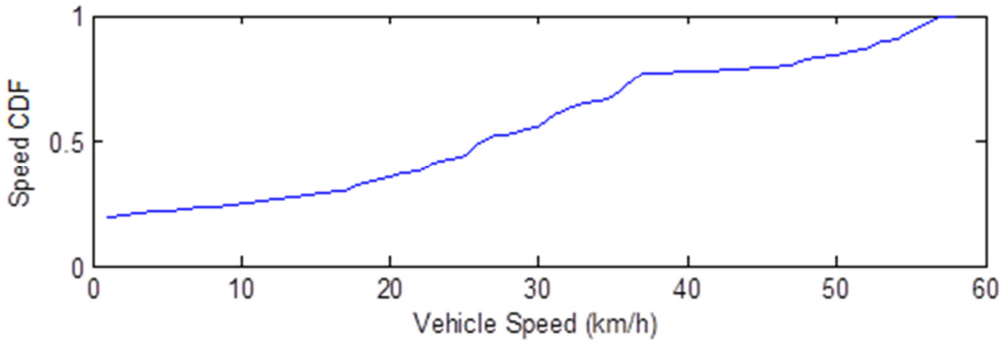

Figure 85: FU505 Speed Distribution

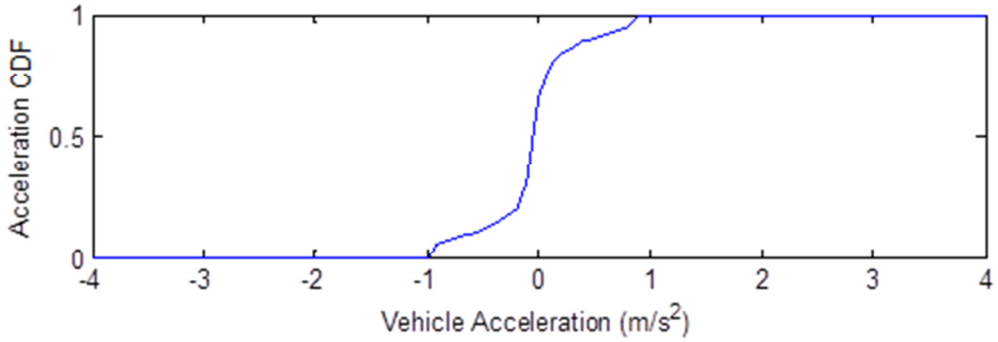

Figure 86: FU505 Acceleration Distribution

5.2.5.4-Cycle Mixed

In addition to the 4 standard industry cycles described above, a blend of the 4 cycles was also assessed using a weighted average of the consumption performance from the 4 cycles. The relative weightings are shown in Table 15[1].

Table 15: 4-Cycle Mixed Relative Weightings

Drive Cycle	Weighted Value (%)	Description
US06 City	14	Low Speed Aggressive Cycle
US06 Highway	45	High Speed Aggressive Cycle
HWFET	12	Medium Speed Cycle
FU505	29	Low Speed Cycle

5.3. Non-Optimized Rule-Based Strategy System Performance

To provide a baseline performance expectation, the SIL model was run to generate vehicle fuel consumption performance using the initial optimization tuning inputs set to the values presented in Table 13. An EF of 1 was used corresponding to EcoCAR2 rules. These results are shown in Table 16 through Table 18.

Table 16: Non-Optimized SIL Model Consumption Performance CD Mode

Drive Cycle	Fuel Consumed (L)	ESS Energy Consumed (kWh)	Distance (km)	Equiv. Cons. (Lge/100km)
US06 City	0.190	0.3976	2.85	8.24
US06 Hwy	0.064	1.7406	10.04	2.59
HWFET	0.004	2.2585	16.5	1.57
FU505	0.000	0.4410	3.59	1.38
4-Cycle	-	-	-	2.91

Table 17: Non-Optimized SIL Model Consumption Performance CS Mode

Drive Cycle	Fuel Consumed (L)	ESS Energy Consumed (kWh)	Distance (km)	Equiv. Cons. (Lge/100km)
US06 City	0.395	-0.1265	2.85	13.37
US06 Hwy	0.880	-0.4006	10.04	8.31
HWFET	0.995	-0.2719	16.5	5.85
FU505	0.340	-0.2173	3.59	8.80
4-Cycle	-	-	-	8.87

Table 18: Non-Optimized SIL Model Consumption Performance UF Weighted

Drive Cycle	Charge Deplete Range (km)	UF	Equiv. Cons. (Lge/100km)
US06 City	92.9	0.732	9.61
US06 Hwy	74.8	0.666	4.50
HWFET	94.7	0.738	2.69
FU505	105.5	0.768	3.10
4-Cycle	86.6	0.711	4.63

The UF for each cycle was calculated by projecting the CD ESS charge consumption over the cycle distance forward to extrapolate a range to depletion (switchover to CS mode):

$$CD_{range} = \frac{ESS_{capacity}}{(kWh_{elec}^{CD}/d)} \tag{12}$$

where:

(kWh_{elec}^{CD}/d) is the electrical consumption rate of the ESS charge over the drive cycle.

The same tuning was used with the SIL model and evaluated using a recursively-defined EF, as is described in Section 5.4.3. These benchmark results are presented in Table 19.

Table 19: Non-Optimized SIL Model Consumption Performance CD Mode with Recursively-Defined Equivalency Factor

Drive Cycle	Fuel Cons. (L)	ESS Energy Cons. (kWh)	Distance (km)	Equiv. Factor	Equiv. Cons. (Lge/100km)
US06 City	0.395	-0.1265	2.85	2.51	12.60
US06 Hwy	0.880	-0.4006	10.04	2.62	7.59
HWFET	0.995	-0.2719	16.5	2.91	5.49
FU505	0.340	-0.2173	3.59	2.96	7.46
4-Cycle	-	-	-	-	8.00

5.4. Optimized Strategy System Performance of Simplified Model

Since the tuning variables being optimized only minimally affect the vehicle operation during EV mode, as tractive power is primarily derived from the RTM in an EV regime, optimization of CD vehicle operation provides minimal benefits. The only HEV operation occurring during the CD regime is the occasional high-power event in which the vehicle strategy engages AWD series-parallel mode.

GA global optimization was conducted to find a calibration of the strategy input tuning variables which results in the lowest equivalent fuel consumption. The optimization was applied to the simplified model since the SIL model produces results too slowly to be feasible for optimization approaches requiring many simulation iterations.

5.4.1. Equivalency Factor 1 Optimization Results

The tuning calibration resulting from running the global optimization with an EF of 1 is shown in Table 20. These tuning variable inputs produced the best overall equivalent fuel consumption in CS mode over the respective drive cycle.

Table 20: Optimization Results by Drive Cycle with Equivalency Factor 1

	US06 City	US06 Hwy	HWFET	FU505	4-Cycle
MIN_TRQ_{ICE}	23.9	2.52	57.1	11.4	7.7
$OPT\_TRQ_{MOD}^{ICE}$	57.6	27.6	32.6	43.9	48.5
A_{CS}^{+}	0.0473	0.0398	0.047	0.019	0.0461
B_{CS}^{+}	0.1227	0.1915	0.0116	0.1826	0.1789
A_{CS}^{-}	0.0389	0.0335	0.0404	0.0286	0.0016
B_{CS}^{-}	0.0432	0.0001	0.0461	0.0168	0.0081

It can be seen that there are large discrepancies in optimal calibration across the various drive cycles tested.

The drive cycle calibrations were applied to the simplified model, and the overall equivalent consumption calculated for each respective calibration. Each calibration was used for all drive cycles to provide a description of how the different calibrations performed overall. The results are shown in Table 21.

Table 21: Lge/100km Consumption Performance of Simplified Model at Optimal Set-point Calibrations with Equivalency Factor 1

	Calibration				
Simulation	**US06 City**	**US06 Hwy**	**HWFET**	**FU505**	**4-Cycle**
US06 City	15.14	15.56	15.70	15.45	15.15
US06 Hwy	6.17	6.08	6.59	6.15	6.15
HWFET	4.16	4.12	3.84	4.12	4.16
FU505	5.86	5.68	7.24	5.65	5.75
4-Cycle	7.10	7.06	7.72	7.06	7.01

While the optimal calibrations performed the best for their respective drive cycles, as is expected, ideal efficiency is not carried across into the other drive cycles. Operational behaviour resulting from the calibrations significantly alters the overall vehicle consumption. Of particular note are the significant differences in optimal versus non-optimal calibration for the HWFET cycle. This may be due to the significantly lower accelerations seen in the HWFET cycle. Since the optimally calibrated tuning variables largely interact with ICE torque demand, lower median and mean ICE demand can be assumed to have resulted in this observed result. As such, higher sensitivity to calibration tuning is expected for this cycle.

5.4.2. Sensitivity of Results to Equivalency Factor

In order to better understand the effect electricity-gasoline EF has on the optimal calibration of the control strategy, a sensitivity study was conducted. Separate optimization runs were conducted for EFs ranging from 0.5 to 4. The resultant calibrations are shown in Figure 87 and Figure 88.

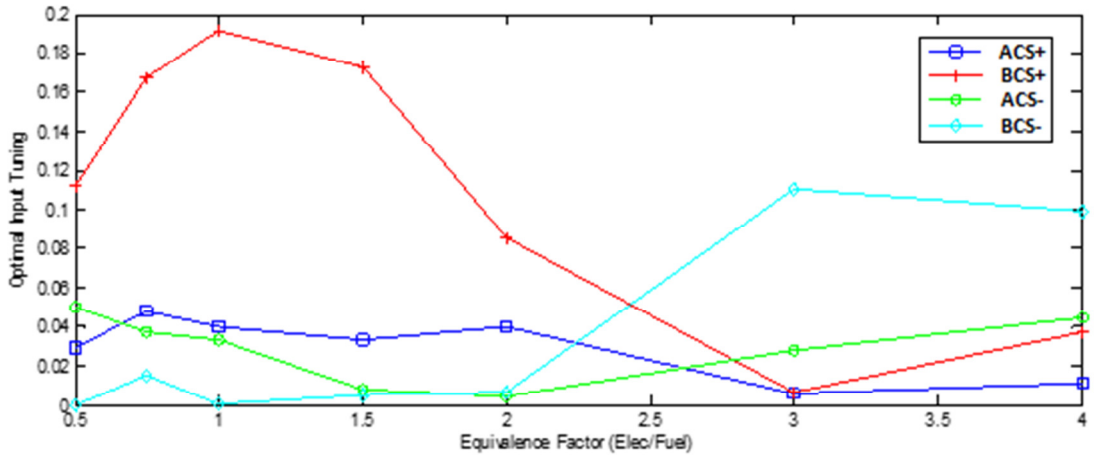

Figure 87: US06 Highway BAS Charge Sustain Algorithm Tuning Variable Optimization Equivalence Factor Sensitivity

As expected, the general trend seen is that higher EFs result in tuning calibrations that produce a strategic bias towards accumulating excess charge in the ESS. This makes sense, as excess charge at the end of a drive cycle is given greater credit, while deficit charge is allocated a greater penalty.

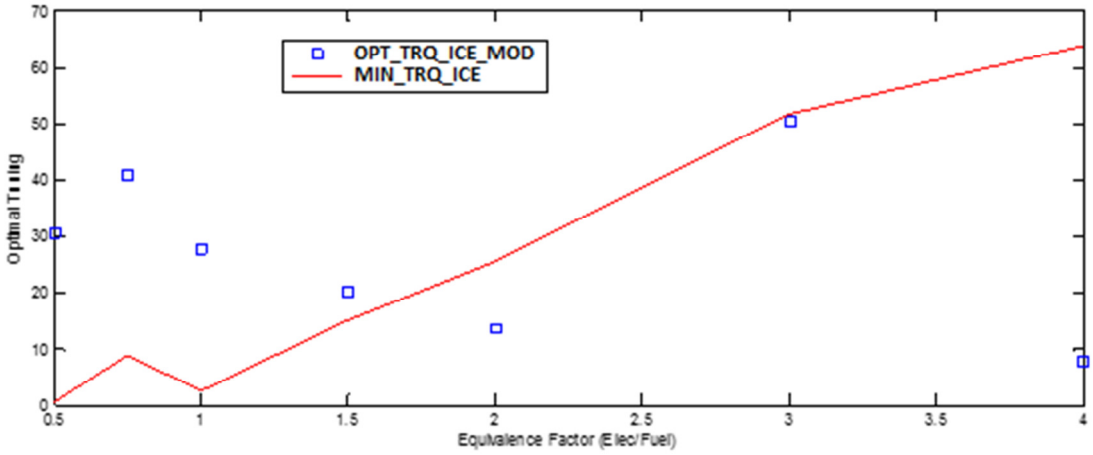

Figure 88: US06 Highway Engine Torque Tuning Variable Optimization Equivalence Factor Sensitivity

5.4.3. Recursive Equivalency Factor Analysis Scheme

While the EF was set to 1 to account for energy use directly in determining equivalent consumption, perhaps it is more reasonable and more realistic to base the EF on the different relative values of stored versus saved electrical and fuel stored energy. If an EF that is not 1 is used in the fitness function of the global optimization, the resultant iterative tuning has an effect on the momentary operation of the vehicle. This momentary operation in turn has an effect on the average relative capacity of the stored electrical and fuel energy sources to perform useful work and propel the vehicle.

A recursively-defined EF may be computed in order to generate a fair assessment of the relative value of the two fuel sources based on the performance of the vehicle for that specific calibration. This optimization procedure is shown in Figure 89.

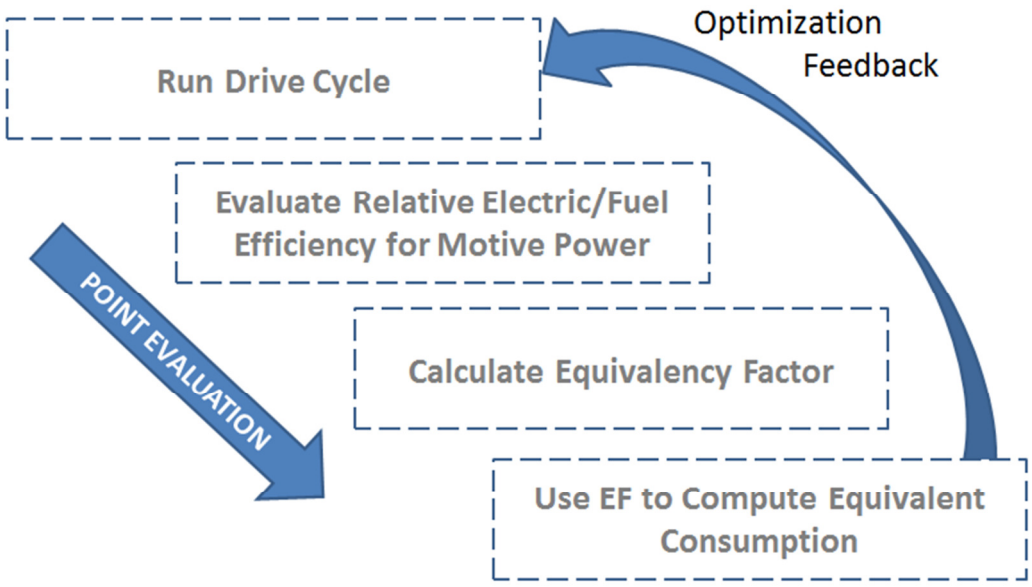

Figure 89: Recursive Equivalency Factor Scheme

This procedure requires the tracking of additional variables compared to the static EF method, including the input and output powers of the ICE versus the MGs.

The iteration step specific EF can be calculated at the end of the drive cycle as:

$$E_{gas}^{elec} = \left[\frac{\int_{t=0}^{t=cycle\ time}(P_{out}^{RTM} + P_{out}^{BAS})}{EC^{ESS}}\right] \Big/ \left[\frac{\int_{t=0}^{t=cycle\ time} P_{out}^{ICE}}{EC^{Fuel}}\right] \quad (13)$$

where:

P_{out} is the output power of the respective component

EC is the energy consumed of the respective component

5.4.4.Recursive Equivalency Factor Optimization Results

The tuning calibration resulting from running the global optimization with a recursively calculated EF is shown in Table 22. These tuning variable inputs produced the best overall equivalent fuel consumption in CS mode over the respective drive cycle when accounting for the surplus or deficit ESS SOC at the end of the cycle using the resultant quotient of electrical system and fuel system propulsion efficiencies.

Table 22: Optimization Results by Drive Cycle with Recursive Equivalency Factor Calculation Applied

	US06 City	US06 Hwy	HWFET	FU505	4-Cycle
MIN_TRQ_{ICE}	22.20	46.10	69.62	1.84	21.16
$OPT\_TRQ_{MOD}^{ICE}$	58.74	55.81	15.27	57.40	54.65
A_{CS}^{+}	0.0274	0.0248	0.0048	0.0001	0.0371
B_{CS}^{+}	0.0260	0.1711	0.0452	0.0027	0.0878
A_{CS}^{-}	0.0409	0.0002	0.0221	0.0500	0.0053
B_{CS}^{-}	0.0483	0.0840	0.0043	0.0172	0.0096

Table 23: Lge/100km Consumption Performance of Simplified Model at Optimal Set-point Calibrations with Recursive Equivalency Factor Calculation Applied

	Calibration				
Simulation	**US06 City**	**US06 Hwy**	**HWFET**	**FU505**	**4-Cycle**
US06 City	14.33	14.65	14.82	14.50	14.41
US06 Hwy	6.09	5.97	6.25	6.06	6.03
HWFET	4.16	4.00	3.65	4.24	4.10
FU505	5.50	5.60	6.27	5.43	5.47
4-Cycle	6.84	6.84	7.14	6.84	6.81

The recursively-computed drive cycle calibrations were applied to the simplified model, and the overall equivalent consumption calculated for each respective calibration. Each calibration was used for all drive cycles to provide a description of how the different calibrations performed overall. The results are shown in Table 23. The final EF used in the optimally-calibrated simulation run for each cycle is shown in Table 24.

Table 24: Optimally-Calibrated Resultant Equivalency Factors

Drive Cycle	**US06 City**	**US06 Hwy**	**HWFET**	**FU505**	**4-Cycle**
Equiv. Factor	2.391	2.263	2.840	2.517	2.407

The discrepancy between vehicle consumption over the calibration-matched cycle versus the other cycles in the test queue is not as great as for the static EF of 1. This suggests that this method of judging the equivalent consumption provides more stable result behaviour across different test cycles. This is partially expected, since the recursive EF scheme tracks the real-time efficiency of the two systems (fuel versus electrical), which prevents a skewed credit or penalty from being applied to the residual ESS SOC difference at cycle end which may result from varying cycle length interacting with behavioural minutiae. Once again, there are the significant differences in optimal versus non-optimal calibration for the HWFET cycle.

5.4.5. Parallel Coordinate Visualization of Recursive Equivalency Factor Optimization

Optimization drive cycle iteration data points collected allow for a representative survey of the search space to understand the effect the tuning variables have on end vehicle fuel consumption rates. Since there are 6 degrees of freedom in the optimally calibrated system, visualization presents a challenge.

Parallel coordinate axis graphs provide a convenient and interactive method of visually describing and interpreting high-dimension data. The following figures were generated using an interactive graphing tool to allow dynamic filtering and axis swapping. The optimization data set used is for the 4-cycle optimization.

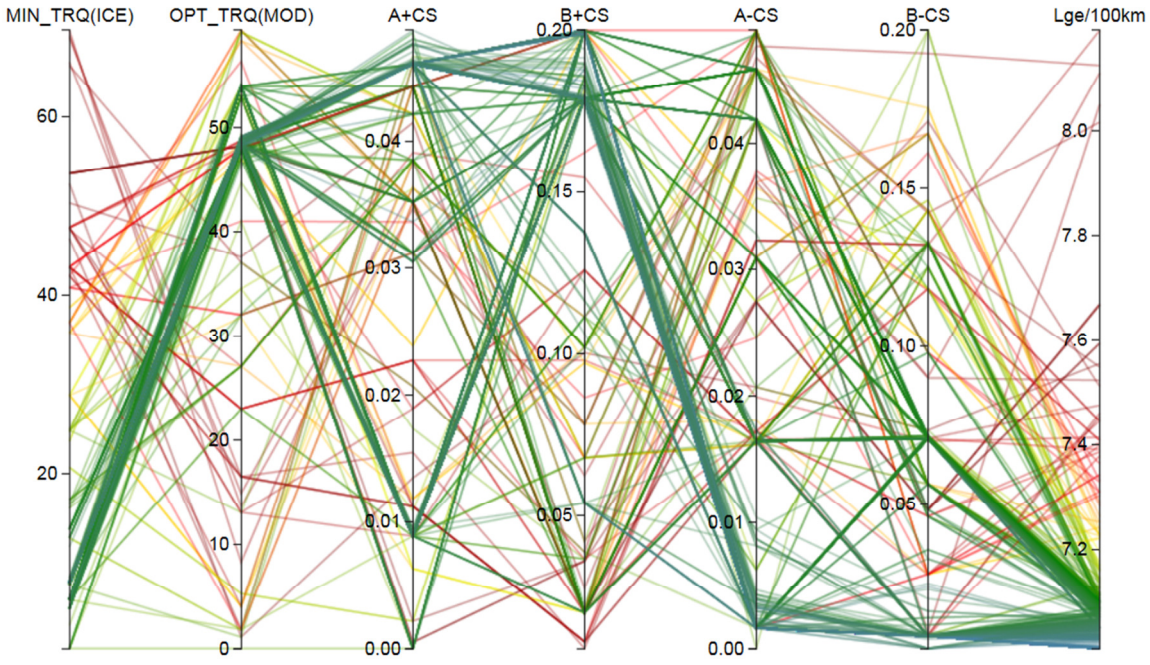

Figure 90: Equivalency Factor 1 4-Cycle Optimization Parallel Axis Plot

Some general qualifications about the data set generated by the GA optimization for the 4-Cycle drive cycle can be made from observation of Figure 90. Few and strong groupings of test calibrations indicate that the optimization routine was able to concentrate within a global minimum relatively quickly. It also suggests that the optimal calibration for the cycle has a relatively wide range of calibrations which produce near-

optimal results. Several secondary groupings can be seen, suggesting a multi-modal search space and the presence of additional local minima. Figure 91 visually identifies a proportional relationship between fuel consumption and the minimum ICE torque tuning variable MIN_TRQ_{ICE}. This is particularly interesting, as there is a consistent correlation between low fuel consumption and lower than expected values for this tuning variable as determined by viewing of the ICE efficiency map. Given the purpose for the tuning variable is to manipulate the ICE torque towards higher values, thus improving its average thermal efficiency, this result suggests that it is only efficient to do so up to a very minor degree (below the optimal set-point there are higher associated consumptions). It is noted that the EF of 1 effectively diminishes the value of leftover stored electrical energy in the ESS at the end of the cycle, which is biased to be higher with higher values of the tuning variable MIN_TRQ_{ICE}.

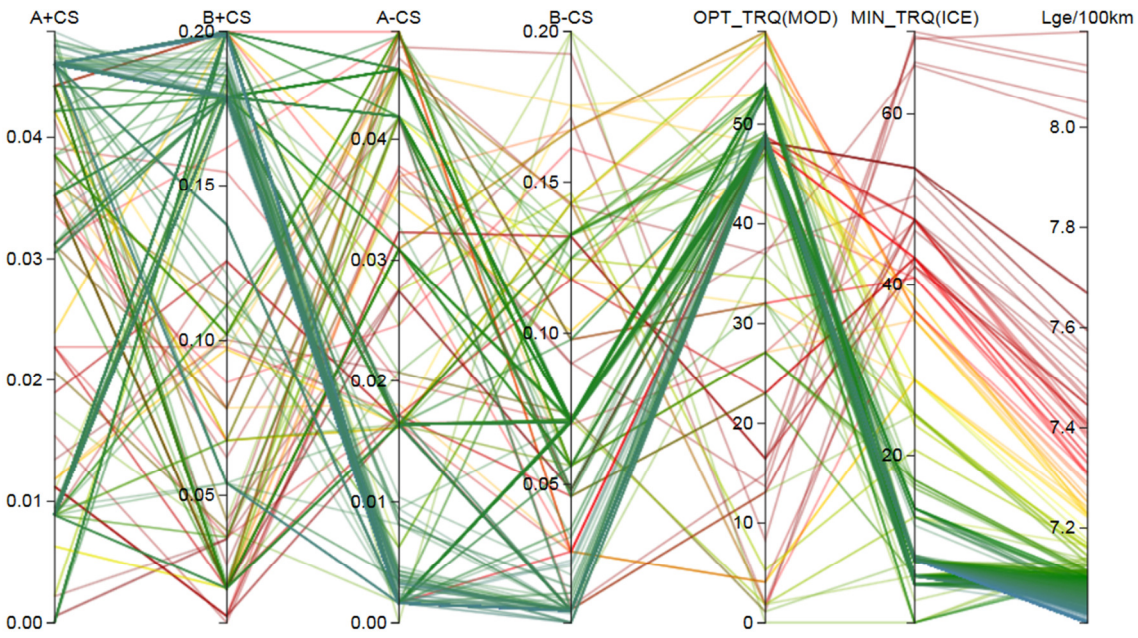

Figure 91: Linear Relationship between Fuel Consumption and Minimum ICE Torque

The same parallel axis plot for the recursive EF evaluation scheme is presented in Figure 92. The relative absence of strong secondary calibration groupings outside of the global optimal grouping and the weaker global optimal grouping suggests a more varied field of

results with weaker relationships. This reduces the confidence in the tuning obtained. None of the calibration variables display a direct functional relationship with fuel consumption. Figure 93 further exhibits this behaviour by showing that poorer performance outputs are resultant from a full range of inputs.

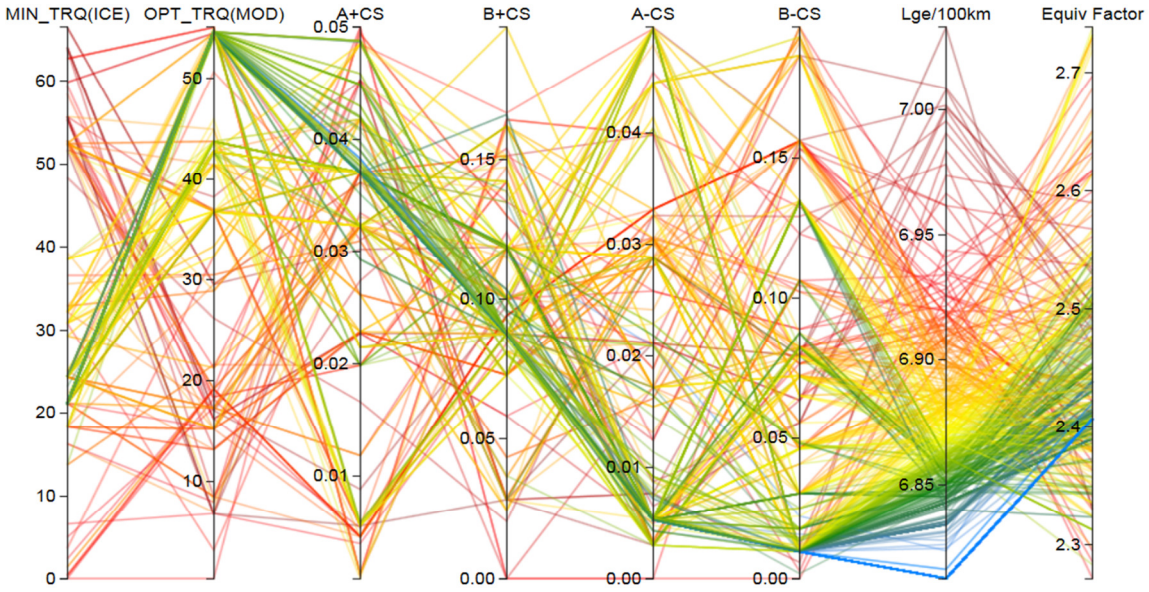

Figure 92: Recursive Equivalency Factor 4-Cycle Optimization Parallel Axis Plot

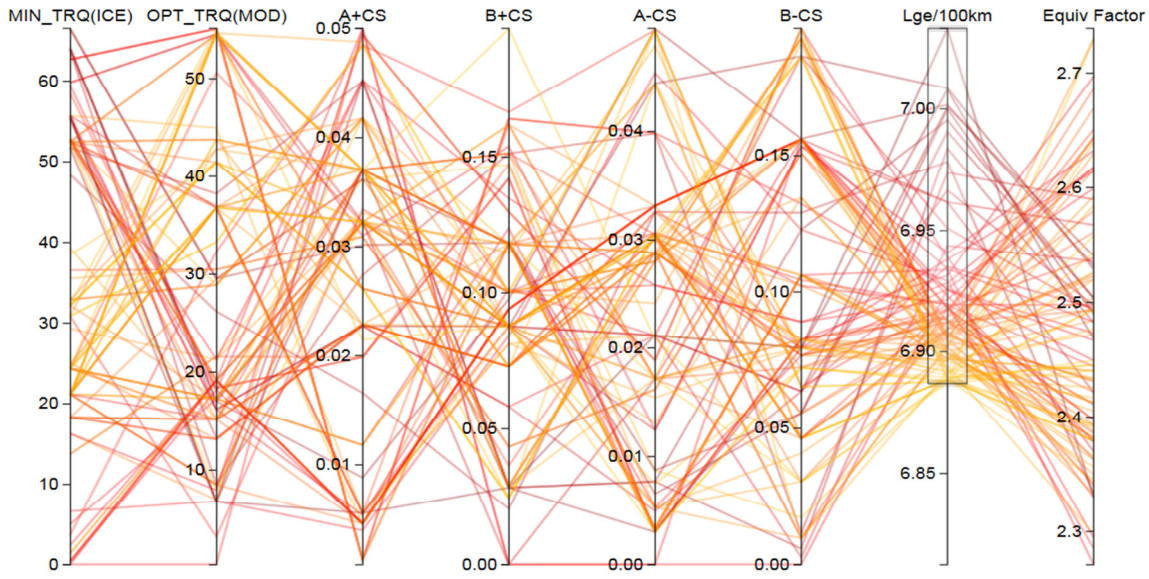

Figure 93: Recursive Equivalency Factor 4-Cycle High Consumption Filtered Data Set

5.5. Translated Optimized Strategy System Performance of SIL Model

The optimized calibration produced using the simplified model was transferred over to the SIL model to assess the effectiveness of the development process. Ideally, optimized efficiency should be observed in the drive cycles matched to their respective tuning calibrations. Results for both an EF of 1 and the recursive EF scheme were assessed. For the recursive calibrations, the equivalent consumption was calculated with an EF determined from the efficiency quotient between electrical and fuel systems to match the recursive EF optimization process described in Figure 89.

5.5.1. Equivalency Factor 1 Optimized

The EF 1 calibrations applied to the SIL model for each drive cycle resulted in vehicle equivalent fuel consumptions as listed in Table 25.

Table 25: Lge/100km Consumption Performance of SIL Model at Optimal Set-point Calibrations with Equivalency Factor 1 Applied

	Calibration				
Simulation	**US06 City**	**US06 Hwy**	**HWFET**	**FU505**	**4-Cycle**
US06 City	13.14	13.22	13.53	13.23	13.23
US06 Hwy	7.91	7.90	7.87	7.94	7.94
HWFET	5.83	5.71	5.36	5.73	5.72
FU505	7.74	7.33	9.43	7.38	7.32
4-Cycle	8.34	8.22	8.81	8.25	8.23

The percentage difference when compared to the simplified model results is indicated in Table 26. It can be seen that the optimal calibrations for the simplified model did not transfer with full certainty to the higher fidelity SIL model.

Table 26: Consumption Percent Difference between Simplified Model and SIL Model for Equivalency Factor 1

	Calibration				
Simulation	**US06 City**	**US06 Hwy**	**HWFET**	**FU505**	**4-Cycle**
US06 City	-13.2	-15.0	-13.8	-14.4	-12.7
US06 Hwy	28.2	29.9	19.4	29.1	29.1
HWFET	40.1	38.6	39.6	39.1	37.5
FU505	32.1	29.0	30.2	30.6	27.3
4-Cycle	17.5	16.4	14.2	16.9	17.5

Table 27 shows the improvement over the benchmark SIL results with the optimized tuning carried over from the MIL optimization. Despite imperfect correlation of optimal calibrations with optimal performance, as seen in Table 25, all cycles saw consumption improvements over the benchmark. Interestingly, the cycles which had results most divergent between MIL and SIL platforms received the greatest percentage improvements further suggesting that result divergence originates in higher cycle sensitivity to the calibration tuning.

Table 27: Consumption Improvement over Benchmark Equivalency Factor 1

Cycle	**Benchmark (Lge/100km)**	**Optimized (Lge/100km)**	**Improvement (%)**
US06 City	13.37	13.14	1.7
US06 Hwy	8.31	7.90	4.9
HWFET	5.85	5.36	8.4
FU505	8.80	7.38	16.1
4-Cycle	8.87	8.23	7.2

5.5.2. Recursive Equivalency Factor Optimized

The recursive EF scheme resultant calibrations applied to the SIL model for each drive cycle resulted in vehicle equivalent fuel consumptions as listed in Table 28. The EF for each simulation was calculated using the same methodology as the simplified model optimization process.

Table 28: Lge/100km Consumption Performance of SIL Model at Optimal Set-point Calibrations with Recursive Equivalency Factor Scheme

	Calibration				
Simulation	**US06 City**	**US06 Hwy**	**HWFET**	**FU505**	**4-Cycle**
US06 City	12.59	12.89	13.06	12.68	12.64
US06 Hwy	7.69	7.48	7.04	7.73	7.68
HWFET	5.77	5.45	5.25	5.61	5.75
FU505	7.22	7.91	8.72	7.08	7.32
4-Cycle	8.01	8.12	8.16	7.98	8.04

The percentage difference when compared to the simplified model results is indicated in Table 29. It can be seen that the optimal calibrations for the simplified model did not transfer with full certainty to the higher fidelity SIL model. The transfer to the higher fidelity model provided better certainty than for the static EF of 1.

Table 29: Consumption Percent Difference between Simplified Model and SIL Model for Recursive Equivalency Factor Scheme

	Calibration				
Simulation	**US06 City**	**US06 Hwy**	**HWFET**	**FU505**	**4-Cycle**
US06 City	-12.1	-12.0	-11.9	-12.6	-12.3
US06 Hwy	26.3	25.3	12.6	27.6	27.4
HWFET	38.7	36.3	43.8	32.3	40.2
FU505	31.3	41.3	39.1	30.4	33.8
4-Cycle	17.1	18.7	14.2	16.7	18.0

Table 30 shows improvement over the benchmark SIL results with the optimized tuning carried over from the MIL optimization, which is smaller than for an EF of 1.

Table 30: Consumption Improvement over Benchmark Recursively-Defined Equivalency Factor

Cycle	Benchmark (Lge/100km)	Optimized (Lge/100km)	Improvement (%)
US06 City	12.60	12.59	0.1
US06 Hwy	7.59	7.48	1.4
HWFET	5.49	5.25	4.4
FU505	7.46	7.08	5.1
4-Cycle	8.00	8.04	- 0.5

5.6. SIL Model Behaviour for Optimal Calibrations

In order to better explain the reasons behind the output divergence between the MIL and SIL model results for a given optimal calibration, detailed model output is presented in the following sub-sections. The cycle resulting in the most highly correlating MIL and SIL results, US06 City was chosen for closer investigation. In addition the unique relationships noted in output performance for the HWFET motivated closer investigation. The calibrations resulting from the recursively-defined EF were selected due to their better overall data correlations.

5.6.1. US06 City Cycle Behaviour for Optimal Calibration

Figure 94 shows overall vehicle behaviour over the US06 City cycle with the optimal calibration. Note that the direction convention for the BAS is inverted. Figure 95 shows vehicle acceleration and hybrid mode selection. Mode changes are relatively infrequent considering the dynamic nature of the drive cycle. Disturbances in vehicle acceleration are kept to a minimum through most mode changes however one major disturbance is noted early in the cycle which coincides with a large accelerator pedal request from the driver. Mode transitions seem to have been effective with the selected calibration in maintaining vehicle driveability.

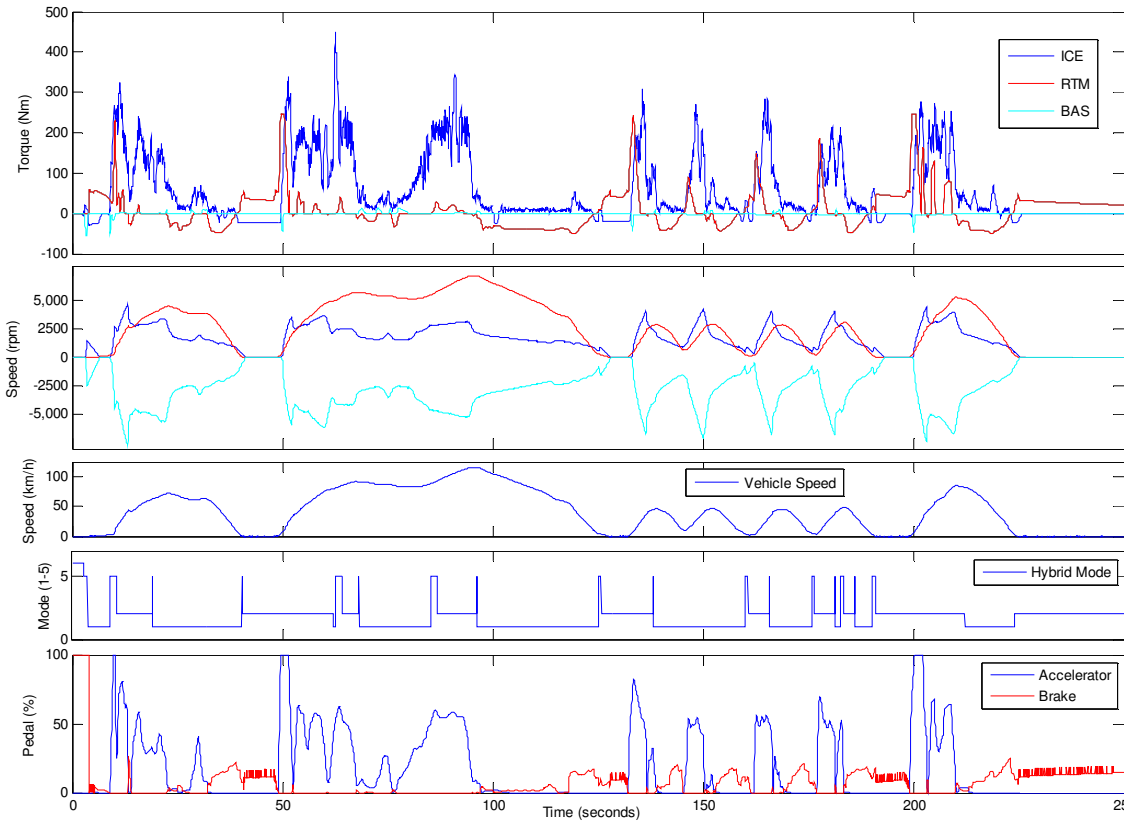

Figure 94: Overall Vehicle Behaviour over US06 City Cycle

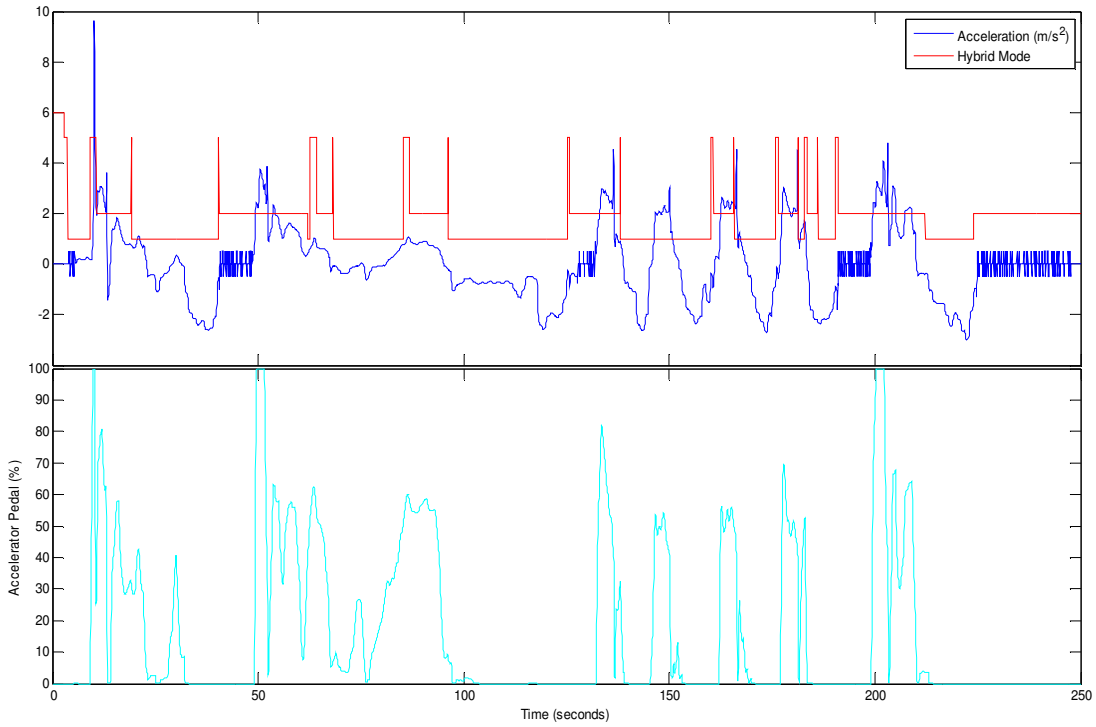

Figure 95: Vehicle Acceleration and Hybrid Mode Transitions over US06 City Cycle

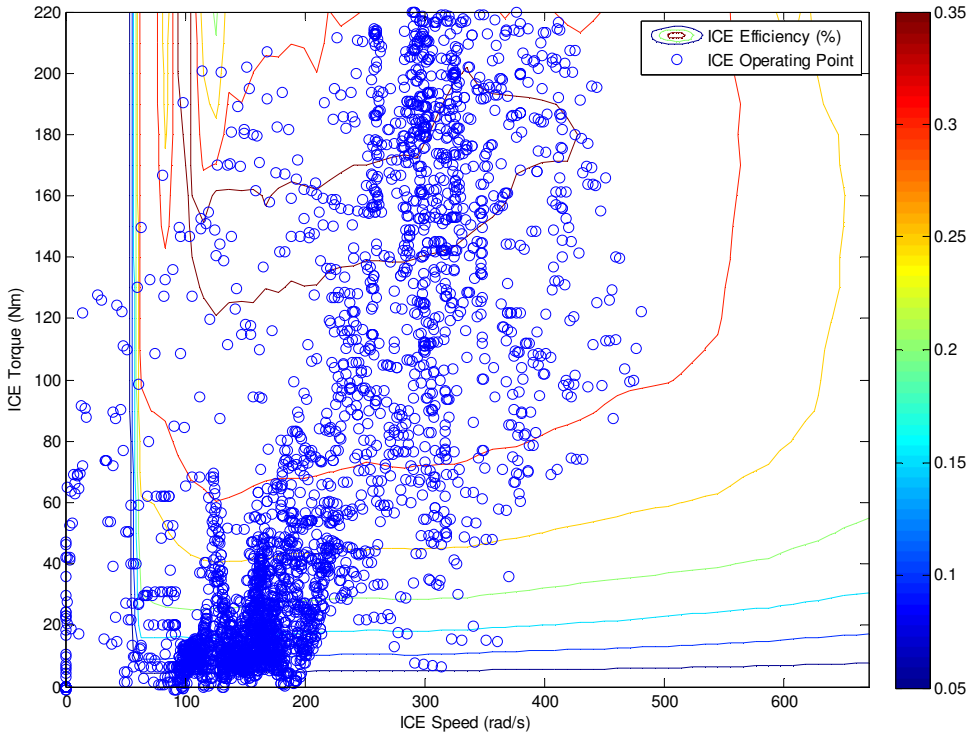

Figure 96: ICE Operation over US06 City Cycle

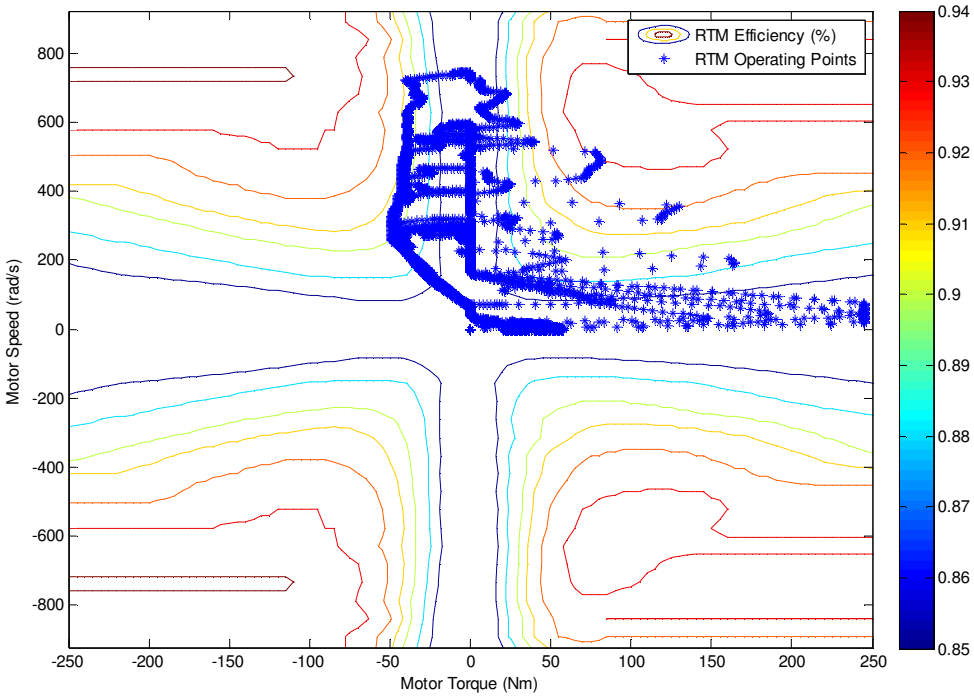

Figure 97: RTM Operation over US06 City Cycle

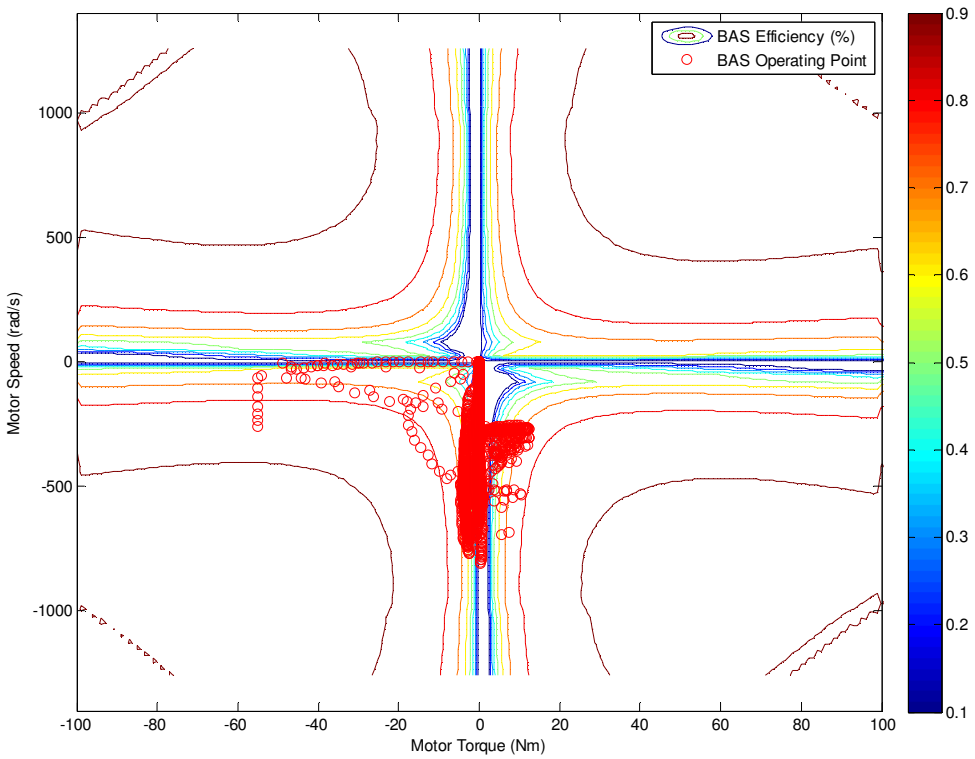

Figure 98: BAS Operation over US06 City Cycle

Figure 96, Figure 97, and Figure 98 show the operation conditions for the ICE, RTM, and BAS respectively. The RTM operation clearly displays phase in and trail off of regenerative braking during accelerator pedal tip-out throughout the cycle. In addition, the larger positive torque states represent the parallel AWD operation mode in response to large torque requests from the driver. The BAS operation is highly limited for this cycle and calibration with only very minor resistance provided correlating with the MIN_TRQ_{ICE} calibration variable. Since all tuning variables have direct impact on BAS torque, this implies a lower sensitivity to the calibration for the US06 City cycle, which correlates with the reduced results divergence between the MIL and SIL model platforms.

Figure 99 shows the breakdown of cycle time spent in each mode by percentage time. A large fraction is spent in the series-parallel AWD mode as a result of the high acceleration demands of the cycle. The total time spent in transition states is small, suggesting successful execution of the strategy-independent framework.

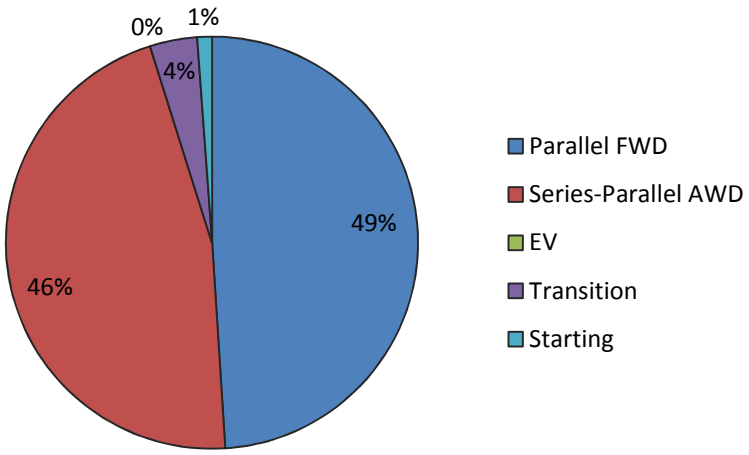

Figure 99: Hybrid Mode Selection over US06 City Cycle

To validate that the calibration functions adequately, the target speed versus actual vehicle speed are plotted in Figure 100. The curves achieve a 96.6% fit suggesting driveability is adequate. Fit was calculated according to the following equation[49]:

$$fit = 100\left(1 - \frac{\sqrt{\sum\left(V_{veh} - V_{cycle}\right)^2}}{\sqrt{\left(V_{cycle} - \overline{V_{veh}}\right)^2}}\right) \tag{14}$$

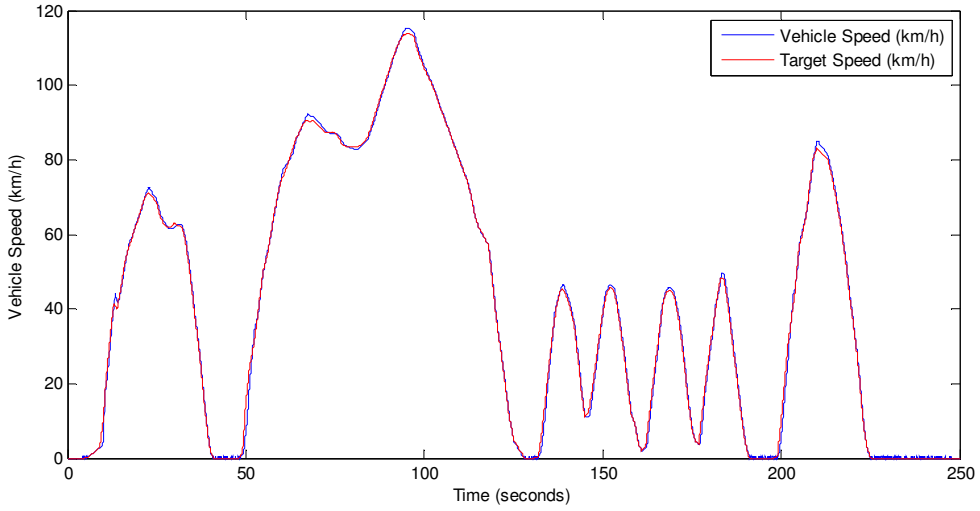

Figure 100: Driver Operation Validation US06 City Cycle

5.6.2. HWFET Cycle Behaviour for Optimal Calibration

Figure 101 shows overall vehicle behaviour over the HWFET cycle with the optimal calibration. Note that the direction convention for the BAS is inverted. Figure 102 shows vehicle acceleration and hybrid mode selection. Mode changes are very infrequent over the cycle due to the low acceleration. This is of great benefit to vehicle driveability over consistent speed cycles such as HWFET. Vehicle acceleration is generally contained within 1.5 m/s^2 providing for a generally smooth and consistent vehicle feel. Mode transitions seem to have been effective with the selected calibration in maintaining vehicle driveability, as all notable acceleration disturbances are correlated with a counterpart disturbance in accelerator pedal input.

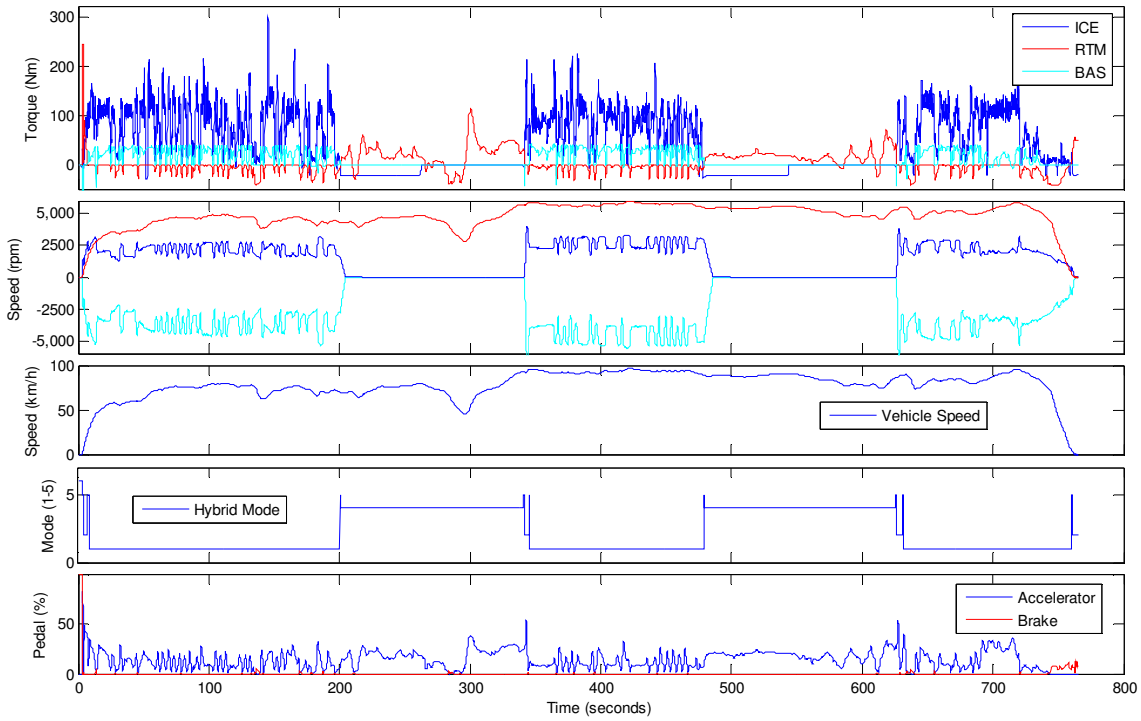

Figure 101: Overall Vehicle Behaviour over HWFET Cycle

Figure 103, Figure 104, and Figure 105 show the operation conditions for the ICE, RTM, and BAS respectively. The RTM operation shows a non-varied cluster of positive-torque points correlating with the EV periods of operation, which is along highly uniform points in the cycle. The BAS operation shows a much larger region of typical operation correlating with the high calibration value for MIN_TRQ_{ICE}. Since all tuning variables

have direct impact on BAS torque, this dense grouping implies a higher sensitivity to the calibration for the HWFET cycle, which correlates with the highly divergent results between the MIL and SIL model platforms.

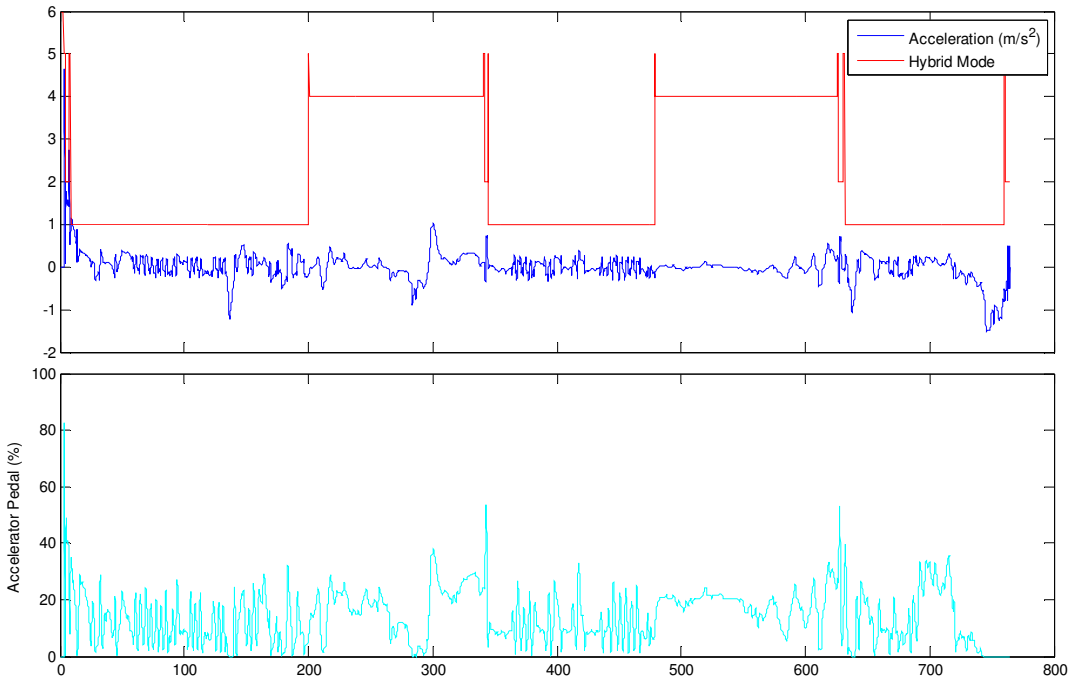

Figure 102: Vehicle Acceleration and Hybrid Mode Transitions over HWFET Cycle

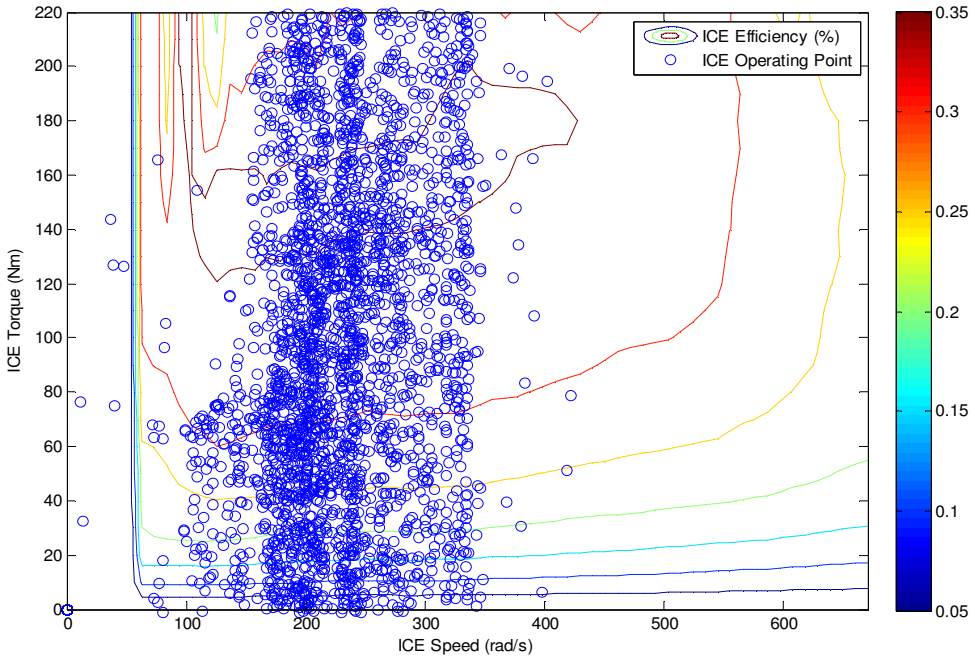

Figure 103: ICE Operation over HWFET Cycle

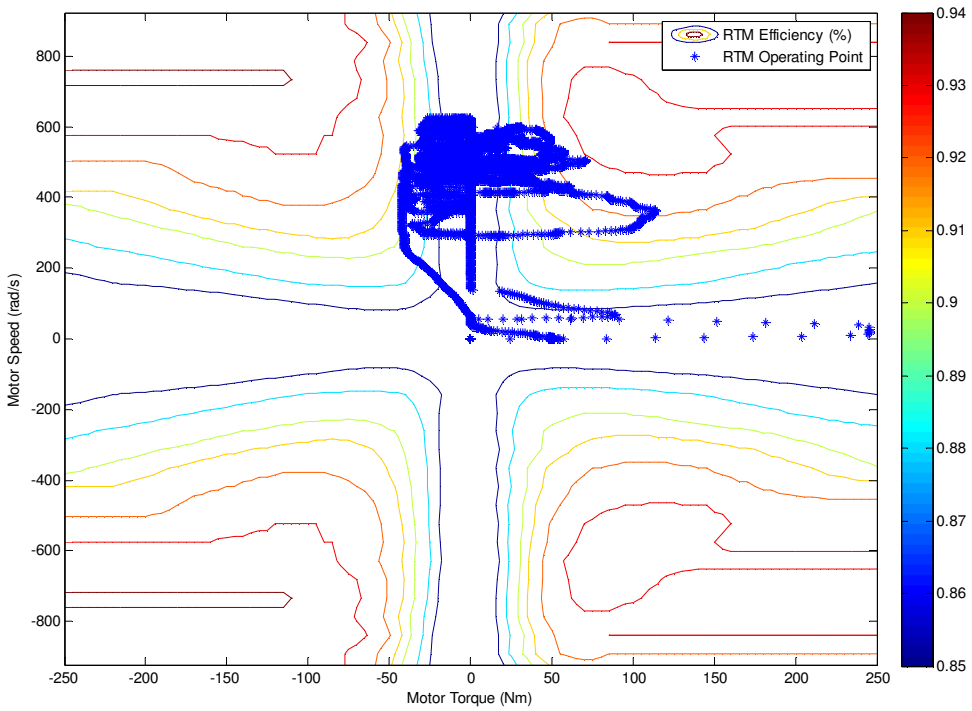

Figure 104: RTM Operation over HWFET Cycle

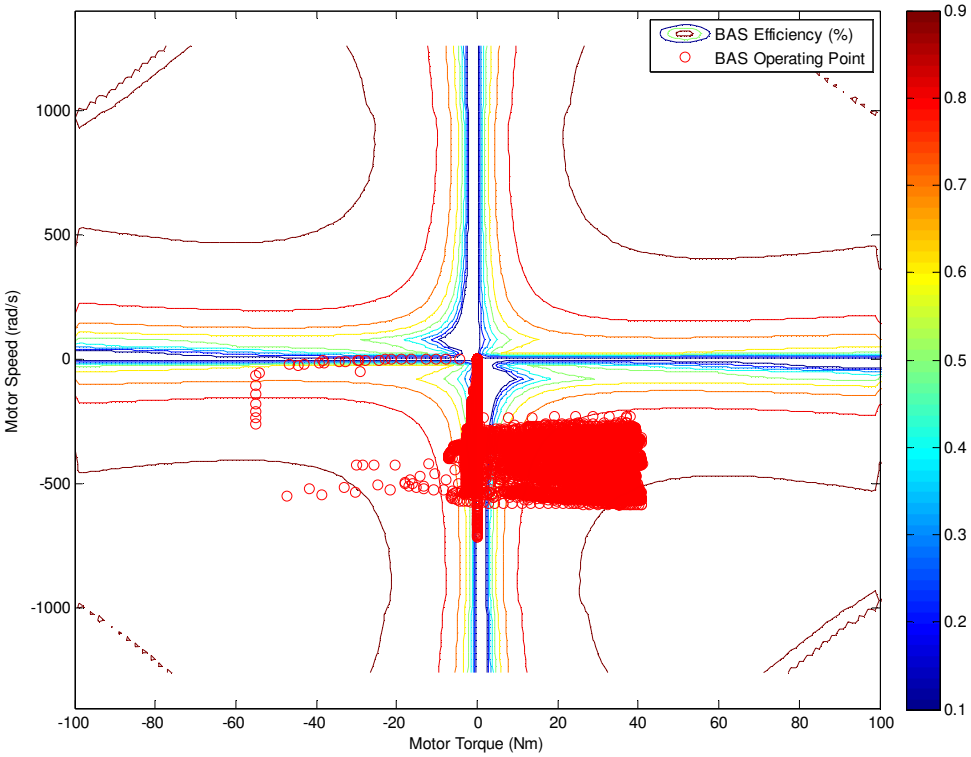

Figure 105: BAS Operation over HWFET Cycle

Figure 106 shows the breakdown of cycle time spent in each mode by percentage time. The large EV mode fraction highlights the charge-accumulating nature of the parallel FWD mode for this calibration and cycle. The total time spent in transition states is minimal, suggesting stability of the strategy under somewhat uniform loading.

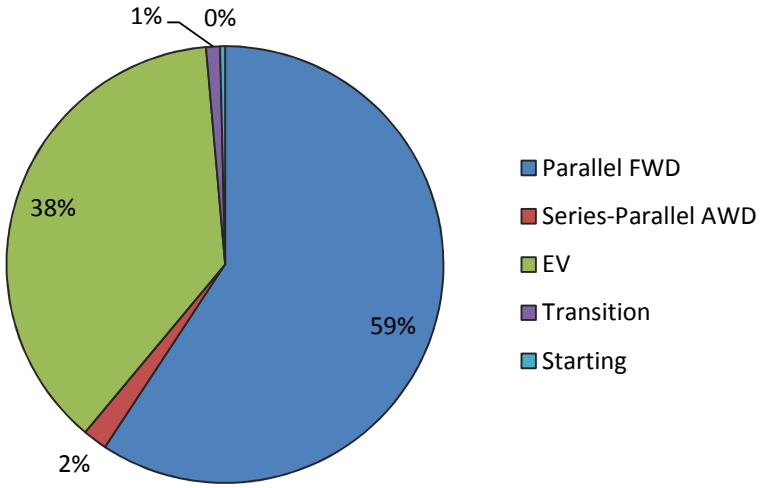

Figure 106: Hybrid Mode Selection over HWFET Cycle

To validate that the calibration functions adequately, the target speed versus actual vehicle speed are plotted in Figure 107. The curves achieve a 98.1% fit suggesting driveability is adequate.

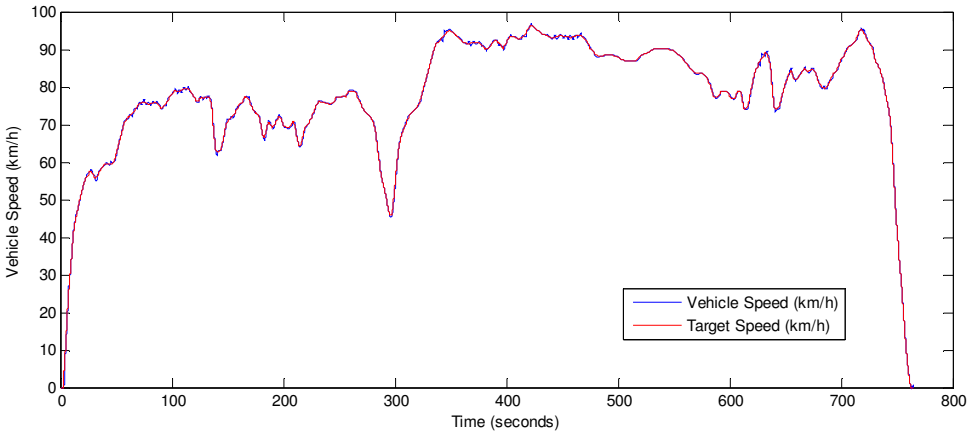

Figure 107: Driver Operation Validation HWFET Cycle

5.7. Performance Evaluation Summary

Tuning calibration of the rule-based control strategy was completed with the intent of providing a path for validation of the dual development platform approach for control system optimization and implementation. As the SIL and MIL platforms were developed largely in parallel with work product from different controls development team members being incorporated into the end results, comparison of strategy dependent benefits resulting from changes calibrated in the MIL platform to performance benefits for the same calibration applied to the SIL model allows assessment of the usefulness of this developmental approach. Performance benefit carry over between the MIL and SIL platform demonstrates the benefits of using a parallel path development approach. This method allows simulation runtime advantages associated with simplified models to be used in the development of advanced control strategies, while robust and safety-critical development of lower level functionality can be developed in parallel using a high fidelity SIL/HIL test platform.

Chapter 6: Conclusions and Recommendations

6.1. Strategy-Independent Controls Implementation and Effects

The controls logic hierarchy developed was designed with the intention of allowing for strategy-independent robust operation of the UVic EcoCAR2 PHEV architecture. The proposed structure allows for any general energy management strategy to be employed so long as output requests are limited to torque requests for the RTM, BAS, and ICE, with an additional signal defining which operating regime the vehicle is presently requested to run in based on the torque set-point values.

The developed hierarchy functions well as a platform for control strategy implementation within the vehicle. A rule-based energy management strategy was used to validate operation of the platform, with global optimization of tuning variables providing for a wide range of operational testing coverage of the platform. In all cases, the vehicle completed the drive cycles tested. Detailed review of the optimal calibration for US06 City and HWFET drive cycles suggested adequate driveability throughout the cycle. Some vehicle acceleration disturbances were noted during the US06 City cycle corresponding to large driver acceleration pedal requests.

The final resultant system provides a foundation for further development and safe in-vehicle testing of novel energy management strategies. Safety-critical and diagnostic function can be further developed in isolation using the standard MBD process described in Chapter 3, while new energy management strategies can be readily ported into the platform for simulated or in-vehicle test evaluation.

6.2.Two-Model Development Approach

The energy management strategy development path proposed relied on a two-model approach. A simplified model simulation platform using quasi-static forward-looking power loss techniques was used to develop an optimally tuned strategy, which was then ported into the SIL development platform for operational testing. The underlying models were constructed to accept the same inputs, with the SIL model containing more advanced modeling of vehicle communications and controller I/O, as well as higher

fidelity plant component models with realistically represented sub-component ECU functionality. These two models produce varying results, but some comparison validation was used to show that the models behaved relatively similarly on an aggregate energy-use basis for the US06 City and Highway cycles. The HWFET and FU505 cycles displayed more significant aggregate result variance.

The rule-based control strategy used in validating the development approach contains optimized tuning variables which are highly interactive with instantaneous operating conditions within the vehicle powertrain. For example, BAS assist and desist functionality during parallel operating regimes is scaled to be proportional to instantaneous ICE torque production as reported by the ICE ECU. As a result, the charge-following strategy employed is sensitive to minutiae in the torque requests sent to the ICE. Additionally, various driveline tuning functions, as discussed in Chapter 4, were used to tune the vehicle for smooth operation. The cumulative effect of the dynamic response differences in each component model combined with these controller elements were responsible for significant differences in the overall equivalent fuel consumption yielded by a particular energy management calibration when evaluated on each model.

The optimized calibrations derived from the simplified model demonstrate a significant pitfall in using global optimization techniques to improve vehicle efficiency. While each cycle performed significantly better than the benchmark tuning when optimally calibrated, efficiency was significantly degraded when cycles were run on calibrations which were optimally tuned to other cycles. This was most significantly noted for the HWFET cycle. These results are likely attributed to the fact that the HWFET cycle has the lowest acceleration profiles, and consequently has the greatest sensitivity to the dynamic response of each component model when being controlled via the energy management strategy as developed. Consequently, the HWFET cycle also had the worst divergence of results between the simplified model and the SIL model.

The recursive EF assessment method described in Chapter 5 allows for a more realistic accounting of surplus or deficit ESS SOC when determining cycle CS equivalent consumption. This evaluation method does pose some issues when trying to apply global

optimization techniques. The recursive evaluation scheme readjusts the EF for each cycle run based on the aggregate minutiae of the electrical system and ICE efficiency performance throughout the cycle. This relocation of the design target provides additional reason to doubt that a global optimal calibration has been achieved. As a result, a small variance in operation, caused by differences between model development platforms, or just as relevantly, variance between modeled and in-vehicle behaviour, becomes more likely to result in large variance in aggregate vehicle efficiency. Thus, optimally calibrating an energy management strategy using this methodology may also be more susceptible to driver behaviour differences and differences in drive cycle characteristics, making it in practice a less useful driver for design optimization.

Despite the absolute aggregate consumption variances between the MIL and SIL modeling platforms, the optimized calibrations produced in the MIL platform produced efficiency improvements in the SIL model compared to the benchmark calibration. Since the benchmark calibration was set based on engineering intuition, these results validate the usefulness of the two-model development approach. A slight decay in vehicle efficiency was noted for the 4-cycle test when results were assessed using a recursively-defined EF. This may have been the result of trying to combine multiple drive cycle test results into one aggregate value using the weighted average method.

6.3.Recommended Future Vehicle Work

Additional vehicle work is required to allow for the UVic PHEV architecture to reach its operational potential, and to allow UVic vehicle controls development research to be highly effective moving forward. This work includes mechanical upgrades to the vehicle and controls updates to the low-level component operation.

6.3.1. Mechanical Deficiencies

The controls development discussed uses a two-model development process and industry-standard MBD procedures for controls testing and refinement. The final step in this process uses vehicle testing to further refine operation, with the end goal being complete synchronization of the modeled simulation results and real-world in-vehicle results.

Mechanical unreliability in the BAS-ICE belt drive interface has consistently presented challenges to the development team. It also prevented full realization of operational flexibility of the control system due to the need to artificially restrict BAS torque input to well below the component capacity to try to protect against mechanical failure of the interface.

The design deficiency exists at the interface between the belt sprocket and the ICE crank shaft. The passenger side crankshaft interface is not designed to allow significant transmission of driveline torque, as it is only used for relatively low level BAS systems in the stock HEV configuration. Repeated mechanical failures of the keyway torque interface and crankshaft itself prohibited rigorous in-vehicle testing and detailed ICE behaviour testing.

A possible solution to the deficiency is the design of an outboard bearing system built into the crank case cover of the ICE. This bearing would support an idler shaft which can be interfaced to the crankshaft end and belt pulley sprocket. Such a configuration would reduce or eliminate the bending moment induced on the crank shaft by the belt pulley system, greatly improving mechanical reliability. Improved reliability would allow for more rigorous vehicle testing and further development of the control platform.

6.3.2. Engine-Throttle Relationship Verification

A significant potential for variance between the SIL model and the in-vehicle behaviour presently persists due to uncertainties in the ICE response to throttle input. The stock vehicle configuration uses an analog voltage input from the drive accelerator pedal to request torque at the ICE ECU. The maximum and minimum torque curves of the ICE are known, but the response curve of the throttle request between maximum and minimum values is not known. The response is presently modeled in the SIL platform as linear between minimum and maximum torque capacity.

Inconsistency between assumed and actual throttle response curve at the ICE will result in inconsistent torque production at mode transitions. This can cause driver startle and driver irritation, which should generally be avoided. Since the vehicle architecture relies

on relatively frequent mode transitions, this effect may become significant during in-vehicle operation.

Developing a response map for the throttle pedal input simply requires static point testing of the ICE torque output on varying throttle inputs at various speeds. This can be accomplished by using the BAS as a dynamometer, while setting the transmission to neutral. The BAS would control the ICE to the desired speed using a speed control PI algorithm, and the reported torque from the BAS would be recorded at each operating point to develop the map.

6.3.3.Use of Manumatic Transmission Functionality

Present operation of the transmission relies on automatic control. The transmission gearing is controlled based on torque status signals sent by the ICE ECU as well as sensed operation status within the transmission. This means that the instantaneous gear selection is not directly controllable by the UVic VSU. As a result, controller wheel torque calculations use a “soft” estimation of present gear ratio based on present vehicle speed. This soft gearing estimation is a continuous curve constructed from the GM shift map of the transmission. This allows for elimination of the potential for gear selection bounces that would exist if explicit gear ratio were used in the vehicle control.

Explicit gear selection capability would allow for explicit gear ratios to be used in wheel torque calculations. This would allow for better drive feel tuning and improve the functionality of mode transitions. Implementation would require additional I/O configuration and testing to link into the transmission ECU and replicate upshift and downshift input I/O sent by the stock vehicle manumatic shift PRINDL functions. Thus gears could be selected in the same manner as when a driver is piloting the stock vehicle in manumatic mode.

6.4.Recommended Future Research Development of Work

6.4.1.Application of Industry Standard Driveability Tools

AVL-DRIVE is an industry-standard simulation add-in tool for objectively measuring vehicle driveability. It uses vehicle data including longitudinal acceleration, pedal

request, and vehicle velocity to produce standardized metrics which describe the driver experience. The software tool can interface with the vehicle SIL simulation to aid in driveability tuning in a simulated environment[50].

Part of the developmental motivation behind the strategy-independent controls platform was the need to apply driveability constraints to a highly flexible optimized energy management strategy while not influencing the functional flexibility of the powertrain. Employing AVL-DRIVE would allow more precise tuning of the mode transitions using objective modeled results feedback. Testing the transition algorithms for a wide variety of fabricated inputs would allow for enhancement of underlying controls platform, further improving the end drive experience of the vehicle while demonstrating future advanced energy management strategies in the vehicle. Academic database searches reveal a lack of research which integrates this tool into works. An associated challenge is that for output of AVL-DRIVE to be meaningful, the vehicle model needs to be of high enough fidelity to capture secondary vehicle handling effects resulting from powertrain control inputs.

6.4.2. Development of Higher Accuracy Lightweight Models for Optimization

The two-model development approach used to validate and optimize high level energy management strategies has been demonstrated to be sensitive to the dynamic behaviour of individual powertrain components irrespective of validating overall power loss similarity. While global optimization would ideally be applied to the highest accuracy models available, computational resource limitations present a challenge. The dynamic sensitivities not captured in a simplified quasi-static power loss model has been shown to create significant divergence in aggregate EC results between the MIL and SIL platforms for lower power drive cycles.

One possible approach is the development of individual component meta-models which more accurately represent dynamic component behaviour. *Murgovski et al.* describe an automated process for developing highly accurate quasi-static component meta-models from proprietary dynamics models[49]. The meta-models could be developed from the detailed SIL platform models to fully capture the dynamic behaviour of each subsystem.

This would be especially beneficial for the ICE and ESS models, which are of much higher fidelity in the SIL model than in the simplified optimization model.

It is essential that component models used in the simplified model maintain a fast enough runtime to be useful for optimization to retain the purpose of the two-model approach. The goal of producing meta-models of each component would be a better carry-over of optimal efficiency between the two platforms, to allow for the development process to be fully realized in future powertrain controls research at UVic using the developed PHEV.

6.4.3.Development of Quasi-Optimal Rule-Based Controls Strategy

The rule-based control strategy that was developed used engineering intuition to establish the basic framework of operation. This includes definition of individual hybrid mode regimes as well as rules for transition between them. Thus the optimization of the specific calibration for the strategy is constrained these definitions which are intrinsic to the strategy.

Work by *Kaban* on the application of dynamic programming to the UVic EcoCAR2 PHEV architecture provides for a useful roadmap in understanding ideal operating characteristics for given drive cycles without the constraints of driveability or driver interaction[4]. Consolidation of these results into a quasi-optimal strategy framework via redefinition of mode behaviour and inter-mode transitions would theoretically provide a better starting point for global optimization of calibration variables as presented, allowing for greater EC improvements. The strategy-independent nature of the control system platform developed would allow for rapid redeployment with new underlying strategy fundamentals.

6.5.Summary of Contributions

The controls development process and associated vehicle simulation platforms were conceived to address the expanding developmental burden associated with implementing advanced control strategies within high DOF HEV architectures. With academic research and development efforts being primarily directed at energy management algorithms,

considerable challenges associated with validation of vehicle control systems for such advanced architectures constitute a barrier to real-world testing of researched strategies.

Through breaking up the vehicle control system into a distinct logic hierarchy, energy management strategy can be effectively delineated from overall control system integration challenges. This effectively allows for a parallel development path to implementation of advanced strategies within a real vehicle while retaining robustness, driveability, and safety-critical considerations as part of the final design execution. The rule-based energy management strategy employed was optimally calibrated using a simplified parallel model platform, and then the calibration results were ported to the advanced SIL control development environment. Carry-over of efficiency improvements validates the proposed approach and the implementation of a strategy-independent vehicle control system for the selected PHEV architecture.

Bibliography

[1] "EcoCAR2: Plugging into the Future, Non-Year-Specific Rules, Rev: N," ed: Argonne National Laboratory, 2014.

[2] J. Wise, "A Real-Time Hybrid Vehicle Control Strategy and Testing Platform," Master of Applied Science, Department of Mechanical Engineering, University of Victoria, Victoria, BC, 2011.

[3] J. Waldner, "Development of a 2-Mode AWD E-REV Powertrain and Real-Time Optimization-Based Control System," Master of Applied Science, Department of Mechanical Engineering, University of Victoria, Victoria, BC, 2011.

[4] S. Kaban, "Performance Modeling and Benchmark Analysis of an Advanced 4WD Series-Parallel PHEV Using Dynamic Programming," Master of Applied Science, Department of Mechanical Engineering, University of Victoria, Victoria, BC, 2015.

[5] R. Capata and A. Coccia, "Procedure for the Design of a Hybrid-Series Vehicle and the Hybridization Degree of Choice," *Energies,* vol. 3, pp. 450-461, 2010.

[6] (2004). *A Short Field Guide to Hybrids*. Available: http://www.greencarcongress.com/2004/08/a_short_field_g.html

[7] C. Manzie, *Relative Fuel Economy Potential of Intelligent, Hybrid and Intelligent-Hybrid Passenger Vehicles*, First ed. Amsterdam, The Netherlands: Elsevier.

[8] (2011). *History of Hybrid Vehicles*. Available: http://www.hybridcars.com/history/history-of-hybrid-vehicles.html

[9] M. J. Kamper and R. Wang, "Hybrid Electric Vehicles," in *Discussion Forum: Electric Vehicles vs Hybrid Vehicles*, Electrical Machines Laboratory, University of Stellenbosch, Stellenbosch, South Africa, 2008.

[10] Y. A. Cengel and M. A. Boles, *Thermodynamics: An Engineering Approach*, 6th ed. New York, NY: McGraw-Hill Companies Inc., 2008.

[11] M. A. Delucchi and T. E. Lipman, *Lifetime Cost of Battery, Fuel-Cell, and Plug-in Hybrid Electric Vehicles*, First ed. Amsterdam, The Netherlands: Elsevier.

[12] S. J. Clegg, "A Review of Regenerative Braking Systems," *Institute of Transport Studies, University of LEEDS,* vol. Working Paper 471, 1996.

[13] (2015). *Average Annual Miles per Driver by Age Group*. Available: http://www.fhwa.dot.gov/ohim/onh00/bar8.htm

[14] SAE, "Standard J2841: Utility Factor Definitions for Plug-in Hybrid Electric Vehicles Using 2001 U.S. DOT National Household Travel Survey Data," ed, 2001.

[15] "Autonomie GM LE9 Engine Operational Dataset," ed. Argonne National Laboratory: Autonomie, 2012.

[16] W. Rippel, "Induction Versus DC Brushless Motors," in *Tesla Motors Blog* ed, 2007.

[17] R. Krishnan, *Electric Motor Drives: Modeling, Analysis, and Control* Upper Saddle River, New Jersey: Prentice-Hall Inc., 2001.

[18] N. Omar, et al., "Standardization Work for BEV and HEV Applications: Critical Appraisal of Recent Traction Battery Documents," *Energies,* vol. 5, pp. 138-156, 2012.

[19] T. Markel and A. Simpson, "Energy Storage Systems Considerations for Grid-Charged Hybrid Electric Vehicles," Institute of Electrical and Electronics Engineers Computer Society, Piscataway, NJ, Chicago, IL, United States2005.

[20] (2007). *Report: Toyota Will Delay Use of Li-Ion in the Prius*. Available: http://www.greencarcongress.com/2007/06/report_toyota_w.html

[21] H. Kelly, "Energy Efficiency and Renewable Energy Program," Argonne National Laboratories, Electric-Drive Vehicle Programs, US DOEAugust 30, 2012.

[22] R. Kotz and M. Carlen, "Principles and Applications of Electrochemical Capacitors," *Electrochimica Acta,* vol. 45, pp. 2483-2498, 2000.

[23] A. Rufer and P. Barrade, "A supercapacitor-based energy storage system for elevators with soft commutated interface," in *36th IAS Annual Meeting - Conference Record of the 2001 Industry Applications, Sep 30-Oct 4 2001*, Chicago, IL, 2001, pp. 1413-1418.

[24] (2014). *U.S. PEV Sales by Model*. Available: http://www.afdc.energy.gov/data/10567

[25] (2014). *U.S. HEV Sales by Model*. Available: http://www.afdc.energy.gov/data/10301

[26] Mazda. *i-STOP Idling Stop Technology*. Available: http://www2.mazda.com/en/technology/env/i-stop/

[27] *Case Study: Toyota Hybrid Synergy Drive*. Available: http://www.ae.pwr.wroc.pl/filez/20110606092430_HEV_Toyota.pdf

[28] L. Zhou, et al., "Design, Modeling and Simulation of a E-REV Using a Saturn VUE Platform, GM 2-mode Transmission and a Rear Traction Motor," 10PFL-0573/2010-01-0830 (PFL100), Advanced Hybrid Vehicle Powertrains (Part 2 of 3), 2010 World Congress & Exhibition, 2010.

[29] M. Mattsson and J. Hordsson, "Marine Hybrid Electric Powertrain - Analysis of Hybrid Features and Simulation of Fuel Consumption for Vessels up to 40m," Master of Science, Automotive Engineering, Chalmers University of Technology, Goteborg, Sweden, 2010.

[30] "Greenhouse Gas Reduction Strategies in the Transport Sector," OECD/ITF2008.

[31] J. J. Corbett and P. Fischbeck, "Emissions from Ships," *Science,* vol. 278, pp. 823-824, 31 October 1997 1997.

[32] R. McLaren, et al., "A survey of NO_2:SO_2 emission ratios measured in marine vessel plumes in the Strait of Georgia," *Elsevier: Atmospheric Environment,* vol. 46, pp. 655-658, 2012.

[33] *Marine Emissions*. Available: http://www.bcairquality.ca/topics/marine-emissions.html

[34] "Canada/US Emission Control Area (ECA) For Ships," ed. Vancouver, Ottawa, Halifax: Environment Canada, Transport Canada, Government of Canada, 2009.

[35] P. Di, et al., "Diesel Particulate Matter Exposure Assessment Study for the Ports of Los Angeles and Long Beach," California Environmental Protection Agency2006.

[36] W. L. R. Emmet, Sc.D., General Electric Company, "The Electrical Propulsion of Ships," in *American Institute of Electrical Engineers*, 1913, pp. 43-60.

[37] *Vacon AC drives save fuel at sea*. Available: http://www.vacon.com/Default.aspx?id=464736

[38] "Regulatory Announcement: EPA Issues New Test Methods for Fuel Economy Window Stickers," Environmental Protection Agency2006.

[39] L. Larsson and C. R. Raven, *Ship Resistance and Flow*: The Society of Naval Architects and Marine Engineers, 2010.

[40] "2012 EcoTec 2.4L I-4 VVT (LE9): Product Highlights," ed: General Motors, 2013.

[41] "Autonomie GM 6T40 Automatic Transmission Operational Dataset," ed. Argonne National Laboratory: Autonomie, 2012.

[42] J. Jancowski-Walsh, et al., "Refinement of Series-Parallel Multiple-Regime Vehicle Architecture Using 2013 Chevrolet Malibu Platform," presented at the SAE Powertrains Fluids and Lubricants, 2014.

[43] D. Prescott, et al., "Implementation of Series-Parallel Multiple-Regime Vehicle Architecture Using 2013 Chevrolet Malibu Platform," presented at the SAE Powertrain Fluids and Lubricants, Malmo, Sweden, 2013.

[44] C. S. Carlson, *Effective FMEAs*, First ed.: Wiley, 2012.

[45] D. Prescott, et al., "Modeling and Simulation Activities Summary for Rapid Prototype Development of Series-Parallel Multiple-Regime Vehicle Architecture, unpublished," 2014.

[46] A. J. Wheeler and A. R. Ganji, *Introduction to Engineering Experimentation*, Second ed. Upper Saddle River, New Jersey: Pearson Education Inc., 2004.

[47] L. Guzzella and A. Sciarretta, "Vehicle Propusion Systems," ed: Spriner, 2005.

[48] H. Vazquez-Leal, et al., "High Accurate Simple Approximation of Normal Distribution Integral," *Mathematical Problems in Engineering,* vol. 2012, 2012.

[49] N. Murgovski, et al., "A methodology and a tool for evaulating hybrid electric powertrain configurations," *International Journal of Electric and Hybrid Vehicles,* vol. 3, pp. 219-245, 2011.

[50] Mathworks. *AVL-DRIVE: A Tool for Objectively Measuring Vehicle Driveability*. Available: http://www.mathworks.com/products/connections/product_detail/product_35936.html?refresh=true

Appendix A – System Interfacing Details

The vehicle-controller interface includes CAN, digital, and analog signal connections between the various ECUs and the VSU. The connections between these components and the interface design at each controller are described in this appendix.

Table 31 shows the digital and analog interfacing at the VSU (MABX). It also highlights hardware interfacing differences between the HIL simulation test platform and the vehicle, which result from omitted model functionality. These functions were omitted due to not providing sufficient utility motivation for inclusion within the simulation. Figure 109 shows the functional digital and analog connections between the VSU and the vehicle powertrain components

Table 31: MicroAutoBoxII VSU Interfacing

PIN	MABX FUNCT	CONTROLLER FUNCTION	Veh	HIL
1 E	VDRIVE	VDRIVE – MABX Required		
1 M	Group 3 Ch 3	ICE Run Crank Control Out		
1 W	ADC Type 1 Con 1 Ch 4	Brake Pedal Input		
1 Y	ADC Type 1 Con 1 Ch 3	Charge Plug Proximity		
1 a	ADC Type 1 Con 1 Ch 2	Accel Pedal Pos Voltage #2		
1 b	ADC Type 1 Con 2 Ch 1	ACCM L/S Pressure Sensor		
1 c	ADC Type 1 Con 1 Ch 1	Accel Pedal Pos Voltage #1		
2 C	DAC 4	Accel Pedal Out to ECM V2		
2 D	DAC 2	Accel Pedal Out to ECM V1		
2 L	Group 2 ch 6	IMS C Gateway		
2 T	Group 2 ch 2	IMS P		
2 c	VBAT prot	DIGIO THRES		
3 B	Group 1 ch 5	Magna Wake		
3 F	GND	Ground 1		
3 G	GND	Ground 2		
3 H	GND	Ground 3		

3	K	Group 2 ch 1	IMS N Gateway		
3	L	Group 2 ch 7	IMS P/N Gateway		
3	M	REMOTE	WAKE		
3	T	Group 2 ch 3	IMS P/N		
3	V	VBAT	12V Power 1		
3	W	VBAT	12V Power 2		
3	X	VBAT	12V Power 3		
3	Y	Group 4 ch 1	ICE On Switch		
4	A	Group 1 ch 2	APM Ena		
4	B	Group 1 ch 6	MPDM ENA		
4	E	Group 6 ch 3	ESS Charging Indicator Light		
4	L	Group 2 ch 8	Magna PCM Shutdown		
4	S	TPU ch 14	Charge Plug Control Pilot		
4	T	Group 2 ch 4	IMS C		
4	Y	Group 4 ch 2	Charge-Sustaining Switch		
5	A	Group 1 ch 3	ACCM Ena		
5	B	Group 1 ch 7	ChargeA Wake Cmd		
5	E	Group 6 ch 4	GFI Light Ground-Fault (Red)		
5	F	Group 6 ch 8	VehicleReady Indicator (Blue)		
5	L	Group 3 ch 1	BMS VEH_WAKE		
6	A	Group 1 ch 4	TM4 Enable		
6	L	Group 3 ch 2	Charge Plug Contactor Command		
6	Y	Group 4 ch 3	Regen Off Switch		
6	a	Group 5 ch 1	Key Accessory Wake Signal		
6	b	Group 5 ch 4	Key Run Crank Signal		

The vehicle controls interfacing functionality is distributed across four CAN busses, each responsible for different component groups within the vehicle. The UVic CAN bus includes all major powertrain components added to the stock vehicle. A lower baud rate CAN bus is also used for control of the MPDM, a CAN-based relay controller used to switch on ancillary low voltage components in the vehicle including cooling pumps and cooling fans. The stock ICE has also been separated from the stock GM high speed CAN bus to facilitate individual control of its functions. The overall CAN architecture is shown in Figure 108.

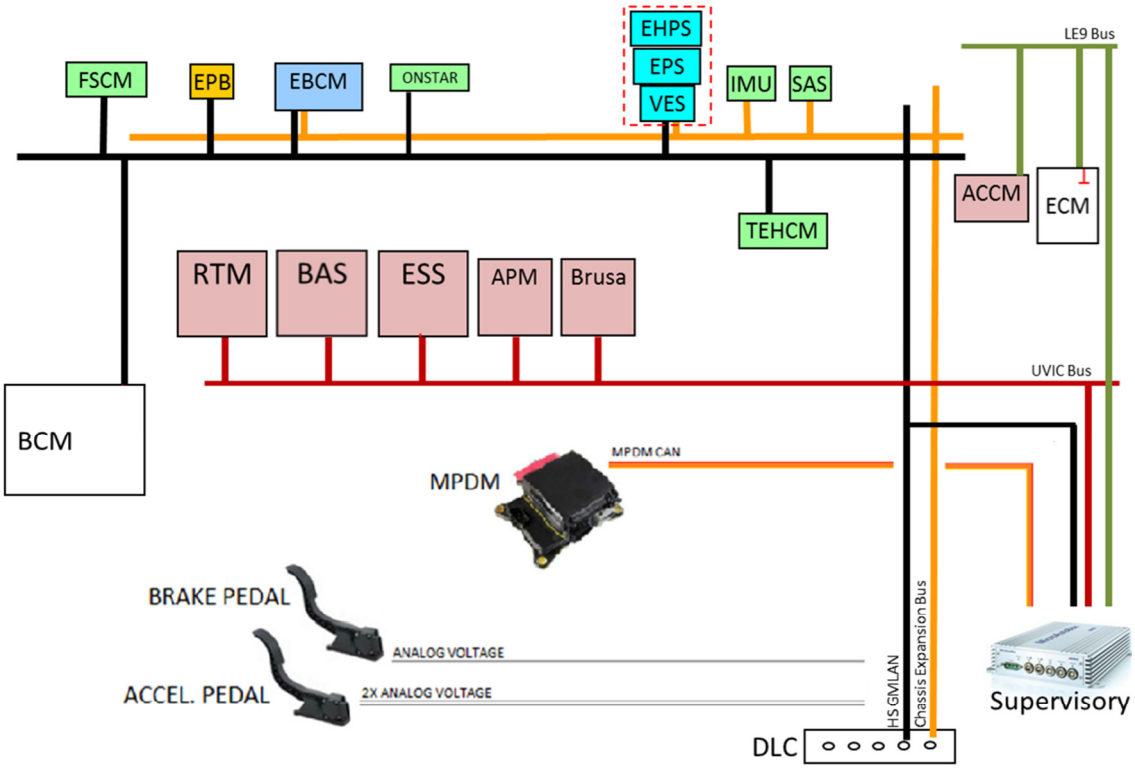

Figure 108: Vehicle CAN Architecture

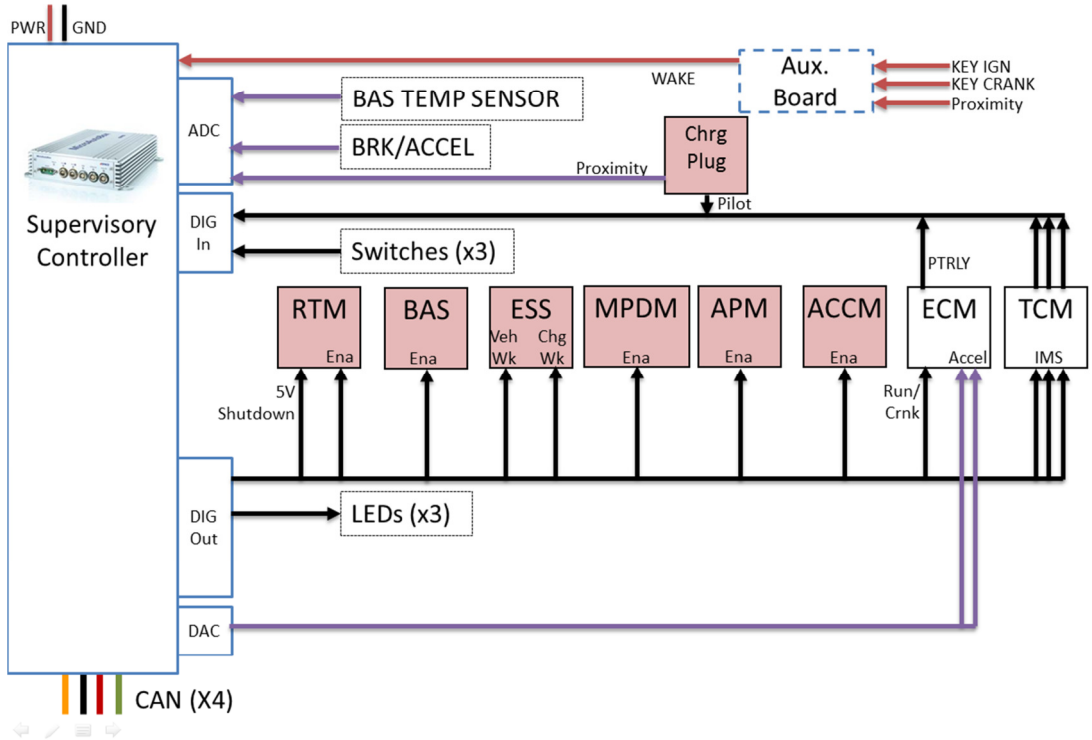

Figure 109: Vehicle Control System Connections

Appendix B – Development of Transmission Gearing Estimation Curve and Rationale

A lack of explicit control of transmission gear selection at the supervisory control level of the vehicle presents an operational challenge. Given the differing drive advantage ratios across the torque-producing components (MGs and ICE), wheel torque output was the variable used in interpreting driver torque requests from the vehicle accelerator pedal and propagating these requests through the controls system.

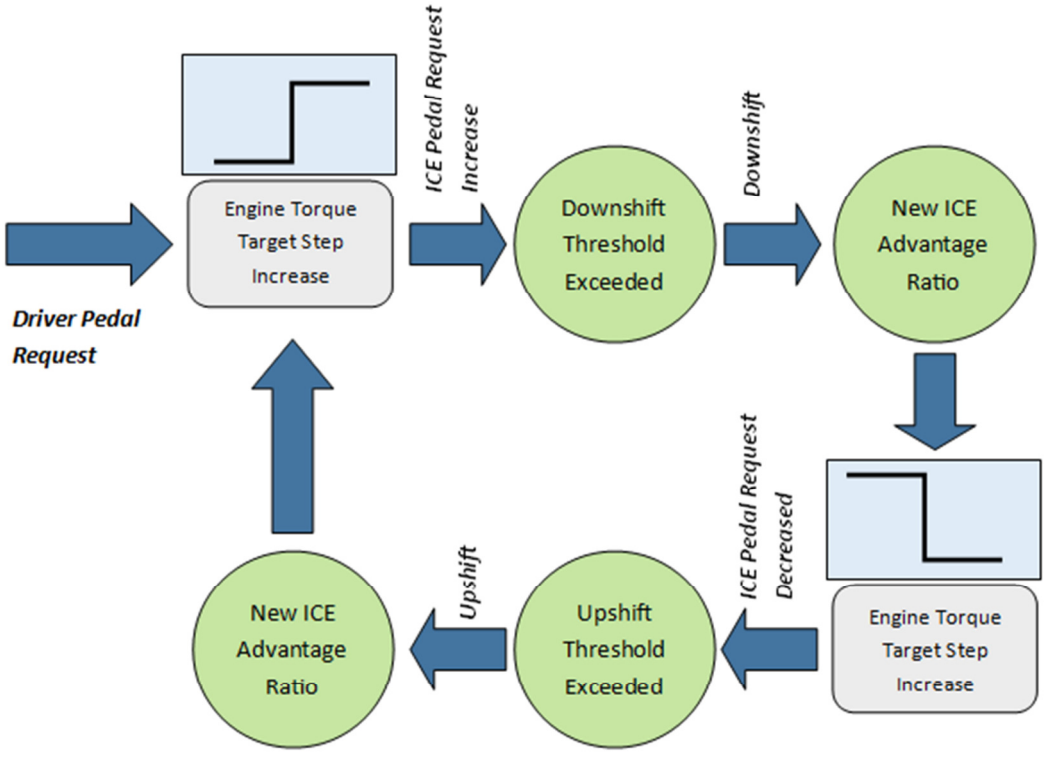

Figure 110: Transmission Gear Bounce Scenario

The instantaneous gear ratio of the transmission is available as a signal on the GM stock high speed bus. This can be used to calculate the instantaneous torque advantage of the

ICE and BAS at a given moment, however, this does not present a suitable control execution method. Complications arise from the fact that transmission gear selection is controlled indirectly through a combination of transmission output shaft speed (proportional to vehicle speed) and ICE pedal input position. Since the ICE pedal input position is also the control path for ICE torque set point, the ICE torque request is indirectly tied to transmission gear selection.

When using wheel torque control targets to calculate component command outputs at the VSU, the transmission gear is required. Direct use of the instantaneous transmission gear ratio has the risk of generating gear selection bounce and consequently poor vehicle driving characteristics. This process flow is shown in Figure 110.

In order to prevent this undesirable behaviour, wheel torque targets are instead multiplied by an advantage ratio curve extrapolated from the shift map of the transmission as a function of vehicle speed only as shown in Figure 111.

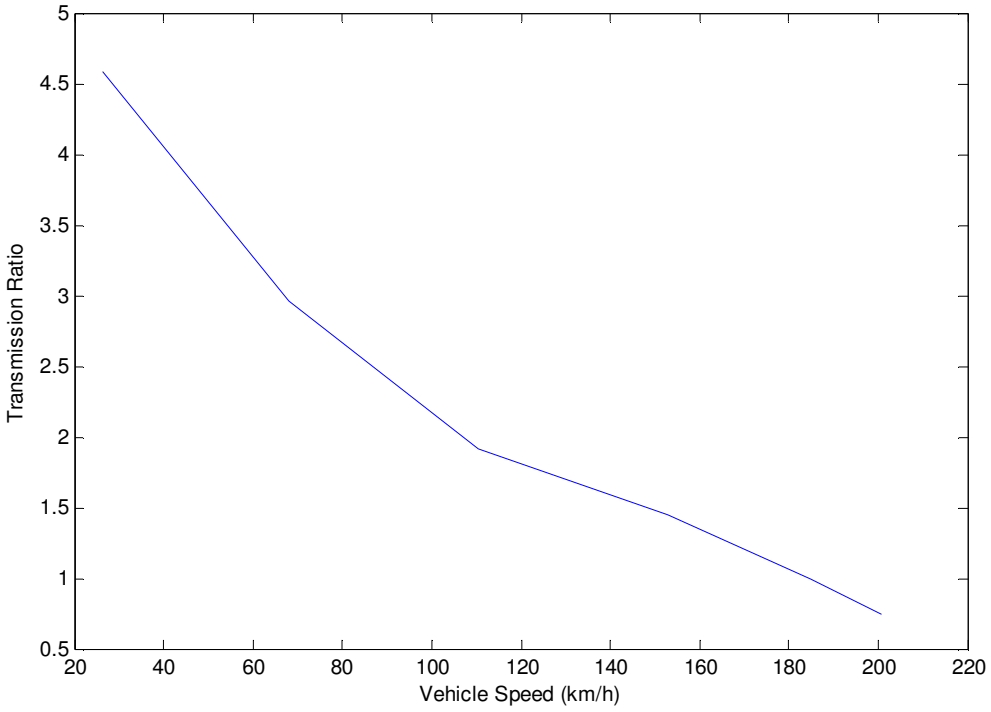

Figure 111: Transmission Ratio Estimator Curve

Maximum accelerator pedal position was used to build the ratio curve to reflect the fact that the full throttle input range for the ICE is available to use, with throttle response behaviour ideally mimicking the stock vehicle. This allows for the ICE torque command to be more consistently predictable. Large steps in the input torque command to the ICE could still indirectly cause a transmission downshift, but this will no longer be followed by the potential for an inadvertent bounce back to the previous gear ratio, as there will be no effect on the ICE torque command.

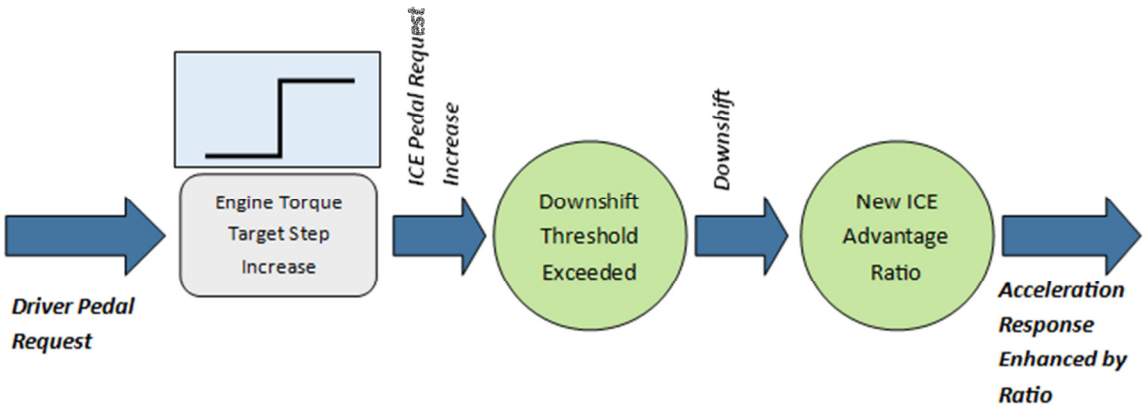

Figure 112: Engine Torque Target Increase Results in No Bounce Acceleration

Appendix C – Optimization Routine Sample Code

Running the Optimization:

```
function [Output] = RunCarOpt(OptInput);
%=========================================
%Function calls optimization routine to
%allow for batch optimization queues

%input array is:
%1-generations
%2-population
%3-drive cycle name
%4 equivalence factor
%5 recursive equivalence factor on/off

%Name1 = US06 City
%Name2 = US06 Hwy
%Name3 = HWFET, Name4 = FU505
%=========================================

%load cycle data
load Drive_Cycles/US06_Hwy.mat;
load Drive_Cycles/US06_City.mat;
load Drive_Cycles/UDDS.mat;
load Drive_Cycles/HWFET.mat;
load Drive_Cycles/Schedule_FU505.mat;

%declare global variables
global Schedule;
global Equiv;
global Recursive;

Equiv=OptInput(4);
Recursive=OptInput(5);

%set cycle based on input
if (OptInput(3)==1)
    Schedule=US06_City
    Cycle='US06City'
elseif (OptInput(3)==2)
    Schedule=US06_Hwy
    Cycle='US06Hwy'
elseif (OptInput(3)==3)
    Schedule=HWFET
    Cycle='HWFET'
elseif (OptInput(3)==4)
    Schedule=FU505
    Cycle='FU505'
end
```

```
%sets up optimization parameters
generations = OptInput(1);
population = OptInput(2);
simulations = (generations+1)*population+100;

%sets up optimization iteration results
global Opt
Opt=zeros(simulations,11);
global counter
counter = 1; %counter for populating results

%optimization initialization of search field
initial = [12 45 0.005 0.02 0.0166 0.0334]
lb = [0 0 0 0 0 0]
ub = [60 70 0.05 0.2 0.05 0.2]

%Call optimization=============
OptimalResults = ga(@ObjFunc, 6, [], [], [], [], lb, ub, [],
gaoptimset...
    ('PopulationSize', population, 'Generations', generations,...
    'TolFun', 0.0000001, 'TimeLimit', 60000,...
    'PlotFcns', {@gaplotbestf, @gaplotstopping},...
    'PopInitRange', [lb; ub],  'StallGenLimit', 10));
%==============================

%save results to file
save(strcat('Results_', date, '_', Cycle, 'gen',
num2str(generations),...
    'pop', num2str(population), 'equiv', num2str(Equiv),...
    'R', num2str(Recursive), '.mat'), 'Opt');
save(strcat('Optimal_', date, '_', Cycle, 'gen',
num2str(generations),...
    'pop', num2str(population), 'equiv', num2str(Equiv),...
    '.mat'), 'OptimalResults');

end
```

Calculating the Objective Function Value:

```
function [Output] = ObjFunc(Coeff);
%=============================================
%function calls the vehicle simulation and uses
%the results to calculate the overall consumption
%which serves as the optimization objective
%function
%=============================================

%Sets Tuning Variables per Optimization Routine
set_param('MalibuSuperBAS/Controller/Outside Numerics/ENG_TUNE',...
    'OFFSET', num2str(Coeff(1)));
set_param('MalibuSuperBAS/Controller/Outside Numerics/ENG_TUNE',...
    'MIN', num2str(Coeff(2)));
```

```
set_param('MalibuSuperBAS/Controller/Outside Numerics/BAS_TUNE',...
    'Apos', num2str(Coeff(3)));
set_param('MalibuSuperBAS/Controller/Outside Numerics/BAS_TUNE',...
    'Bpos', num2str(Coeff(4)));
set_param('MalibuSuperBAS/Controller/Outside Numerics/BAS_TUNE',...
    'Aneg', num2str(Coeff(5)));
set_param('MalibuSuperBAS/Controller/Outside Numerics/BAS_TUNE',...
    'Bneg', num2str(Coeff(6)));

%Sets CS Mode
set_param('MalibuSuperBAS/Controller/CS Mode Sw', 'Mode', num2str(1));

%run simulation
sim('MalibuSuperBAS');
run EquivCons;
CS_Cons = TotConsEquiv_Lge100km; %Equivalent gas Consumption in CS Mode

%declare global values for storing results
global counter;
global Opt;
global Equiv;
global Recursive;

%store values==================
%Opt(counter, 1) = UNUSED;
%Opt(counter, 2) = UNUSED;
%Opt(counter, 3) = UNUSED;
Opt(counter, 4) = CS_Cons;
Opt(counter, 6) = Coeff(1);
Opt(counter, 7) = Coeff(2);
Opt(counter, 8) = Coeff(3);
Opt(counter, 9) = Coeff(4);
Opt(counter, 10) = Coeff(5);
Opt(counter, 11) = Coeff(6);

%Stores value of equivalence factor
if Recursive == 1
    Opt (counter, 5) = ELEC_Eff(end)/ENG_Eff(end);%recursive EF
end
if Recursive == 0
    Opt (counter, 5) = Equiv;
end

counter = counter+1;
%============================
%%%%%%%%%%%%%%%%%%%%%%%%%%%%%%

%send results back to optimizatio routine
Output = CS_Cons;

end
```

Calculating Equivalent Consumption:

```
%%%%%%%%%%%%%%%%%%%%%%%%%%%%%%%%%%%%%%%%%%%%%%%%%%%$$$$$$
%Script Calculates Equivalent CS Consumption
%%%%%%%%%%%%%%%%%%%%%%%%%%%%%%%%%%%%%%%%%%%%%%%%%%%%$$$$$

%declare global variables for access
global Equiv;
global Recursive;

%Calculate non-recursive EF consumption
if Recursive == 0;
    Dist_km = O_VehDist(end); %Distance travelled over cycle
    ESSEnergy_kWh = -O_ESSE(end); %Electrical Energy Consumed at ESS
    E_Consumption = ESSEnergy_kWh/Dist_km*100; %ESS Consumption per
100km
    Fuel_L = O_Fuelkg(end)/0.7583;%E85 Fuel Use in Kg
    Fuel_L100km = Fuel_L/Dist_km*100;%Fuel Consumption
    TotGasEquiv_L = (ESSEnergy_kWh/8.895)*Equiv+Fuel_L; %Gasonline
                                                    %Equivalent Usage
    TotConsEquiv_Lge100km = TotGasEquiv_L/Dist_km*100; %Gasoline
                                    %Equivalent Fuel Consumption Rate
end

%Calculate recursive EF consumption
if Recursive == 1;
    EF = ELEC_Eff(end)/ENG_Eff(end);%recursive EF

    Dist_km = O_VehDist(end); %Distance travelled over cycle
    ESSEnergy_kWh = -O_ESSE(end); %Electrical Energy Consumed at ESS
    E_Consumption = ESSEnergy_kWh/Dist_km*100; %ESS Consumption per
100km
    Fuel_L = O_Fuelkg(end)/0.7583;%E85 Fuel Use in Kg
    Fuel_L100km = Fuel_L/Dist_km*100;%Fuel Consumption
    TotGasEquiv_L = (ESSEnergy_kWh/8.895)*EF+Fuel_L; %Gasonline
                                                %Equivalent Usage
    TotConsEquiv_Lge100km = TotGasEquiv_L/Dist_km*100; %Gasoline
                                    %Equivalent Fuel Consumption Rate
end
```